

Science Driven Optimization of the LSST Observing Strategy

Prepared by the LSST Science Collaborations,
with contributions from the LSST Project.

Contributing Authors

Željko Ivezić ([ivezic](#)),¹ Beth Willman ([bethwillman](#)),² Stephen Ridgway ([StephenRidgway](#)),³ Phil Marshall ([drphilmarshall](#)),⁴ Lynne Jones ([rhiannonlynne](#)),⁵ Rahul Biswas ([rbiswas4](#)),⁶ Timo Anguita ([tanguita](#)),⁷ Ohad Shemmer ([ohadshemmer](#)),⁸ David Nidever ([dnidever](#)),⁹ Eric Gawiser ([egawiser](#)),¹⁰ Michelle Lochner ([MichelleLochner](#)),¹¹ Will Clarkson ([willclarkson](#)),¹² Knut Olsen ([knutago](#)),¹³ Dave Monet ([dgmonet](#)),¹⁴ Lucianne Walkowicz ([lmwalkowicz](#)),¹⁵ Peregrine McGehee ([pmmcgehee](#)),¹⁶ Michael B. Lund ([lundmb](#)),¹⁷ Chuck Claver ([cclaver](#)),¹⁸ Seth Digel ([sethdigel](#)),¹⁹ Ashish Mahabal ([AshishMahabal](#)),²⁰ Eric Bellm ([ebellm](#)),²¹ Andy Connolly ([connolly](#)),²² Michael Strauss ([michaelstrauss](#)),²³ Jason Rhodes ([jasondrhodes](#)),²⁴ Marcelles Soares-Santos ([soares-santos](#)),²⁵ Carl Grillmair ([cgrillmair](#)),²⁶ Christina Peters ([cmp346](#)),²⁷ David Trilling ([davidtrilling](#)),²⁸ Eric Neilsen ([ehneilsen](#)),²⁹ Federica Bianco ([fedhere](#)),³⁰ Josh Meyers ([jmeyers314](#)),³¹ Someone Calledknawro ([knawro](#)),³² Stefano Valenti ([svalenti](#)),³³ Peter Yoachim ([yoachim](#)),³⁴ Christopher Stubbs ([astrostubbs](#)),³⁵ Jay Strader ([caprastro](#)),³⁶ *your name here*, and the LSST Project and Science Collaborations

¹University of Washington, ...

²LSST, ...

³NOAO, ...

⁴SLAC, ...

⁵University of Washington, ...

⁶University of Washington, ...

⁷UNAB, Chile, ...

⁸Some Institute, Somewhere, ...

⁹LSST, ...

¹⁰Rutgers, ...

¹¹UCL, ...

¹²University of Michigan-Dearborn, ...

¹³NOAO, ...

¹⁴USNO, ...

¹⁵Adler Planetarium, ...

¹⁶IPAC, ...

¹⁷Vanderbilt University, ...

¹⁸LSST, ...

¹⁹SLAC, ...

²⁰Some Institute, Somewhere, ...

²¹Some Institute, Somewhere, ...

²²University of Washington, ...

²³Princeton, ...

²⁴JPL, ...

²⁵Some Institute, Somewhere, ...

²⁶Some Institute, Somewhere, ...

²⁷Some Institute, Somewhere, ...

²⁸Some Institute, Somewhere, ...

²⁹Some Institute, Somewhere, ...

³⁰Some Institute, Somewhere, ...

³¹Some Institute, Somewhere, ...

³²Some Institute, Somewhere, ...

³³Some Institute, Somewhere, ...

³⁴Some Institute, Somewhere, ...

³⁵Some Institute, Somewhere, ...

³⁶Michigan State, ...

Contents

Preface	7
Guidelines for Authors	8
0 Template Science Chapter	11
0.1 Introduction	11
0.2 Example Science Project Section	11
1 Introduction	13
1.1 Synoptic Sky Surveying at Universal Cadence	14
1.2 Beyond the Baseline Observing Strategy	14
1.3 Evaluation and Optimization of the LSST Observing Strategy	14
1.4 Outline of This Paper	15
2 Some Example Observing Strategies	17
2.1 Introduction	17
2.2 The Baseline Observing Strategy	18
2.3 Some Simulated Alternative Observing Strategies	25
2.4 Analysis of NEO/PHA completeness	33
2.5 Ongoing and Future Work	37
2.6 Summary	38
3 Solar System	41
3.1 Discovering Solar System Objects	41
4 The Galaxy	43
4.1 Introduction	43
4.2 Some general considerations for Milky Way metrics	43
4.3 Summary table of Milky Way science cases	45
4.4 The spatial structure of the Milky Way	45
4.5 Metallicity and age mapping in the Milky Way	46
4.6 Star Formation History of the Milky Way	47
4.7 Dust in the Milky Way	48
4.8 Microlensing in the Milky Way with LSST	49
4.9 The Galactic Plane Should Be Part of the Main Deep-Wide-Fast Survey	50
4.10 Milky Way Metrics: future work	53
5 Mapping Our Galaxy: Positions, Proper Motions and Parallax	55
6 Variables and Transients	59
6.1 Introduction	59
6.2 Metrics for Transients and Variables	60
6.3 Periodic Variable Stars	62
6.4 Non-periodic Variables	64
6.5 Periodic Transient Events	65
6.6 Transient Events	66

Contents

6.7	Rolling Cadence	69
7	Cosmology	73
7.1	Introduction	73
7.2	Large Scale Structure: Testing Dithering Patterns and Timescales to Improve Survey Uniformity	74
7.3	Suppressing systematic effects	75
7.4	Supernova Cosmology and Physics	78
7.5	Strong Gravitational Lens Time Delays	85
7.6	AGN Science	89
8	Deep Drilling Fields	95
8.1	Introduction	95
9	Special Surveys	97
9.1	Introduction	97
9.2	The Magellanic Clouds	97
9.3	Short Exposure Survey- Introduction	100
10	Tensions and Trade-offs	107
	References	109

Preface

This is a community white paper outlining various science cases and the impacts that observing strategy will have on them, quantified using the Metric Analysis Framework. We will describe various strategies and tradeoffs that impact the observing cadence (visit sequence), the current cadence baseline, and future directions for the optimization of the survey strategy. We aim to publish this white paper on arXiv, and invite community feedback.

The timescale for producing this white paper, started before and finished after the Observing Strategy workshop at the August 2015 LSST Project and Community workshop, is many months.

Messages

The main points we aim to convey in this white paper are as follows:

- We have a pretty good idea of how we would deploy LSST: there is a baseline strategy and a corresponding simulated visit sequence, with which it can be demonstrated that the data required for the promised science can be delivered.
- However, the baseline strategy is not set in stone, and can and will be optimized. Even small changes could result in significant improvements to the overall science yield.
- These improvements can be predicted via analysis of the outputs of the LSST Operations Simulator, OPsim, using the Metric Analysis Framework (MAF). Once the baseline visit sequence has been evaluated with a given science case's metrics, all other proposed visit sequences can be compared against it, automatically.
- The LSST observing strategy evaluation and optimization process will be as open and inclusive as possible. We invite all stakeholders to participate.

Project start: July 2015.

Guidelines for Authors

Phil Marshall

Since this is a community white paper, contributions are welcome from everyone. Read on for how to make a contribution, and how you should structure that contribution.

0.0.1 How to Get Involved

The first thing you should do is read and absorb the current version of the white paper, which you should be able to [view on GitHub](#). (You can also [download the “raw” PDF](#), which is hyper-linked for easier navigation.) You will then be able to provide good feedback, which you should do via the [GitHub issues](#). Browse the existing issues first: there might be a conversation you can join. New issues are most welcome: we’d like to make this white paper as comprehensive as possible.

To edit the white paper, you’ll need to “[fork](#)” its [repository](#). You will then be able to edit the paper in your own fork, and when you are ready, submit a “[pull request](#)” explaining what you are doing and the new version that you would like to be accepted. It’s a good idea to submit this pull request sooner rather than later, because associated with it will be a discussion thread that the writing community can use to discuss your ideas with you. For help getting started with `git` and [GitHub](#), please see this [handy guide](#).

0.0.2 Chapter and Section Design

For a high-level justification of the following design, please see [Section 1.3](#). In short, we’re aiming for modular sections (that are easy to write in parallel, and then re-arrange within chapters later) focused on one science project each, and quantified by one (or maybe two) figures of merit (which will likely depend on other, lower-level metrics). Each section can be thought of as an observing proposal, demonstrating the performance achievable given various assumptions about the time awarded.³⁷

The first section of each science chapter needs to be an *introduction* that outlines, very briefly, the commonality of the key science projects contained in it: what is to be measured, in broad-brush terms, and why this is of interest. Then, suppose we were to design an LSST survey to enable these measurements: qualitatively, what might it look like, in terms of the choices we are able to make? This chapter introduction can eventually (when the results are in!) summarize, again, in very broad brush terms, the results of a number of investigative sections, one on each science case.

The individual sections following this introduction will then need to describe the particular discoveries and measurements that are being targeted in each *science case*. It will be helpful to think of a “science case” as a “science project” that the section leads *actually plan to do*. Thinking this way means that the sections can follow the tried and tested format of an observing proposal: a brief description of the investigation, with references, followed by a technical feasibility piece. This latter part will need to be quantified using the MAF framework, via a set of metrics that need

³⁷These notes on the white paper design are adapted from the notes at [whitepaper/notes/chapter-template.md](#)

to be computed for any given observing strategy to quantify its impact on the described science case. Ideally, these metrics would be combined in a well-motivated figure of merit. The section can conclude with a discussion of any risks that have been identified, and how these could be mitigated.

The following chapter shows a template introduction and science case section for you to work from. The latter is checked into the repository as `section-template.tex`. For an example of a section being developed according to the above guidelines, please take a look at [Section 7.5](#).

0 Template Science Chapter

Editor Name(s)

0.1 Introduction

General introduction to the chapter's science projects.

Overview of observing strategy needed by those projects, bringing out common themes or points of tension.

0.2 Example Science Project Section

Author Name(s)

A short preamble goes here. What's the context for this science project? Where does it fit in the big picture?

0.2.1 Target measurements and discoveries

Describe the discoveries and measurements you want to make.

Now, describe their response to the observing strategy. Qualitatively, how will the science project be affected by the observing schedule and conditions? In broad terms, how would we expect the observing strategy to be optimized for this science?

0.2.2 Metrics

Quantifying the response via MAF metrics: definition of the metrics, and any derived overall figure of merit.

0.2.3 OpSim Analysis

OpSim analysis: how good would the default observing strategy be, at the time of writing for this science project?

0.2.4 Discussion

Discussion: what risks have been identified? What suggestions could be made to improve this science project's figure of merit, and mitigate the identified risks?

Go to: • [the start of this section](#) • [the start of the chapter](#) • [the table of contents](#)

1 Introduction

Phil Marshall, Zeljko Ivezic, Beth Willman, ...

The Large Synoptic Survey Telescope (LSST) is a dedicated optical telescope with an effective aperture of 6.7 meters, currently under construction on Cerro Pachón in the Chilean Andes. The telescope and camera will have a huge field of view, 9.6 deg^2 , and the étendue, i.e., the product of collecting area and field of view will be significantly larger than any other telescope. Thus this telescope is designed for wide-field deep imaging of the sky; its mantra is “Wide-Deep-Fast”, i.e., the ability to cover large swaths of sky (“Wide”) to faint magnitudes (“Deep”) in a short amount of time (“Fast”), allowing to scan the sky repeatedly.

The science case for the LSST is based broadly on four science themes:

- Dark energy and dark matter (via strong and weak lensing, large-scale structure, and supernovae);
- Exploring the transient and variable universe;
- Studying the structure of the Milky Way galaxy and its neighbors via resolved stellar populations;
- An inventory of the Solar System, including Near-Earth Asteroids and Potential Hazardous Objects, Main-Belt Asteroids, and Kuiper-Belt Objects.

These themes, together with *many* other science applications, are described in detail in the [LSST Science Book](#), produced by the LSST Project Team and Science collaborations in 2009. The present white paper represents an important next step in science planning beyond the Science Book. In particular, we now need to quantify how well the LSST (for a given realization of its cadence) will be able to carry out its science goals; indeed, we will use this quantification to refine and optimize the cadence itself.

The Science Book is six years old. In those six years, some of the science themes described in there have evolved or become obsolete, while new science opportunities and ideas have arisen. Moreover, our understanding of the capabilities (such as system response and therefore depth, telescope optics, and so on) have matured considerably. The present document endeavors to explore the principal science themes as described in the Science Book, but is not slaved to them, and where appropriate, we will point out relevant updates to the Science Book.

1.1 Synoptic Sky Surveying at Universal Cadence

Synoptic Surveying with LSST - the basic observing strategy determined by key projects described in the LSST Science Requirements Document, and constrained by the LSST’s design ([Ivezic et al. 2008](#)).

1.2 Beyond the Baseline Observing Strategy

Optimizing the Observing Strategy: what perturbations are we permitted to introduce, to maximize the system’s science capabilities? What are our constraints? And our opportunities?

1.3 Evaluation and Optimization of the LSST Observing Strategy

The first step towards a science-based optimization of the LSST observing strategy is a *science-based evaluation of the baseline LSST observing strategy*. After simulating a sample observing schedule consistent with this strategy (see [Chapter 2](#)), we then need to quantify its value to each science team. This is what the LSST DM Sims team’s “Metric Analysis Framework” was designed to enable. Once the fiducial strategy has been evaluated in this way, then any other strategy can be evaluated in the same terms, using the same code, and we will be able to start optimizing the strategy through iterations between OPSIM and MAF.

With this program in mind, it makes sense to define *one “Figure of Merit” (FoM) per science project*, that captures the value of the observing strategy under consideration to that science team. This FoM will probably be a function of several “metrics” that quantify lower-level features of the observing sequence. For Figures of Merit to be directly comparable between disparate science projects, they need to be dimensional, and have the same units. One natural choice could be the *information gained* by the science team, in bits. This is a well-defined statistical quantity, albeit not yet one in common use. A given observing schedule’s value would then depend on both this information gain, but also *how much that information is worth to the whole community*. It is at this point that the debate could become heated: probably the best we can do in Cadence Diplomacy is to quantify all the information gains implied by each proposed change to the baseline observing strategy, combine them to see whether it makes everyone happy, and iterate. In this way we might hope to minimize the debates about the less quantifiable worth of each piece of information.

We are some way from being able to define information-based Figures of Merit for most science cases – but the metrics that they will depend on will be easier to derive. Writing this white paper is an opportunity to think through the Figure of Merit for each science project that we as a community want to carry out, and how that measure of success is likely (or even known) to depend on metrics that summarize the observing sequence presented to us. Thinking about the problem in terms of science projects, each with a Figure of Merit, encourages us to design modular document sections, with one science project and one Figure of Merit per section.

This will have the happy side-effect of allowing the chapters to be straightforwardly re-arranged as we go, to make the white paper easier to read. It will also naturally lead to the definition of

a suite of MAF super-metrics, can be evaluated on any future OPSIM output database. A table in each section showing the values of the metrics and the FoM, for different schedules, for that science project, will be very helpful. The metric names in these tables should match the metric class names in the `sim_maf_contrib` module. In principle these tables could be auto-generated by the MAF framework, and extended as OPSIM is repeatedly reconfigured and run.

For an example of how all this could look, please see the [lens time delays section](#). The MAF subsections are still under development there, but keep checking back to see it come together during the August 2015 workshop week. Templates for the chapters and sections can be found in [Chapter 0](#).

1.4 Outline of This Paper

The rest of this white paper is structured as follows. In [Chapter 2](#) we describe a number of OPSIM simulated observing schedules (“cadences”) explored by the LSST Sims team in summer 2015 in preparation for this paper: they include a “baseline cadence”, and then some small but interesting perturbations to it. Then, we present the science cases considered so far, organised into the following chapters:

- [Chapter 3: Solar System](#)
- [Chapter 4: The Galaxy](#)
- [Chapter 5: Mapping Our Galaxy: Positions, Proper Motions and Parallax](#)
- [Chapter 6: Variables and Transients](#)
- [Chapter 7: Cosmology](#)
- [Chapter 8: Deep Drilling Fields](#)
- [Chapter 9: Special Surveys](#)

Finally, in [Chapter 10](#) we bring the results of all the science metric analyses together and discuss the tensions between them, and the trade-offs that we can anticipate having to make.

Go to: • [the start of this section](#) • [the start of the chapter](#) • [the table of contents](#)

2 Some Example Observing Strategies

Željko Ivezić and the LSST Simulations Team, LSST Project Science Team, and Others

Summary: In this chapter (which was originally prepared as the standalone report available from <http://www.astro.washington.edu/users/ivezic/lsst/cadexp2.pdf>) we analyze and compare the performance of a number of simulated LSST observing strategies (“cadences”) which were developed in support of the LSST 2015 Observing Strategy Workshop. A candidate new Baseline Cadence, [enigma_1189](#), was found adequate and is proposed as a replacement for the previous Baseline Cadence ([opsim3.61](#)). Simulations that only implemented Universal Cadence proposal imply a margin of about 40% relative to the design specifications for the main survey sky coverage and the number of visits per field from the Science Requirements Document. This margin can be used to increase the sky coverage of the main survey, the total number of visits per field, or to implement special programs, such as deep drilling fields and Galactic plane coverage. Several simulations analyzed here quantitatively explore these strategic options. Additional simulations show that the effects of variations of the visit exposure time in the range 20-60 seconds on surveying efficiency can be predicted using simple efficiency estimates. Various modifications of baseline cadence (e.g. Pan-STARRS-like cadence, no visit pairs, sequences with 3 and 4 visits) indicate a large parameter space for further optimization, especially for time-domain investigations and detailed coverage of special sky regions.

2.1 Introduction

With the release of the latest version of Operations Simulations (hereafter OPSIM) code (version 3.2.1) for simulating LSST deployment, and the active development of Metrics Analysis Framework (MAF, currently version 0.2) for analyzing OPSIM outputs, we can now begin to undertake systematic and massive investigations of various LSST deployment strategies.

The optimization of the ultimate LSST observing strategy will be done with significant input from the community. To facilitate this process, the first of a series of meetings, named “LSST & NOAO Observing Cadences Workshop”, was held during the [LSST 2014 meeting](#) in Phoenix, AZ, August 11-15, 2014. The next workshop, named “LSST Observing Strategy Workshop”, will be held [after the LSST 2015 meeting](#) in Bremerton, WA, August 20-22, 2015.

In part as a preparation for this upcoming workshop, the LSST Simulations Team and the Project Science Team have designed, executed and analyzed a number of simulated surveys. The cadence strategies for these surveys, while similar to Baseline Cadence, are modified to study the impact of various strategy variations on the scientific potential of LSST. The cadence set also includes a candidate baseline cadence replacement.

An initial analysis of these simulated surveys is presented here. MAF reports for all simulated cadences are available from

<http://tusken.astro.washington.edu:8080/?runId=2>

OPSIM databases investigated in this section:

<i>enigma_1189 — the new Baseline Cadence.</i>	18
<i>ops2_1098 — Only Universal Cadence, with pairs of visits.</i>	25
<i>ops2_1092 — A Pan-STARRS-like observing strategy.</i>	26
<i>ops2_1093 — Only Universal Cadence, no visit pairs.</i>	27
<i>kraken_1032 — Baseline Cadence, but with no visit pairs.</i>	29
<i>ops1_1163 — Baseline Cadence, but with 33% shorter exposure time.</i>	29
<i>ops1_1164 — Baseline Cadence, but 100% longer exposure time.</i>	30
<i>ops1_1162 — Baseline Cadence, but with doubled u-band exposure time.</i>	31
<i>ops1_1161 — Baseline Cadence, but with doubled u-band exp. time and Baseline NE Spur.</i>	32
<i>ops2_1096 — Only Universal Cadence, with relaxed airmass limit.</i>	33
<i>ops2_1097 — Only Universal Cadence, with stringent airmass limit.</i>	33
<i>ops2_1094 — NEO test: no request for pairs of visits.</i>	34
<i>enigma_1257 — NEO test: pairs of visits (as in the Baseline Cadence).</i>	34
<i>enigma_1258 — NEO test: triplets of visits.</i>	34
<i>enigma_1259 — NEO test: quads of visits.</i>	34

Go to: • [the start of this section](#) • [the start of the chapter](#) • [the table of contents](#)

2.2 The Baseline Observing Strategy

The current “official” (managed by the LSST Change Control Board) Baseline Cadence, `opsim3.61`, was produced with an old version of OPSIM code. We first introduce a candidate replacement simulation that was produced using the latest version (v3.2.1) of OPSIM code, and then proceed with the analysis of other simulations that modify observing strategy in various informative ways. Suggestions for further tool development, and a summary of the main cadence questions addressed here are available at end of this document.

`enigma_1189`

the new Baseline Cadence.

The candidate replacement “Baseline Cadence” candidate, `enigma_1189`, has the following basic properties¹:

¹See <http://tusken.astro.washington.edu:8080/summaryStats?runId=1>

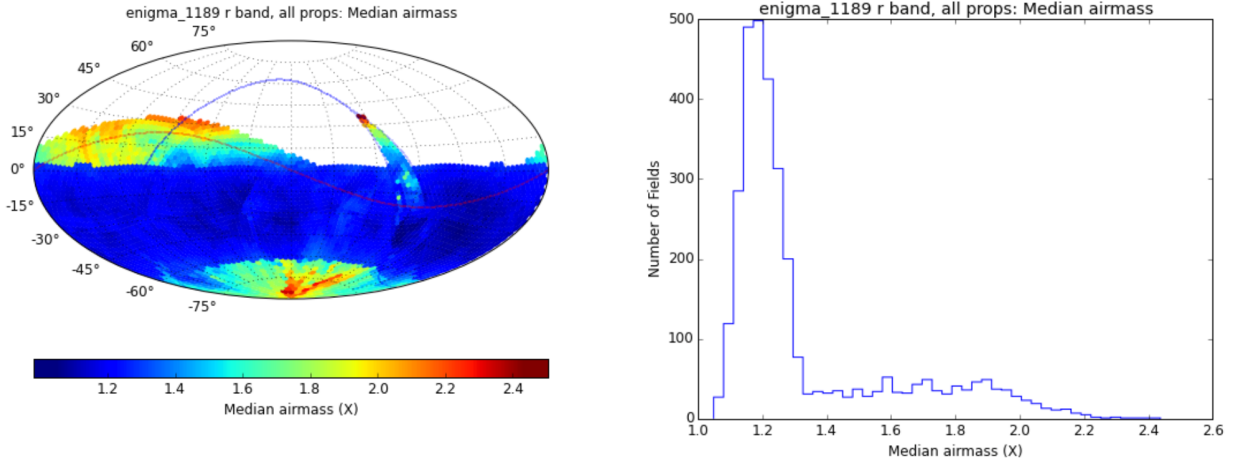


Figure 2.1: The median airmass in the r band across the sky for simulated cadence [enigma_1189](#) is shown in Aitoff projection of equatorial coordinates in the left panel. The corresponding histogram is shown in the right panel. For the main survey area, the maximum allowed airmass was set to 1.5.

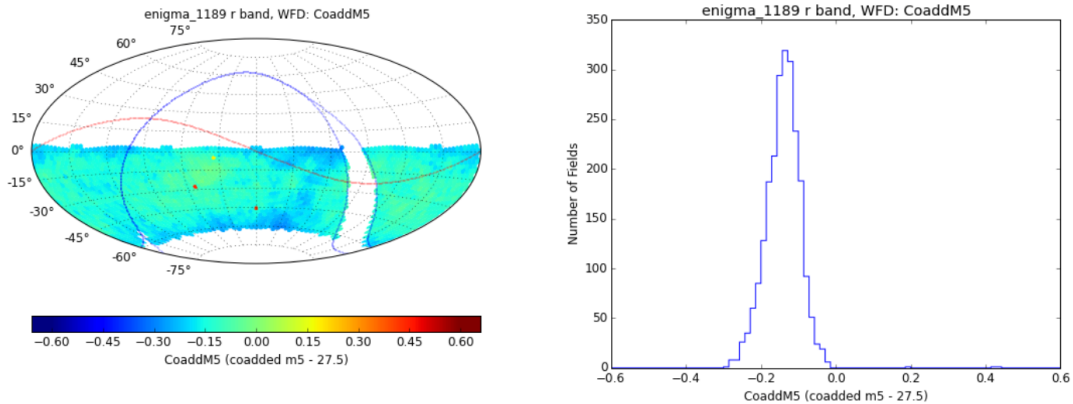
1. The total number of visits is 2,469,307, with 85.4% spent on the Universal proposal (the main deep-wide-fast survey), 6.4% on the North Ecliptic proposal, 1.7% on the Galactic plane proposal, 2.1% on the South Celestial pole proposal, and 4.5% on the Deep Drilling cosmology proposal.
2. The median number of visits *per night* is 815, the range is 35 to 1104, with 3062 observing nights. The mean slew time is 6.9 seconds (median: 4.8 sec) and the total open shutter time is 4.06 Msec. The median total open shutter time (per night) as a fraction of the observing time (the ratio of the open shutter time and the sum of the open shutter time, readout time and slew time) is 73%. The 25%-75% quartiles for the number of filter changes per night are 2 and 7, with the mean of 4.6. The total number of filter changes is 15,364.
3. In the r band, the median seeing is 0.77 arcsec, the median airmass is 1.23, and the median 5σ depth for point sources is 24.5. The variation of the median airmass for the r band observations with the position on the sky is shown in [Figure 2.1](#).
4. For the 2,293 fields (somewhat overlapping) from the Universal Cadence area (also known as WFD – wide, fast, deep), the median number of visits in the $ugrizy$ bands is (63, 89, 202, 202, 182, 181), respectively. Not only that these medians exceed the requested number of visits (design specification from the SRD²) of (56, 80, 184, 184, 160, 160) in the $ugrizy$ bands, but the minimum number of visits per field over this area does so, too. This result is quite encouraging given that only 85% of observing time was spent on the Universal Cadence proposal. The mean number of visits over the Universal Cadence area, summed over all bands, is 920.
5. The coadded 5σ depth³ for point sources in the $ugrizy$ bands is (26.1, 27.3, 27.4, 26.7, 25.4,

²The LSST Science Requirements Document (SRD) is available as <http://ls.st/lpm-17>

³Note that these values depend on externally supplied values for fiducial single-epoch 5σ depths; the following values were used in analysis described here: (24.45, 25.17, 24.67, 24.27, 23.57, 22.36) in the $ugrizy$ bands, respectively. These values are progressively deeper towards the blue bands and shallower towards the red bands, compared to the values listed in Table 2 from the latest version (v3.1) of the LSST overview paper: (23.68, 24.89, 24.43, 24.00,

:

CoaddM5 OpsimFieldSlicer r band, WFD npz JSON



Coadded depth in filter r, with design value subtracted (27.5), for all WFD proposals. More positive numbers indicate fainter limiting magnitudes.

<i>Median:</i>	27.39
<i>Mean:</i>	27.39
<i>Rms:</i>	0.05
<i>N(-3Sigma):</i>	2.00
<i>N(+3Sigma):</i>	3.00
<i>Count:</i>	2293
<i>25th%ile:</i>	27.36
<i>75th%ile:</i>	27.42
<i>Min:</i>	27.24
<i>Max:</i>	27.97

Figure 2.2: A screen grab from web-based MAF analysis of simulated cadence [enigma_1189](#). The coadded 5σ depth for point sources in the *r* band across the main survey area (WFD=“wide-fast-deep”) is shown in the top left corner, in Aitoff projection of equatorial coordinates. The red line shows the Ecliptic and the blue line shows the Galactic equator (it bifurcates around the so-called “Galactic confusion zone”). The distribution of the limiting depth across this area is shown as a histogram in the top right corner. The basic statistics for this distribution are listed in the bottom left.

24.4), respectively. The distribution of coadded depth across the sky is fairly uniform; for an example see [Figure 2.2](#).

6. For the 2,293 fields from the Universal Cadence area, the median seeing is 0.75 arcsec in the *r* band and 0.74 arcsec in the *i* band. The median airmass in the *urz* bands is 1.25, 1.20 and 1.26 (the maximum allowed airmass for the Universal Cadence area was set to 1.5). The median sky brightness in the *ury* bands is 22.0 mag/arcsec², 21.1 mag/arcsec², and 17.3 mag/arcsec², respectively.
7. Restricted to the Universal Cadence fields, a unique area of 18,000 sq.deg. received at least 898 visits (summed over bands; the SRD design value is 825).

23.45, 22.60). This discrepancy is due to the Project software evolution falling behind continuing improvements in the system performance estimates and will be rectified by introducing automated version control system across the Project.

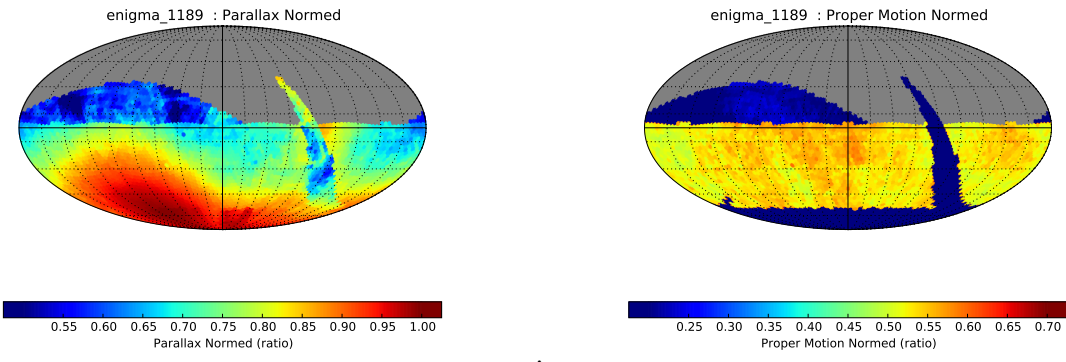


Figure 2.3: The trigonometric parallax errors (left) and proper motion errors (right), normalized by the values for idealized perfectly optimized cadences (parallax: all the observations are taken at maximum parallax factor, resulting in a peak at the South Ecliptic pole; proper motion: a half of all visits are obtained on the first day and the rest on the last day of the survey), obtained for simulated cadence `enigma_1189` are shown in Aitoff projection of equatorial coordinates.

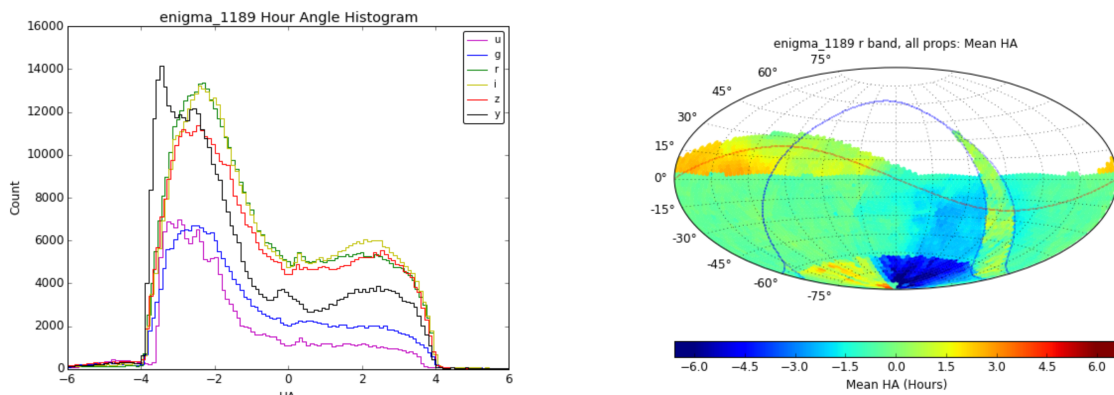


Figure 2.4: Histograms in the left panel show the distribution of hour angles (HA) in 6 bands for all proposals from simulated cadence `enigma_1189` (the distributions are similar for WFD fields considered alone). Note the bias towards observations west from the meridian. The right panel shows the distribution across the sky of the mean HA for all observations in the *r* band.

8. The median trigonometric parallax and proper motion errors are 0.57 mas and 0.16 mas/yr, respectively, for bright sources (limited by assumed systematic errors in relative astrometry of 10 mas), and 5.5 mas and 1.6 mas/yr for points sources with $r = 24$ (assuming flat spectral energy distribution), over the Universal Cadence fields. The variation of parallax and proper motion errors across the sky is visualized in Figure 2.3.

For comparison, the current Baseline Cadence, `opsim3.61` (obtained with old OpSim code), delivered 2,651,588 visits, or 7.4% more than `enigma_1189` (this is due to known effects and changes in the code, such as more pre-scheduled down time in the new version). Perhaps the most important (and undesired!) difference between the two simulations is that the new candidate Baseline Cadence spent 6.4% of the observing time on North Ecliptic Spur proposal (vs. 4% spent on corresponding Universal North proposal in `opsim3.61`), and less than 90% of time on the Universal proposal (the main wide-deep-fast survey).

Analysis of the hour angle distribution, shown in Figure 2.4 and Figure 2.5, reveals a strong

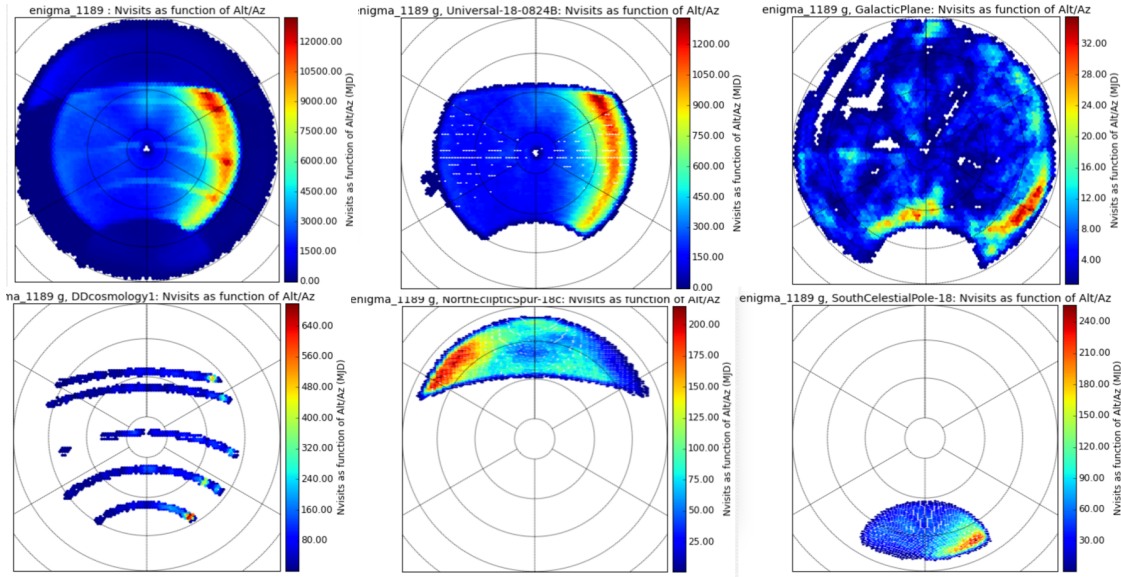


Figure 2.5: The color-coded map in the top left panel shows the g band visit count from Baseline Cadence simulation [enigma_1189](#) in the equal-area Lambert projection of the horizontal coordinate system (altitude-azimuth), with north on top and west towards the right. The horizon corresponds to the largest circle. Five implemented proposals are shown separately in other panels (top row: Universal and Galactic Plane, bottom row: Deep Drilling fields, North Ecliptic Spur, and South Celestial Pole region). The Universal cadence was limited to airmass below 1.5, while other proposals sampled higher airmass, too (see the histogram in [Figure 2.1](#)). Note the strong propensity of Universal fields for westward observations (the median airmass is about 1.2).

bias towards observations west from the meridian for the main survey. *This pattern is not fully understood at this time* and may be caused by specific features of the cost function implemented in the OpSim code.

Another potentially undesirable feature, seen in practically all simulations analyzed here, is that up to about a quarter of visits in the main survey area represents the third, the fourth and sometimes even the fifth visit to a field in the same night. For a large number of time-domain programs, these visits could be used instead to decrease the field inter-night revisit time. For more

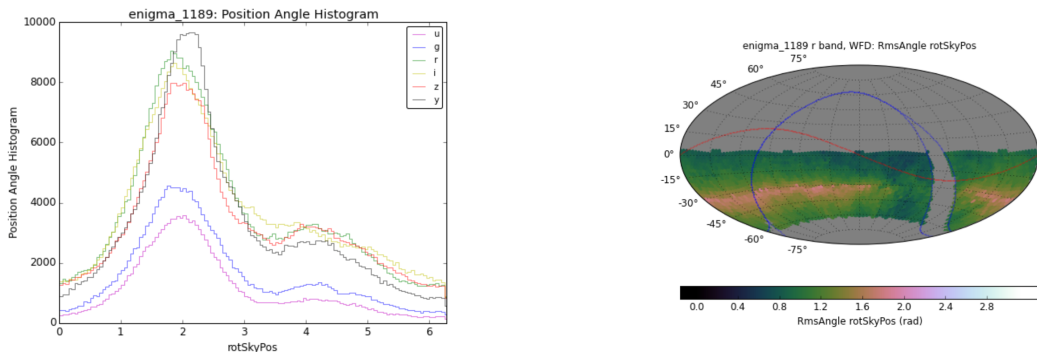


Figure 2.6: The left panel shows the position angle distribution (in radians) in each band for the main survey fields in [enigma_1189](#). The position angle is the angle between “up” in the image and North on the sky. The variation of the root-mean-square scatter of the r band distribution across the sky is shown in the right panel.

2.2 The Baseline Observing Strategy



Figure 2.7: The median inter-night gap (or revisit time) is shown in Aitoff projection for all proposals and all filters for candidate Baseline Cadence [enigma_1189](#). On average, fields in the main survey get revisited about every 3 days.



Figure 2.8: The median inter-night gap for r band visits is shown in Aitoff projection for all proposals and all filters for candidate Baseline Cadence [enigma_1189](#). On average, fields in the main survey get revisited in the r band about every 15 days.

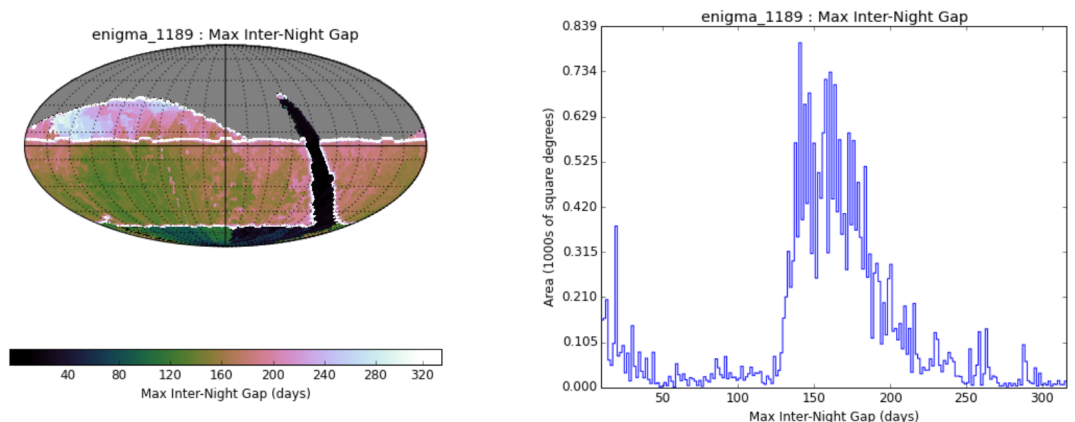


Figure 2.9: The maximum inter-night gap (or revisit time) is shown in Aitoff projection for all proposals and all filters for candidate Baseline Cadence [enigma_1189](#).



Figure 2.10: The fraction of simulated Type Ia SNe at a redshift of 0.5 detected pre-peak in any filter for candidate Baseline Cadence [enigma_1189](#). About 40% of all such SNe from the main survey will be detected before their maximum brightness.

details, see [Section 2.4](#). The position angle distributions for this simulation are shown in [Figure 2.6](#).

Time-domain metrics

The analysis of metrics designed for time-domain science has not been performed yet in detail, except for the analysis of asteroid completeness discussed in [Section 2.4](#). MAF already includes several sophisticated metrics, e.g., period recovery for variable stars, which will be described in a later version of this report.

As a brief illustration of time-domain analysis, [Figure 2.7](#) shows the median revisit time distribution when all bands are considered, and [Figure 2.8](#) shows the median revisit time distribution in the band. On average, fields in the main survey get revisited about every 3 days using all filters, and every 15 days when using only r band visits (30 days when using only u band visits is the longest median revisit time). [Figure 2.9](#) shows the maximum inter-night gap, which on average is about 5-6 months.

The temporal sampling for this simulation is sufficient to enable a large recovery fraction for SNe. [Figure 2.10](#) shows that a large fraction of LSST SNe will be detected before their maximum brightness. Similar MAF metrics that explore various quality cuts on SNe light curves (e.g. “detected at least 6 times, at least 3 pre-peak, at least 3 post-peak, with observations in at least 3 filters”).

Intra-night revisit time distribution is discussed in more detail in §[2.4](#).

Special Proposals

Regarding the special proposals, here we only provide the basic performance parameters. With the exception of the Deep Drilling proposal, these proposals are essentially strawman placeholders. The North Ecliptic proposal (6.4% of the observing time) obtained an additional 300 visits per field, summed over *griz* bands. These fields are placed along the northern part of the Ecliptic. The Galactic plane proposal (1.7%) obtained 30 visits per band in all six bands, across the region extending in Galactic latitude 10 degrees from the Galactic center, with the boundary approaching

the Galactic equator linearly with longitude, and the zone ending at $l = 90$ deg. and at $l = 270$ deg. The South Celestial pole proposal (2.1%) obtained 30 visits per band in all six bands, for fields centers with Dec < -62.5 deg. The Deep Drilling cosmology proposal (4.5%) included 5 fields, with each obtaining several thousand visits per band. The coadded 5σ depths for these fields are much fainter than for the main survey: the medians values are (28.5, 28.6, 28.8, 28.2, 27.7, 26.0) in the *ugrizy* bands, respectively.

Conclusions:

The candidate Baseline Cadence, [enigma_1189](#), appears to be an adequate replacement for the current baseline cadence ([opsim3.61](#)). Based on this preliminary analysis, there are no major problems with its performance. While there are patterns which are not fully understood (most notably the observing bias towards west), or undesired (unnecessary revisits of the same field in the same night), [enigma_1189](#) is used as a benchmark cadence, and referred to as “Baseline Cadence”, in the rest of this document⁴

An important feature of [enigma_1189](#) simulation is that the mean slew time of 6.9 sec is very close to the minimum possible slew time of about 4.5 sec. The implication is that the surveying efficiency, assuming 30 sec exposure time per visit, can be increased by at most about 6% (that is, the total open-shutter time is within about 6% from its possible maximum, given everything else unchanged). Nevertheless, there are other survey aspects, including sky coverage and temporal sampling functions, that can be further optimized, as discussed in ??.

Go to: • [the start of this section](#) • [the start of the chapter](#) • [the table of contents](#)

2.3 Some Simulated Alternative Observing Strategies

We now describe some alternatives to the Baseline Cadence that were explored. These OPSIM databases are all available for further testing with science-based MAF metrics.

ops2_1098

Only Universal Cadence, with pairs of visits.

Motivation and description: Formally, $\sim 90\%$ of observing time is allocated to the main Universal Cadence program (WFD). The remaining observing time is allocated to other programs, such as “Deep Drilling” programs (see Section 3.4 and Tables 22-26 in the SRD). With this simulation, we wished to find out what would be the effect of ignoring special programs and spending all of the observing time on the main Universal Cadence program.

⁴ Assuming that additional analysis will not uncover any major deficiencies, this simulation will be discussed by the Project Science Team and proposed for adoption as the new Baseline Cadence to the Change Control Board. The target date for this proposal is late September 2015.

Expectations: About 2.11 million visits (85% of 2.47 million visits) from Baseline Cadence ([enigma_1189](#)) were allocated to WFD cadence. Here we expect that all of these 2.47 million visits will be allocated to WFD cadence.

Analysis Results: This simulated cadence is named [ops2_1098](#). Compared to the Baseline Cadence [enigma_1189](#):

1. The total number of visits is close to the expected value: 2.45 million. The minimum number of visits per field for the 2,293 WFD fields in Baseline Cadence is 968 for this simulation, compared to 898 for Baseline Cadence.
2. The median number of visits per night and the mean slew time are essentially the same as for Baseline Cadence (810 vs. 815 and 7.2 sec vs. 6.9 sec).
3. The median seeing, sky brightness and airmass in the r and i bands are essentially the same as for WFD fields in Baseline Cadence.
4. The median trigonometric parallax and proper motion errors are improved by about 8%, with improvements commensurate with the increase in the number of visits.
5. This simulation also shows observing bias towards west (that is, additional special programs in [enigma_1189](#) are not responsible for this bias).

Conclusions: [ops2_1098](#), using only uniform cadence proposal, delivered 99.2% of the number of visits obtained by Baseline Cadence. Therefore, *the “filler” aspect of other proposals does not have a major impact on the surveying efficiency*. The minimum number of visits per field for the 2,293 WFD fields in Baseline Cadence is 968 (the SRD design value is 825 and the stretch goal value is 1000). Although the sky coverage of these 2293 fields is about 18,000 sq.deg., their cumulative area is 22,000 sq.deg. With proper dithering, the effective number of visits could be increased to $968 \times 22 / 18 = 1183$ (or the WFD area increased from 18,000 sq. deg.; see analysis of [ops2_1092](#) below). This increase is an improvement of 43% relative to the SRD design specification of 825 visits over 18,000 sq.deg. However, note again that there are no other programs in this simulation (i.e., if other programs were allocated 10% of the observing time, the implied overall “over-performance” in the number of visits would be about 30%).

[ops2_1092](#)

A Pan-STARRS-like observing strategy.

Motivation and description: ”Pan-STARRS-like cadence attempts to apply a uniform cadence strategy throughout the survey region, which is maximized and defined by $\text{Dec} < +15 \text{ deg}$ (about 27,400 deg²). The maximum acceptable airmass is kept at its default value of 1.5 (which excludes fields with $\text{Dec} < -78 \text{ deg}$ and $\text{Dec} > +18 \text{ deg}$). This simulation utilizes uniform cadence and no other proposal, and requires pairs of visits as in Baseline Cadence.

Expectations: The total number of visits should be roughly the same as in Baseline Cadence, but spread over a 42% larger sky area (3,255 fields instead of 2,293), with fewer visits per field.

Analysis Results: This simulated cadence is named [??](#). Compared to the Baseline Cadence [enigma_1189](#):

1. The total number of visits is 2.47 million, and essentially identical to the number of visits in Baseline cadence.
2. The mean number of visits per field is 758.5, which is 98% of the number of visits for WFD fields obtained by Baseline Cadence (but here the sky area is 42% larger).
3. The median number of visits per night and the mean slew time are essentially the same as for Baseline Cadence.
4. The median seeing, sky brightness and airmass in the r and i bands for WFD fields are essentially the same as in Baseline Cadence.
5. The median trigonometric parallax and proper motion errors show uniform behavior over the entire enlarged area (see [Figure 2.11](#)), with the values similar to those obtained for Baseline Cadence.
6. This simulation also shows observing bias towards west.

Due to increased sky area, which samples regions that can never achieve low airmass, the median coadded depth is about 0.15 mag shallower for this simulation than for Baseline Cadence. As a result, the counts of galaxies per unit area down to a fixed SNR would decrease by about 15-20%. At the same time, the area outside the Galactic plane is increased by about 30%, and thus the total number of galaxies would be increased by about 10%, compared to WFD fields in Baseline Cadence. However, the increased median airmass also results in larger seeing, especially for the borderline regions, as illustrated in [Figure 2.12](#). The increased median seeing would decrease the number of galaxies effectively resolved for weak lensing by about 3-5%. In addition, the additional area has somewhat larger extinction due to interstellar dust which further decreases the galaxy counts (this impact of dust extinction is not yet implemented in MAF). As a result of these effects, the two strategies result in similar weak lensing galaxy samples.

Conclusions: When only the Universal Cadence proposal is employed, the survey area could be increased by about 40%, while still delivering the mean number of fields at the level of 98% of that in Baseline Cadence (or 92% of the SRD design value of 825). Hence, simulations [ops2_1092](#) and [ops2_1098](#) demonstrate that the “survey reserve”, relative to the Universal Cadence design specifications from the SRD, can be used to i) increase the number of visits per field over the WFD area, or ii) increase the surveyed area while keeping the number of visits per field statistically unchanged, or iii) increase both area and the number of visits, and/or iv) execute additional programs (the current baseline).

[ops2_1093](#)

Only Universal Cadence, no visit pairs.

Motivation and description: The main goal of this simulation was to assess the impact of the requirement for visit pairs on the survey efficiency (Baseline Cadence requests two visits per night to the same field, separated in time by about an hour, and driven by asteroid orbit determination). It is plausible that the removal of this requirement could result in a more efficient survey. In order

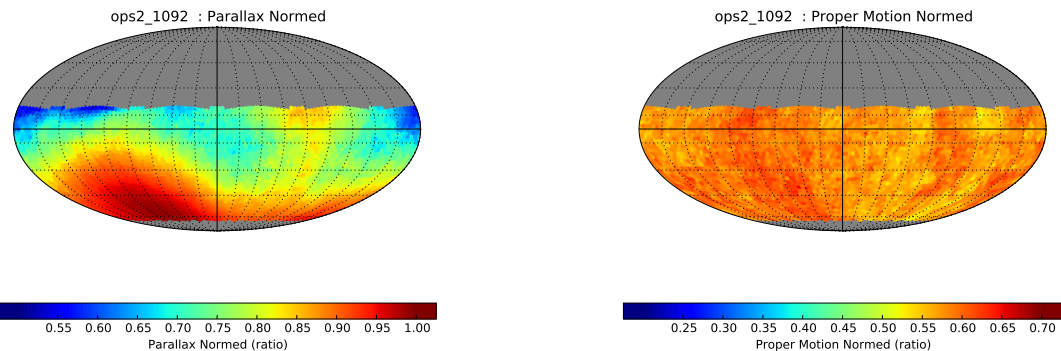


Figure 2.11: The trigonometric parallax errors (left) and proper motion errors (right) for simulated cadence ops2_1092 (“Pan-STARRS-like” cadence), normalized by the values for idealized perfectly optimized cadence, are shown in Aitoff projection of equatorial coordinates (compare to Figure 2.3).

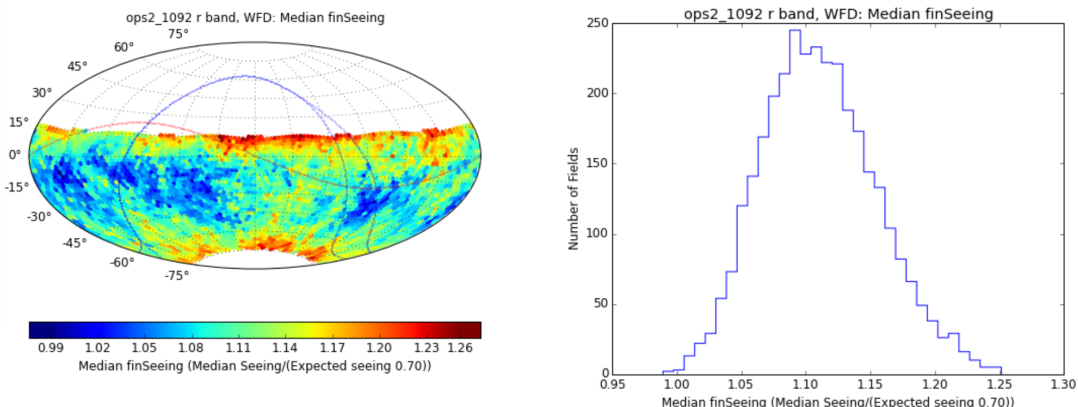


Figure 2.12: The median seeing in r filter, for simulated cadence ops2_1092 (“Pan-STARRS-like” cadence), normalized by expected value (0.70). Note that fields with the most positive and most negative declination have on average larger values. For comparison, the median normalized seeing for WFD fields in Baseline Cadence is 1.08, with a negligible fraction of fields with values above 1.18.

to allow as simple analysis as possible, only the Universal Cadence proposal is requested. Hence, this simulation should be directly compared to simulation [ops2_1098](#).

Expectations: If the requirement for visit pairs decreases surveying efficiency, then this simulation should deliver more than 2.45 million visits delivered by [ops2_1098](#).

Analysis Results: This simulated cadence is named [ops2_1093](#). Compared to [ops2_1098](#):

1. The total number of visits is 2.45 million, identical to [ops2_1098](#).
2. The median slew time, and the median coadded depth and seeing in the r band are essentially identical, too.
3. The median airmass in the r band of 1.26 is a bit higher than 1.20 obtained for [ops2_1098](#).

4. The median fraction of revisits faster than 30 minutes of 0.35 is smaller than 0.39 for [ops2_1098](#), and is consistent with the absence of pair contributions (that is, such revisits are due to field edge overlaps, and unintentional revisits, in case of [ops2_1093](#)).

Conclusions: The comparison of this simulation and [ops2_1098](#) shows that requiring pairs of visits (in a given observing night) does not result in an appreciable loss of surveying efficiency. Indeed, pairs of visits result in a better short-timescale coverage that would enhance many types of time-domain science (and, of course, it's crucial for asteroid science).

`kraken_1032`

Baseline Cadence, but with no visit pairs.

Motivation and description: The main goal of this simulation was to assess the impact of the requirement for visit pairs on the survey efficiency. Instead of the idealized case above which compared only the Universal Cadence proposal fields, in this more realistic case *all proposals from Baseline Cadence are executed*. Hence, this simulation should be compared to Baseline Cadence ([enigma_1189](#)).

Expectations: A slight, or no, increase in surveying efficiency and thus the total number of visits is expected when compared to Baseline Cadence.

Analysis Results: This simulated cadence is named [kraken_1032](#). Compared to [enigma_1189](#),

1. The total number of visits is 2.53 million, or 2.4% more than in Baseline Cadence.
2. The mean slew time is 5.8 sec, or 16% shorter than for Baseline Cadence. This decrease in the mean slew time implies an efficiency increase of 2.8% and explains the actual 2.4% improvement implied by the total number of visits. Note that this simulation has the shortest mean slew time of all simulations investigated here (the nominal shortest slew and settle time is about 4.5 sec).
3. The median airmass in the r band is slightly larger for this simulation than for Baseline Cadence: 1.29 vs. 1.23.

Conclusions: Unlike the comparison of [ops2_1093](#) and [ops2_1098](#), here the removal of visit pair requirement results in a 16% shorter mean slew time and consequently in 2.4% more visits.

`ops1_1163`

Baseline Cadence, but with 33% shorter exposure time.

Motivation and description: The optimal exposure time per visit for the main survey, in the limit of a single value for all bands and at all times, is in the range of about 20–60 seconds (see Section 2.2.2 in the LSST overview paper, arXiv:0805.2366, version 3.1). This simulation investigates the effect of decreasing the exposure time per visit to 20 seconds (from its nominal value of 30 seconds). The shorter exposure time results in 0.22 mag shallower faint limit per visit (the

effect is larger in the *u*-band, see [ops1_1162](#)).

Expectations: The total number of visits is expected to increase by about 50%, compared to [enigma_1189](#), to 3.70 million, for the same survey efficiency. However, the shorter exposure time will have a significant impact on the survey efficiency: assuming a slew time of 7 sec, the efficiency drops from 73% to 65% (comparing $30/(30+4+7)$ vs. $20/(20+4+7)$). Therefore, the expected increase in the number of visits is about 32% and the expected number of visits is 3.2 million.

Analysis Results: This simulated cadence is named [ops1_1163](#). Compared to Baseline Cadence:

1. The total number of visits is 3.29 million, representing an increase of 33% that is very close to the expected value of 32%.
2. The median number of visits per night is 1091, or about 34% more than for Baseline Cadence. The total open shutter time is 11% smaller for this simulation, and easily understood as due to expected 11% decrease due to smaller surveying efficiency (the mean slew time is practically the same as in Baseline Cadence, 6.8 sec vs. 6.9 sec).
3. The main survey (WFD, 18,000 sq. deg.) fields received 32% more visits than in Baseline Cadence. The increase in the minimum number of visits over that area is 7% (from 898 to 961). In addition, another 1,000 sq. deg. (6% of the nominal WFD) area has more than 961 visits.
4. Most other performance parameters are essentially unchanged: the fraction of visits spent on the main survey (84% vs. 85%), the median seeing in the r band (0.78 arcsec vs. 0.77 arcsec), and the median airmass (1.24 vs. 1.23).

Conclusions: The comparison of [ops1_1163](#) and [enigma_1189](#) simulations demonstrates that the effect of shorter exposures can be easily understood using simple efficiency estimates. With the visit exposure time is decreased from 30 sec to 20 sec, the surveying efficiency and the total open shutter time drops by ~10%, while the number of (shorter exposure time) visits (for all proposals) increases by 33%.

[ops1_1164](#)

Baseline Cadence, but 100% longer exposure time.

Motivation and description: This simulation investigates the effect of increasing the exposure time per visit to 60 seconds (from its nominal value of 30 seconds). The longer exposure time results in 0.38 mag deeper faint limit per visit (the effect is larger in the *u*-band, see [ops1_1162](#)).

Expectations: The total number of visits is expected to decrease by about a factor of 2 in case of no significant impact on the survey efficiency. However, the longer exposure time improves efficiency by a factor of $2*(34+7)/(64+7)-1=15\%$, and thus the expected total number of visits is $0.5*1.15 = 58\%$ of the the number of visits in Baseline Cadence (assuming the same mean slew time of 7 seconds).

Analysis Results: This simulated cadence is named [ops1_1164](#). Compared to Baseline Cadence:

1. The total number of visits is 1.42 million or 58% of the visits obtained with Baseline Cadence, and the total open-shutter time is 15% higher than for Baseline Cadence. Both results are in good agreement with above expectations.
2. The median number of visits per night is 472, or 58% of the value obtained with Baseline Cadence. The mean slew time is 0.1 sec longer than that obtained with Baseline Cadence.
3. This simulation has significantly different time allocation per proposal, compared to Baseline Cadence: 69% spent on the Universal proposal (vs. 85%) and 18% spent on the North Ecliptic proposal (vs. 6%) (with smaller and less important differences for other proposals). Because of these differences, *the results of this test may not be very robust*.

Conclusions: Simple estimates of the total number of visits and the improvement in efficiency are in good agreement with delivered values. Of course, the increased efficiency comes at the cost of fewer visits, which is disadvantageous for time-domain science.

Note to OpSim team: **this simulation should be repeated** with the requested number of visits per field set to 60% of the values used for Baseline Cadence for **all** proposals. For example, instead of (75, 105, 240, 240, 210, 210) for Universal-18-0824B proposal, (45, 63, 144, 144, 126, 126) should be used. This way the additional observing time due to improved surveying efficiency will be allocated to all proposals, including Universal Cadence. *This simulation will be repeated with the same North Ecliptic Spur proposal as used for [enigma_1189](#), and with the modified requested number of visits.*

ops1_1162

Baseline Cadence, but with doubled u-band exposure time.

Motivation and description: The read-out noise in the u band is not negligible compared to the background noise as in other bands, due to darker u band sky. The current best estimates for survey performance (see Table 2 in the LSST overview paper, arXiv:0805.2366, version 3.1) indicate that the *coadded* depth in the *u* band could be improved by 0.24 mag by increasing the exposure time per visit from 30 seconds to 60 seconds⁵ (assuming the same total exposure time, which implies a decrease in the number of visits by a factor of two). To keep the total exposure time in the *u* band unchanged, the requested number of visits in this simulation is decreased by a factor of 2 relative to Baseline Cadence specification.

Expectations: The total exposure time in the *u* band should remain unchanged. The single visits depth should be 0.38 mag deeper due to twice as long exposure time (the gain of 0.24 mag related to read-out noise effects is not yet implemented in the OPSIM code so MAF outputs may be a bit

⁵In the background-limited case, a factor of two increase of the exposure time results in 0.38 mag deeper data. Since in the *u* band the read-out noise is not negligible compared to the background noise, the total noise increases by less than a factor of $\sqrt{2}$ and there is an extra depth improvement of 0.24 mag (see eq. 7 and Table 2 the overview paper). Conversely, when exposure time is shorter than 30 seconds, there is an extra penalty of 0.16 mag, in addition to a loss of depth of 0.22 mag due to shorter exposure time in the limit of negligible read-out noise.

confusing).

Analysis Results: This simulated cadence is named [ops1_1162](#). Compared to Baseline Cadence ([enigma_1189](#)):

1. The total number of visits is 2.21 million or 89.5% of the Baseline Cadence values. The fraction of time allocated to the main survey is 77% vs. 85% for Baseline Cadence, and for the NE spur proposal 14% vs. 6%. Given that the NE spur proposal was different than for [enigma_1189](#), this simulation needs to be rerun.

Conclusions: The u band exposure time can be increased from 30 seconds to 60 seconds without a significant impact on the survey efficiency. This change would result in a gain of about 0.2 mag in the coadded depth. However, the number of visits in the u band would be decreased by about a factor of two, with a negative impact on time-domain science. *This simulation will be repeated with the same North Ecliptic Spur proposal as used for [enigma_1189](#) to make conclusions more robust and precise.*

[ops1_1161](#)

Baseline Cadence, but with doubled u -band exp. time and Baseline NE Spur.

Motivation and description: This simulation is similar to [ops1_1162](#), which increased the exposure time per visit in the u -band from 30 seconds to 60 seconds, with the requested number of visits decreased by a factor of 2. This change resulted in a gain of about 0.24 mag in the coadded depth. Since the number of u band visits in [ops1_1162](#) was decreased by about a factor of two, with a negative impact on time-domain science, this simulation does not change the nominal requested number of visits per field. Hence, the coadded depth in the u band in this simulation would be improved by about 0.6 mag.

Expectations: Given that about 5% of all visits are allocated to the u band, the total number of visits may decrease by up to about 5%, resulting in about 0.03 mag shallower data in bands other than u band.

Analysis Results: This simulated cadence is named [ops1_1161](#). Compared to Baseline Cadence ([enigma_1189](#)):

1. The total number of visits is 2.36 million or 95.5% of the Baseline Cadence values. The fraction of time allocated to the main survey is 78% vs. 85% for Baseline Cadence, and for the NE spur proposal 13% vs. 6%. Given that the NE spur proposal was different than for [enigma_1189](#), this simulation needs to be rerun.

Conclusions: When the u band exposure time is increased from 30 seconds to 60 seconds, and the number of visits is kept unchanged, the single-visit and coadded depths would be improved by 0.6 mag. This improvement would come at the expense of about 6% fewer visits in other bands (with about 0.03 mag shallower coadded depths).

ops2_1096

Only Universal Cadence, with relaxed airmass limit.

Motivation and description: What is the effect of changing the airmass limit from 1.5 to 2.0? To avoid complicated analysis, use only Universal Cadence proposal and thus compare to [ops2_1098](#).

Analysis Results: This simulated cadence is named [ops2_1096](#). Compared to [ops2_1098](#), it collected 98.0% visits. This fraction is identical to the loss of efficiency due to slightly longer mean slew time: 8.1 sec vs. 7.2 sec. In addition, [ops2_1096](#) has much worse airmass distributions than [ops2_1098](#), extending to the allowed maximum of 2.0. For example, the median for the r band and WFD fields is 1.33, compared to 1.20 for [ops2_1098](#).

Conclusions: This simulation confirms that it's a bad idea to relax airmass limit: as a result, the airmass distribution always widens. In addition, relaxed airmass limit tends to result in a longer mean slew time. For a given proposal, the airmass limit has to be as tight as possible, while still allowing observations of all requested fields.

ops2_1097

Only Universal Cadence, with stringent airmass limit.

Motivation and description: What is the effect of changing the airmass limit from 1.5 to 1.3? To avoid complicated analysis, we use only the Universal Cadence proposal and thus compare to [ops2_1098](#).

Analysis Results: This simulated cadence is named [ops2_1097](#). Compared to [ops2_1098](#), it collected essentially the same number of visits. The mean slew time is also essentially unchanged (7.4 sec vs. 7.2 sec). The airmass distributions is improved compared to [ops2_1098](#). For example, the median for the r band and WFD fields is 1.14, compared to 1.20 for [ops2_1098](#). The limiting coadded depth in u and g bands is about 0.1 mag deeper than for Baseline Cadence.

Conclusions: It is possible to achieve the same surveying efficiency with much more stringent airmass limit than 1.5, which was used in most simulations to date. *Given this encouraging behavior, an analogous experiment should be executed for Baseline Cadence (i.e. a simulation like [enigma_1189](#), with airmass limit for the main survey set to 1.3) – after the “Western bias” is fixed’.*

Go to: • [the start of this section](#) • [the start of the chapter](#) • [the table of contents](#)

2.4 Analysis of NEO/PHA completeness

Continuing our analysis of some alternatives to the Baseline Cadence, we now investigate a suite of observing strategies for their suitability in supporting Near-Earth Object (NEO) science. As in the previous section, these OPSIM databases are all available for further testing with science-based MAF metrics.

The U.S. Congress has given a mandate to NASA to implement a Near-Earth Object (NEO) Survey program to detect, track, catalogue, and characterize the physical characteristics of near-Earth objects equal to or greater than 140 meters in diameter⁶. The goal is to achieve a completeness of 90%. In recent practice, adopted here, the completeness is evaluated for a subset of NEOs called Potentially Hazardous Asteroids⁷ (PHA), with $H \leq 22$, where H is the absolute magnitude⁸ in the Johnson's V band. While LSST is very competitive in this context, it will also enable analysis of many other Solar System populations (e.g. main-belt asteroids, comets, trans-Neptunian objects). Nevertheless, we focus analysis here on NEOs/PHAs completeness.

Motivation and description:

The baseline cadence implements observing strategy with two visits to a field obtained per night, separated in time by a fraction of an hour. Motivation for a simulation that does require pairs of visits is to gauge its impact on the survey efficiency and other performance parameters. Motivation for simulations with more than two visits to a given field per night is to investigate the feasibility of a more robust approach to linking individual detections into a plausible object track. Although detailed simulations of the performance of image differencing software and orbital determination software indicate that two visits per night are likely to be sufficient, quantitative analysis of other strategies is clearly within the purview of the cadence optimization program. Five simulations are analyzed in this section:

ops2_1094

NEO test: no request for pairs of visits.

enigma_1257

NEO test: pairs of visits (as in the Baseline Cadence). .

enigma_1258

NEO test: triplets of visits.

enigma_1259

NEO test: quads of visits.

Expectations: Analysis of all simulations is repeated three times, with different conditions for what constitutes an object's "discovery": two, three or four detections per night are required, together with at least three such sequences in a 15-day window. When only two detections per

⁶See <http://www.gpo.gov/fdsys/pkg/PLAW-109publ155/pdf/PLAW-109publ155.pdf>

⁷ Potentially Hazardous Asteroids (PHAs) are defined as asteroids with a minimum orbit intersection distance (MOID) of 0.05 AU or less.

⁸Absolute magnitude is the magnitude that an asteroid would have at a distance of 1 AU from the Sun and from the Earth, viewed at zero phase angle. This is an impossible configuration, of course, but the definition is motivated by desire to separate asteroid physical characteristics from the observing configuration.

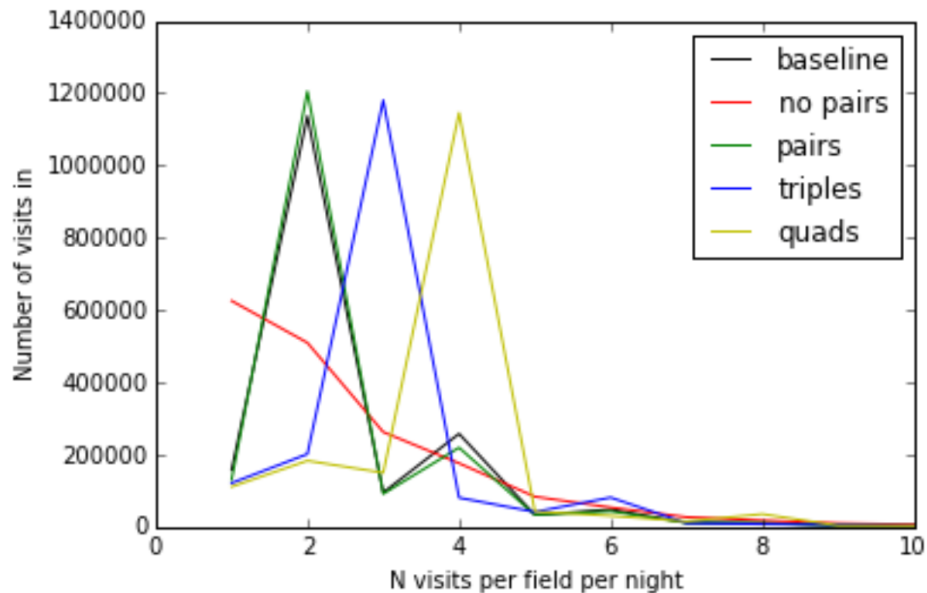


Figure 2.13: The distribution of the number of visits used for nightly sequences of length given on the horizontal axis. Only *griz* bands are used. Note that even “no pairs” simulation ([ops2_1094](#)) includes multiple visits. The highest peak is at the requested number of visits in a sequence.

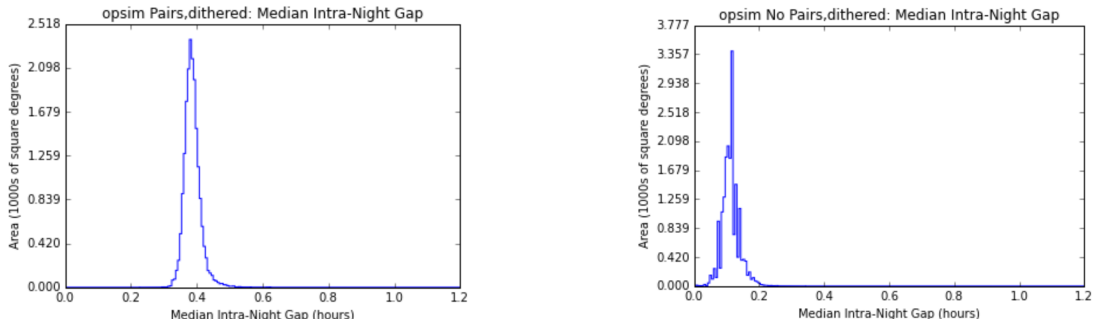


Figure 2.14: The comparison of the median intra-night gap distributions for Baseline Cadence (left) and simulation [ops2_1094](#), which did not request pairs of visits per night. Despite no need for pairs, simulation [ops2_1094](#) produced them “spontaneously”, as well as longer sequences (see Figure 2.13). The mean field revisit time is much shorter (about 6 minutes, see the right panel) than for Baseline Cadence (22 minutes).

night are required, a modest decrease in PHA completeness is expected for simulations that request more than two visits per night because some visits “don’t live up to their full potential”. On the other hand, when more than two detections per night are required, a naive expectation is that PHA completeness for runs with fewer requested visits will drop significantly.

Analysis Results: First, we emphasize that “requested” is not the same as “delivered”: even the “no pairs” simulation [ops2_1094](#) ends up having multiple visits in a given night to the same fields, and when multiple visits per night are requested, not all fields get to have completed sequences. The statistics of how many fields are combined into sequences of a given number of visits is shown in Figure 2.13. As evident, the highest peak is at the requested number of visits in a sequence, but not

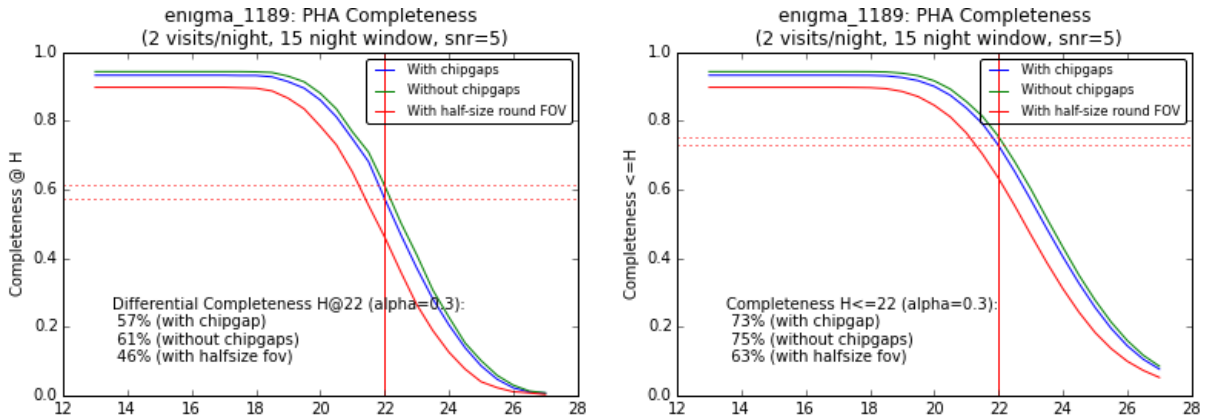


Figure 2.15: The PHA completeness for [enigma_1189](#), as a function of the object’s absolute visual magnitude H on the horizontal axes (left: differential completeness at a given H ; right: cumulative completeness for all objects brighter than a given H). The completeness for $H \leq 22$ NEOs (those with diameters larger than 140m) for this simulation is 73% (blue line in the right panel). The panels also show the effects of ignoring chip gaps (a 2% effect for cumulative $H \leq 22$ completeness) and of decreasing the field-of-view size to a half (i.e. to 4.8 sq. deg; a 10% effect).

:

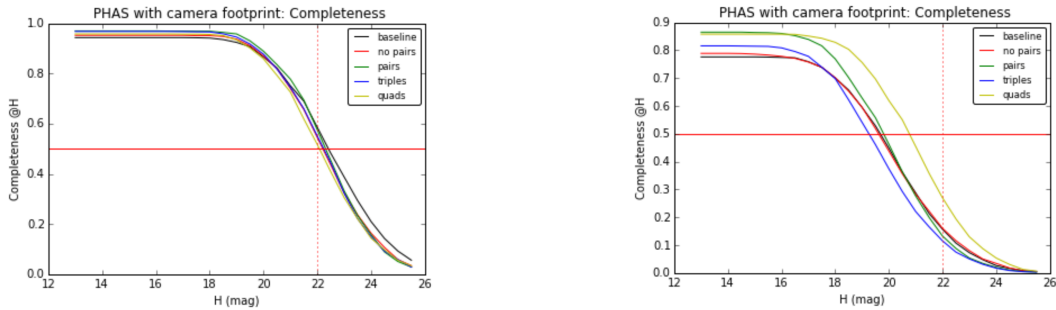


Figure 2.16: The comparison of differential PHA completeness for the five analyzed simulations when requiring two detections per night (left) and four detections per night (right). With two detections per night, all simulations perform similarly but when four detections per night are required, the simulation that has the largest number of such sequences (see [Figure 2.13](#)), performs the best although at an inferior level compared to the left panel (see also [Figure 2.15](#)).

all visits are incorporated into requested sequences: some are in both shorter and longer sequences. In particular, even “no pairs” simulation includes multiple visits to some fields, essentially because the current version of the algorithm is not told not to do so. As illustrated in [Figure 2.14](#), such revisits typically happen within 10 minutes from the first visit. This (unintended) behavior implies that the naive expectation above is probably incorrect, as we discuss in more detail below.

For baseline reference, the PHA completeness for [enigma_1189](#) is shown in [Figure 2.15](#). The baseline cadence achieves a cumulative completeness of 73% for $H \leq 22$ PHAs. This cumulative completeness for $H \leq 22$ is 17% higher than differential completeness at $H=22$ of 56% due to increasing completeness towards smaller H (larger objects). Both differential and cumulative completeness are relevant metrics: the former provides more insight in the behavior of a particular simulation, while the latter is a metric given to NASA by the U.S. Congress. Analysis of results illustrated in

Figure 2.16 can be summarized as follows:

- When NEO discovery algorithm requires pairs of visits, all runs have very similar PHA completeness, with quads run only about 2% lower than the baseline (a differential completeness of 56% at H=22 for [enigma_1189](#))
- When NEO discovery algorithm requires 4 detections per night, the simulation with quads achieves a differential completeness of about 27% at H=22, or about 30% lower completeness than Baseline Cadence.
- When NEO discovery algorithm requires 4 detections per night, Baseline Cadence reaches a differential completeness of about 15% at H=22 (some quads are unintentionally produced by chance, see [Figure 2.13](#)).
- When NEO discovery algorithm requires 3 detections per night, runs which requested triples and quads achieve a differential completeness of about 40% at H=22 (corresponding to a cumulative completeness of about 57% for H \leq 22).

Therefore, going from pairs of visits to triples (both for cadence and NEO detection) reduces completeness (both differential and cumulative) for PHAs with H \leq 22 by about 15-20% (and by about 30% for quads).

Impact on other science programs

The impact of requesting sequences with 3 or 4 visits to the same field on other science programs is not yet analyzed in detail. The impact on static science should be minimal, except perhaps for a bit worse behavior of various systematic errors (because fewer nights, with their observing conditions, are sampled).

For time-domain science, the mean revisit time will increase by about 50% if we go from pairs to triples, and by about a factor of two for quads. This change will have a negative impact on time-domain science programs based on SNe, variable stars, and transient objects, which remains to be quantified.

Go to: • [the start of this section](#) • [the start of the chapter](#) • [the table of contents](#)

2.5 Ongoing and Future Work

2.5.1 Ongoing: Extended time-domain metrics

A number of very sophisticated time-domain metrics have been implemented in recent MAF development cycle (and some were contributed by the community) but they have not been systematically run yet on all available simulations. Time-domain metrics, together with metrics for analyzing special programs (e.g. deep drilling programs), will be further expanded in the next development cycle.

2.5.2 Ongoing: Rolling Cadence experiments

Analysis of a few prototype runs (`ops2_1102`, `enigma_1260`, `enigma_1261`), which implemented the so-called “swiss cheese rolling cadence” is in progress.

2.5.3 Future work

Based on analysis presented here, several recommendations for further cadence exploration, can be made.

1. Further optimization of the main survey (e.g., exposure time in general, and u band exposure time in particular; fixing western bias; optimizing airmass limit and sky coverage; investigations of variable, perhaps SNR-driven, exposure time).
2. Exploration and optimization of temporal sampling function in general, and of Rolling Cadence in particular.
3. NEO completeness studies: what would it take for LSST to reach 90% completeness for 140m and larger NEOs? Based on previous analysis, directions to explore are deeper visits along the Ecliptic and longer survey duration (about 12 years).
4. Exploration of extending the main survey to the Galactic plane (per A. Gould’s proposal, arXiv:1304.3455) and further optimization of Galactic plane and Bulge science programs.
5. Optimization of LMC/SMC coverage (and somewhat less importantly, the South Celestial Pole coverage).
6. Deep drilling optimization (detailed analysis of existing proposals; investigation of gains from going to a larger observing time allocation, e.g. 20%).
7. Twilight short-exposure time observing (per internal Stubbs proposal).
8. Planning commissioning observations (e.g. the tension between going wide to enable self-calibration and dense temporal sampling to obtain various light curve templates and fine tune image differencing and multi-epoch data processing and data analysis software tools).
9. Dynamic cadence explorations (the main goal at this time is to answer: are our tools good enough to act and react swiftly and robustly in operations?).

Go to: • [the start of this section](#) • [the start of the chapter](#) • [the table of contents](#)

2.6 Summary

The most important conclusion of this study is that the upper limit on possible scheduling efficiency improvements for Baseline Cadence is close to 6%. This conclusion is by and large based on the fact that the mean slew time for (candidate) Baseline Cadence is 6.9 sec, and thus only slightly larger than the design specifications for the system slew and settle time of 4.5 sec. Nevertheless, there are a number of features to understand, and some to fix, and there is substantial optimization

potential in temporal sampling functions and further optimization of the sky area and observing strategy details, that can result in enhanced science even with the same integrated open-shutter time (e.g. by obtaining deeper data through an improved sampling of observing conditions).

The main other questions addressed here are:

1. *By what factor could we exceed the SRD design specification for the number of visits if only Universal Cadence proposal was implemented?*

A simulation that only implemented Universal Cadence proposal exceeded the design specification for the number of visits by about 40% (over the design specification for the sky area of 18,000 sq.deg.)

2. *By what factor could we exceed the SRD design specification for the sky coverage if only Universal Cadence proposal was implemented with the design specification for the number of visits?*

This Pan-STARRS-like strategy results in about 40% larger sky coverage (about 25,000 sq.deg.), with the mean number of visits at 92% of the design specification. The total number of visits is the same as for Baseline Cadence, implying similar surveying efficiency.

Therefore, the available “margin” relative to the SRD design specifications for the main survey is equivalent to about 30-40% larger sky coverage, or about 30-40% more visits per field. The SRD assumes that 10% margin will be available for other programs. The implied “survey reserve”, relative to the Universal Cadence design specifications from the SRD, can be used to:

- a) increase the number of visits per field over the WFD area, or
- b) increase the surveyed area while keeping the number of visits per field statistically unchanged, or
- c) increase both area and the number of visits, and/or
- d) execute additional programs (the current baseline).

3. *What is the effect of auxiliary proposals on surveying efficiency?*

A comparison of simulations which only implemented Universal Cadence proposal to those that included all other programs did not show a significant change of efficiency (older simulations, not analyzed here, showed increases in surveying efficiency of up to about 3% due to shorter slewing time).

4. *What is the effect of visit pairs on surveying efficiency?*

Relinquishing the visit pair requirement results in up to 2-3% improvement of the surveying efficiency. The impact on some time-domain science would be positive, while for NEO and main-belt asteroid science it would be strongly negative.

5. *Can the effects of variations of the visit exposure time on surveying efficiency be predicted using simple efficiency estimates?*

Simple estimates based on comparing exposure (open shutter) and total visit times are in good agreement with simulations. Decreasing the visit exposure time to 20 seconds decreases the total open shutter time by 10%, and increasing it to 60 seconds increases the total open shutter time by 16%, relative to Baseline Cadence and standard exposure time of 30 seconds. The number of visits changes by factors of 1.35 and 0.58.

6. *What are the effects of doubling the exposure time only in the u band?*

The effect of doubling the exposure time only in the u band, while simultaneously halving the number of requested visits, has no significant effect on the survey efficiency.

The effect of doubling the exposure time only in the u band, with the number of requested visits unchanged, is a decrease in the number of visits in other bands by about 6%.

7. *What is the impact of hard airmass limit, $X < 1.5$, on the surveying efficiency?*

It is a very bad idea to relax airmass limit! It is possible to achieve the same surveying efficiency with much more stringent airmass limit than 1.5, which was used in most simulations to date.

Go to: • [the start of this section](#) • [the start of the chapter](#) • [the table of contents](#)

3 A Solar System Census

Lynne Jones, David Trilling, Mike Brown, Eric Christensen

3.1 Discovering Solar System Objects

Discovering, rather than simply detecting, small objects throughout the Solar System requires unambiguously linking a series of detections together into an orbit. The orbit provides the information necessary to scientifically characterize the object itself and to understand the population as a whole. Without orbits, the detections of Solar System Objects (SSOs) by LSST will be of limited use; objects discovered with other facilities could be followed up by LSST, but almost the entire science benefit to planetary astronomy would be lost.

Therefore, the primary concern regarding the Solar System is related to the question “Can we link detections of moving objects into orbits?”. This requirement poses varying levels of difficulty as we move from Near Earth Objects (NEOs) through the Main Belt Asteroids (MBAs) and to TransNeptunian Objects (TNOs) and Scattered Disk Objects (SDOs), as well as for comets and for other unusual but very interesting populations such as Earth minimoons.

discuss specific challenges for each population; TNOs and SDOs are relatively easy, MBAs are very numerous, NEOs are hard because of speed, comets and minimoons are hard because of nongravitational forces

Much of the answer to this question comes down to the performance of various pieces of LSST Data Management software. In particular, the false positive rate resulting from difference imaging, the compute limitations of the Moving Object Processing System (MOPS) to extend to high apparent velocities, and the capability to unambiguously determine if a linkage is ‘real’ or not via orbit determination (done as part of MOPS). Additional concerns are related to how well observations widely separated in time can be linked into the ‘discovery’ orbits (i.e. if we have a discovery in year 1, but do not detect the object again until year 3, could these observations be linked?). The answers to these questions range beyond the limits of the OpSim simulated surveys, but bear on the observing strategy requirements for discovering Solar System Objects.

describe current minimum observation requirements for existing surveys, describe current expected requirements for MOPS, describe current effort to understand if MOPS requirements are realistic in LSST context

If we assume various detection requirements, ranging from XXX to the minimum MOPS requirements, we can characterize the performance of available simulated surveys in terms of their expected detection rates for various known populations.

describe completeness metrics for NEOs/MBAs/TNOs/etc - known populations. what do we do about unknown populations?

Beyond this basic but absolutely critical requirement to actually discover SSOs across the Solar System, we can start to look at other science goals: detecting activity, determining colors for moving objects, and measuring shapes and spin states for objects.

describe requirements and challenges for these; why colors are hard, how many objects will we actually be able to determine shape/spin for, how lightcurves may differ from shape/spin

Note: take a look at https://github.com/rhiannonlynne/MafSSO/blob/master/SSO_Analysis.ipynb (an extremely messy ipython notebook, but starting to point at some of the ideas I have for metrics – let's expand on this)

Go to: • [the start of this section](#) • [the start of the chapter](#) • [the table of contents](#)

4 The Galaxy

Will Clarkson, Kathy Vivas, Peregrine McGehee, and others to follow

4.1 Introduction

LSST will significantly advance Milky Way science, on lengthscales from the galactic halo and local volume, right down to sensitive surveys for faint nearby objects to uncover the true state of the Solar Neighborhood. Much more detail about most of these science cases, and specific science questions to be answered, can be found in the LSST Science Book (particularly chapters 6 and 7) and Ivezic et al. (2008 arXiv 0805.2366, in particular Sections 2.1.4 and 4.4); in this chapter we (aim to) present metrics that will allow various observing strategies to be quantitatively assessed in terms of their impact on science cases falling under the general rubric of “The Milky Way.”

Our intention is to decouple the technical issue of coverage on-sky from the science accomplished; for example, if a science case includes regions both inside and outside of the “Wide-Fast-Deep” (WFD) survey, then the metric for a particular science case should produce a quantitative assessment of the science outcome no matter what the distribution of pointings on the sky actually was. As a result, issues to do with areal coverage (for example, whether a census of all nearby brown dwarfs that neglects “low-latitude” fields towards the inner Galaxy, is scientifically unacceptable) should in theory fall out as a result of the metrics assessment process.

This chapter is organized as follows. In Section 4.2 we point out some general considerations specific to much of the Milky Way science area that we recommend MW scientists bear in mind when considering metrics. Because of the large diversity of science cases, Section 4.3 presents the essential aspects of each science case, expressed in terms of observational goals and tracer population. Science cases dominated by in-plane observations are presented first in Table X, as the observing strategy for in-plane observations is currently far from resolved. Then Table Y in this section presents the vital statistics for science cases covered by Wide-Fast-Deep. Sections 4.4-?? then present the metrics and their evaluations for MW science cases. Finally, section 4.10 points the way to anticipated future improvements to this living document in light of expected precursor data.

4.2 Some general considerations for Milky Way metrics

Many of the Milky Way science cases involve Galactic Plane observations almost exclusively. At the time of writing (late August 2015), even the broad parameters of in-plane observations remain to be decided (for example the number of exposures per-filter).

Before launching into the specifics of metrics per-science case, we point out some general factors that are likely to obtain for Milky Way science (all over the sky), which we encourage the reader to incorporate into their thinking when considering possible metrics. [Language will change as metrics are produced.]

We currently envisage these to be implemented as methods that a given science metric would call as part of its chain of evaluation.

1. Observing the “foreground:” By the standards of LSST’s Wide-Fast-Deep survey, many if not most of the objects of interest to Milky Way science are close enough that they will saturate under the Wide-Fast-Deep cadence, or will be impacted by bright foreground objects. With LSST’s saturation limit at 15 second exposure in the neighborhood of $r \sim 17$ (**need confirmation!**), metrics should include in their chain of evaluation, some sensitivity to at least the following implications of foreground observation:

- The upper limit on brightness for which measurements can be made that are sufficiently accurate for a given science case;
- The loss in discovery efficiency due to charge bleeds from objects unrelated to the targets for a given science case.

The discovery efficiency metric may correlate with existing first-order metrics already presented elsewhere; for example, the range of position angles for a field will likely correlate with the discovery efficiency in the presence of charge bleeds, as a wider range of position-angles will reduce the number of exposures in which a given faint target lies underneath the charge bleed from one very bright foreground object. Or, a given dithering strategy might increase discovery efficiency due to pathological, very close, very bright objects being moved into chip-gaps during some of the dithers.

(One suggested observing configuration for the Plane to mitigate the impact of both of these factors, is to split the exposures per pair into unequal-length exposures; perhaps $(1 \times 1s + 1 \times 10s)$, to ensure that nearly every object has an unsaturated exposure in nearly every field. Although we do not wish to suggest a large array of observing strategies at this stage, we do recommend that this option be simulated for in-plane observations.)

2: Crowding and seeing: Metrics for in-plane science must incorporate the impact of spatial confusion on both photometric and astrometric measurements. Both of these depend on seeing. More work remains to be done on the level of sophistication necessary in these considerations; for example, when considering relative proper motion precision, the spatial density of reference stars at similar brightness to the object whose proper motion is desired (to mitigate magnitude-dependent PSF effects like the “fatter-brighter” effect) will in principle impact the proper motion precision attainable. The size of the impact of this effect on proper motion precision should be determined.

3: Relative and absolute metrics: Because even the first-order observation parameters for in-plane observations are somewhat unconstrained, metrics should be sensitive to differences in overall allocation as well as by comparison to the ideal strategy within an allocation. For example, the way in which observations are distributed within a time baseline is not very impactful to many science cases if that baseline is only three years long for OpSim algorithmic reasons! (For example, OpSim might move all the exposures in a galactic plane science case into the first three years to finish short projects early, which would be a disaster for cases that require a long time baseline.)

4.3 Summary table of Milky Way science cases

Here we present a quick-look summary of the Milky Way science cases to-date, with measurement type and tracer population indicated where appropriate. This communicates the importance of certain objects and certain regimes to Milky Way science. Given the considerations outlined in Section 4.2, this overview is split in two tables: Table 1 shows science cases for the five main science cases we have identified for metric development, while while Table Y summarizes the rest in terms of tracers and simple scaling relations (the majority of which can safely assume SRD performance numbers).

All those bullet points from v1 of this chapter are condensed and summarized in these tables.

[Table 1 - measurements and tracers for the five main science cases requiring new metrics.]

[Table 2 - Milky Way science cases not in Table 1; scaling relations from other metrics.]

(*Hierarchical metrics (e.g. github Issue #79)*: since others are developing detailed metrics for fine-grained issues of detectability, in this Chapter we focus our candidate metrics mostly on high-level metrics that might call the variability metrics as functions.)

The following sections describe observing metrics for Milky Way science cases. These have significant (but not exclusive) observation-sets in or towards the Plane. If your science case is not mentioned below, it should be mentioned concisely in Table 2.

Section 4.4: The spatial structure of the Milky Way Galaxy, including the plane, bulge, halo and local volume;

Section 4.5: Metallicity and age mapping in the Milky Way;

Section 4.6: Star formation history of the Milky Way;

Section 4.7: Dust in the Milky Way;

Section 4.8 Microlensing;

Section 4.9 Galactic Plane Science—Case for DWF;

[As of 2015-08-21, the .tex files for these subsections are mostly empty shells. Content to follow.]

[To be resolved: how to ensure Solar Neighborhood science is best represented. Does this deserve a sixth section?]

4.4 The spatial structure of the Milky Way

Author Name(s)

A short preamble goes here. What's the context for this science project? Where does it fit in the big picture?

4.4.1 Target measurements and discoveries

Describe the discoveries and measurements you want to make.

Now, describe their response to the observing strategy. Qualitatively, how will the science project be affected by the observing schedule and conditions? In broad terms, how would we expect the observing strategy to be optimized for this science?

4.4.2 Metrics

Quantifying the response via MAF metrics: definition of the metrics, and any derived overall figure of merit.

4.4.3 OpSim Analysis

OpSim analysis: how good would the default observing strategy be, at the time of writing for this science project?

4.4.4 Discussion

Discussion: what risks have been identified? What suggestions could be made to improve this science project's figure of merit, and mitigate the identified risks?

Go to: • [the start of this section](#) • [the start of the chapter](#) • [the table of contents](#)

4.5 Metallicity and age mapping in the Milky Way

Author Name(s)

A short preamble goes here. What's the context for this science project? Where does it fit in the big picture?

4.5.1 Target measurements and discoveries

Describe the discoveries and measurements you want to make.

Now, describe their response to the observing strategy. Qualitatively, how will the science project be affected by the observing schedule and conditions? In broad terms, how would we expect the observing strategy to be optimized for this science?

4.5.2 Metrics

Quantifying the response via MAF metrics: definition of the metrics, and any derived overall figure of merit.

4.5.3 OpSim Analysis

OpSim analysis: how good would the default observing strategy be, at the time of writing for this science project?

4.5.4 Discussion

Discussion: what risks have been identified? What suggestions could be made to improve this science project's figure of merit, and mitigate the identified risks?

Go to: • [the start of this section](#) • [the start of the chapter](#) • [the table of contents](#)

4.6 Star Formation History of the Milky Way

Author Name(s)

Summary: this important topic does not seem to have been developed in previous versions of the LSST science book or Ivezic et al. (2008). LSST gives the opportunity to survey extensive areas around star formation regions in the Southern hemisphere. Among others, it would allow to study the Initial Mass Function down to the sub-stellar limit across different environments. Young stars are efficiently identified by their variability.

A short preamble goes here. What's the context for this science project? Where does it fit in the big picture?

4.6.1 Target measurements and discoveries

In order to assess the ability of LSST to 1) identify and 2) classify YSO we need to quantify the variability timescales and amplitudes of both Class I/II (stars with disks) and Class III (WTTS). Inclusion of eruptive variables (FUor/Exor) is appropriate as well - see section 8.10.2 in the Science Book.

In brief, WTTS are quasi-periodic with amplitudes of 0.1 to 0.3 mag and periods 1 to 15 days - so comparable to gamma Dor stars (see Figure 8.17 in the SB). Given the temporal evolution of cool spots, a period recovery analysis such as shown for RRL stars (see Figure 8.20 in the SB) is likely difficult. The embedded systems and CTTS are irregular variables but shown have distinctive colors due to extinction + UB/blue excess arising from to accretion shocks.

4.6.2 Metrics

Quantifying the response via MAF metrics: definition of the metrics, and any derived overall figure of merit.

4.6.3 OpSim Analysis

OpSim analysis: how good would the default observing strategy be, at the time of writing for this science project?

4.6.4 Discussion

Discussion: what risks have been identified? What suggestions could be made to improve this science project's figure of merit, and mitigate the identified risks?

Go to: • [the start of this section](#) • [the start of the chapter](#) • [the table of contents](#)

4.7 Dust in the Milky Way

Author Name(s)

A short preamble goes here. What's the context for this science project? Where does it fit in the big picture?

4.7.1 Target measurements and discoveries

Describe the discoveries and measurements you want to make.

Now, describe their response to the observing strategy. Qualitatively, how will the science project be affected by the observing schedule and conditions? In broad terms, how would we expect the observing strategy to be optimized for this science?

4.7.2 Metrics

Quantifying the response via MAF metrics: definition of the metrics, and any derived overall figure of merit.

4.7.3 OpSim Analysis

OpSim analysis: how good would the default observing strategy be, at the time of writing for this science project?

4.7.4 Discussion

Discussion: what risks have been identified? What suggestions could be made to improve this science project's figure of merit, and mitigate the identified risks?

Go to: • [the start of this section](#) • [the start of the chapter](#) • [the table of contents](#)

4.8 Microlensing in the Milky Way with LSST

Author Name(s)

Note: these metrics have already been worked out in some detail by Gould (arXiv). We do not expect to re-invent that wheel here.

A short preamble goes here. What's the context for this science project? Where does it fit in the big picture?

4.8.1 Target measurements and discoveries

Describe the discoveries and measurements you want to make.

Now, describe their response to the observing strategy. Qualitatively, how will the science project be affected by the observing schedule and conditions? In broad terms, how would we expect the observing strategy to be optimized for this science?

4.8.2 Metrics

Quantifying the response via MAF metrics: definition of the metrics, and any derived overall figure of merit.

4.8.3 OpSim Analysis

OpSim analysis: how good would the default observing strategy be, at the time of writing for this science project?

4.8.4 Discussion

Discussion: what risks have been identified? What suggestions could be made to improve this science project's figure of merit, and mitigate the identified risks?

Go to: • [the start of this section](#) • [the start of the chapter](#) • [the table of contents](#)

4.9 The Galactic Plane Should Be Part of the Main Deep-Wide-Fast Survey

Jay Strader

The current baseline cadence (`enigma_1189`) partially excludes the Galactic Plane from the deep-wide-fast survey and instead adopts a nominal 30 visits per filter as part of a special proposal. The basic justification for this cadence is that the crowding and extinction in the plane makes it impossible to achieve many of the extragalactic science goals of the survey. However, much Milky Way science can *only* be accomplished in the plane, so it is not *prima facie* obvious that this area should be excluded from the deep-wide-fast survey. Careful consideration of science goals and metrics is necessary to determine whether the plane should be addressed in a special proposal—and the details of that proposal. Here we briefly highlight the science cases that focus on the Plane and show that despite the challenges, there is compelling support for including the Galactic Plane in the deep-wide-fast survey.

The science cases emphasized below do not require independent single epoch or combined photometry down to the nominal survey magnitude limits. However, it is still desirable to determine quantitative measurements of the effects of crowding and extinction on photometry, proper motions, and parallax as a function of Galactic latitude and filter rather than rough qualitative estimates. This will require image simulations through ImSim at a range of representative Galactic latitudes that are processed through the stack.

4.9.1 Unique Galactic Transients and Variables

Given the challenges of observing in the Plane, a simple increase of the survey area is insufficient justification for standard deep-wide-fast coverage. However, what is relevant is that many classes of important transients and variable stars are mostly or exclusively found in this region. Here we describe a representative (but non-exhaustive) list of these variables and transients.

Stellar-Mass Black Holes

Of the millions of stellar-mass black holes formed through the collapse of massive stars over the lifetime of the Milky Way, only ~ 20 have been dynamically confirmed through spectroscopic measurements (e.g., Corral-Santana et al. 2015). Many questions central to modern astrophysics can only be answered by enlarging this sample: which stars produce neutron stars and which black holes; whether there is a true gap in mass between neutron stars and black holes; whether supernova explosions result in large black hole kicks.

All of these known stellar-mass black holes were discovered as bright X-ray sources, either due to persistent emission or as transient “X-ray novae” due to an increase in the mass accretion rate within the standard disk instability model. This introduces a strong bias in the known black hole candidates: only those with short outburst recurrence times and whose peak X-ray luminosity reaches $\sim 10^{35}$ – 10^{36} erg/s can be detected. Short-period binaries should be preferentially faint (Knevitt et al. 2014) and may be mostly or entirely missed in current samples.

More importantly, there is expected to be a large population of black hole binaries in quiescence with low X-ray luminosities from $\sim 10^{30}$ – 10^{33} erg/s. Such systems can be identified as optical variables that show unique, double-humped ellipsoidal variations of typical amplitude ~ 0.2 mag due to the tidal deformation of the secondary star, which can be a giant or main sequence star. In some cases analysis of the light curve alone can point to a high mass ratio between the components, suggesting a black hole primary; in other cases the accretion disk will make a large contribution to the optical light, and other observations will be required to identify the nature of the binary.

Most black hole candidates have been identified toward the center of the Galaxy, in the Plane: 68% of black hole candidates are located within 5° of the Plane and 92% within 10° of the Plane. Therefore, including the Plane in the deep-wide-fast survey offers the best route to identifying the hundreds of quiescent black hole binaries that should be present. The brighter sources will be amenable to spectroscopy with the current generation of 4-m to 10-m telescopes to dynamically confirm new black holes; spectroscopy of all candidates should be possible with the forthcoming generation of large telescopes.

Other Compact Binaries

The methods discussed above for black holes can also be used to identify white dwarf and especially neutron star binaries, which again are preferentially found in the dense regions of the Galaxy. In some cases the secondaries can show clear ellipsoidal variations and be identified and studied as periodic variables; in other cases the accretion disk light can dominate, resulting in quasi-periodic or non-periodic light curves. Nonetheless, cross-matching LSST variables against the all-sky eROSITA catalog (reaching typical X-ray fluxes of 10^{31} – 10^{32} erg/s at 8 kpc) will reveal hundreds of new neutron star X-ray binaries (Merloni et al. 2012).

From studies of *Fermi* γ -ray sources, it is clear that pulsar surveys miss a huge fraction of pulsars in close binary systems (probably due to the effects of enshrouding material) but that targeted follow-up can detect such pulsars (Ray et al. 2012). Combining these observations with optical spectroscopic data gives the equivalent of a double-lined spectroscopic binary, and can often yield accurate masses for both the neutron star and the secondary. Further, gold-standard Shapiro-delay masses for neutron stars require edge-on orientations that only arise from large samples of objects. Such studies offer the best chance to probe the upper end of the neutron star mass distribution; the maximum mass of neutron stars determines the equation of state of dense matter and is of central interest to both astronomers and nuclear physicists.

A Milky Way Supernova

A supernova in the Milky Way would be among the most important astronomical events of our lifetime, with enormous impacts on stellar astrophysics, compact objects, nucleosynthesis, and neutrino and gravitational wave astronomy. The estimated rate of supernovae (both core-collapse and Type Ia) in the Milky Way is about 1 per 20–25 years (Adams et al. 2003); hence there is a 40–50% chance that this would occur during the 10-year LSST survey.

If fortunate, such an event will be located relatively close to the Sun and will be an easily observed (perhaps even naked-eye) event. However, we must be cognizant of the possibility that the supernova could go off in the mid-Plane close to the Galactic Center or on the other side of the Milky Way—both regions covered by LSST. While any core-collapse event will produce a substantial neutrino flux, alerting us to its existence, such observations will not offer precise spatial localization. The models of Adams et al. (2013) indicate that LSST is the *only* planned facility that can offer an optical transient alert of nearly all Galactic supernovae. Even if the supernova is not too faint, LSST will likely be the sole facility with synoptic observations preceding the explosion, providing essential photometric data leading up to the event—but only if LSST covers the Plane at a frequent cadence.

Novae

Only ~ 15 novae (explosions on the surfaces of white dwarfs) are discovered in the Milky Way each year, while observations of external galaxies show that the rate should be a factor of ~ 3 higher (Shafter et al. 2014). Evidently, we are missing 50–75% of novae due to their location in crowded, extinguished regions, where they are not bright enough to be discovered at the magnitude limits of existing transient surveys. Fundamental facts about novae are unknown: how much mass is ejected in typical explosions; whether white dwarfs undergoing novae typically gain or lose mass; whether the binary companion is important in shaping the observed properties of nova explosions. Novae can serve as scaled-down models of supernova explosions that can be tested in detail, e.g., in the interaction of the explosion with circumstellar material (e.g., Chomiuk et al. 2015). Further, since accreting white dwarfs are prime candidates as progenitors of Type Ia supernovae, only detailed study of novae can reveal whether particular systems are increasing toward the Chandrasekhar mass as necessary in this scenario.

Most novae occur in the Galactic Plane and Bulge, and therefore the quick identification of novae is best enabled by the standard deep-wide-fast cadence. These events will trigger multi-wavelength follow-up ranging from the radio to X-ray and γ -rays; these data are necessary for accurate measurements of the ejected mass.

4.9.2 Microlensing

Gould (2013) shows that coverage of the Plane with the standard deep-wide-fast cadence would be, in essence, an effective intra-disk microlensing survey (in which disk stars are lensed by other objects in the disk, such as exoplanets, brown dwarfs, or compact objects). The lower stellar density compared to past bulge-focused microlensing surveys would be offset by the larger area covered by LSST. The predicted rate of high magnification microlensing events that are very sensitive to planets would be ~ 25 per year. This survey would be able to detect planets at moderate distances from their host stars, a regime poorly probed by standard Doppler and transit techniques. The LSST data alone would not be sufficient: the detection of a slow (\sim days) timescale increase in brightness of a disk star would need to trigger intensive photometric observations from small (1-m to 2-m class) telescopes that would observe at high cadence for the 1–2 months of the microlensing event. This science *requires* the standard deep-wide-fast cadence (with typical inter-night visit times of a few days) to catch lensing events as they start to brighten.

4.9.3 A Three-Dimensional Dust Map of the Milky Way

The Pan-STARRS1 survey (PS1) has produced a three-dimensional dust map of the region of the sky covered in their 3π survey (which excludes a large part of the Galactic Plane toward the south). Such maps are necessary to accurately measure the intrinsic luminosities and colors of both Galactic and extragalactic sources. The PS1 map (Schlafly et al. 2014) saturates at extinctions $E(B - V) > 1.5$ as their tracer stars fall out of the survey catalogs fainter than $g \sim 22$, meaning that this high-fidelity map does not extend uniformly to within a few degrees of the midplane. In addition, it only extends to a distance of about 4.5 kpc. Deep LSST data will allow this map to be extended to much higher extinctions and larger distances. Owing to the high extinction and the use of blue filters, this project is less affected by crowding than other projects requiring photometry in the Plane. Nonetheless, quantitative estimates of the expected photometric accuracy in coadded u and g images at low Galactic latitude are desirable.

4.9.4 Metrics

Using proposed variable star metrics (§6.3), the recovery of accurate periods for variables discussed above should be compared between the baseline cadence and the results of the “Normal Plane” OpSim proposal (in which the portion of the Plane falling within the deep-wide-fast declination limits is observed at the standard deep-wide-fast cadence).

Several focused surveys on the Bulge with the wide-field MOSAIC II and DECam instruments have demonstrated that *differential* photometry is possible in these very crowded regions down to close to the LSST single epoch photometry limits in r and i (e.g., Britt et al. 2014). Therefore, periods and amplitudes for variables can be accurately measured even if precise absolute photometry is not available for every star (even though such photometry should be possible down to at least the main sequence turnoff; Rich 2015). In the Plane, away from the Bulge, the crowding is less extreme, and quantitative limits should be calculated for photometry, proper motion, and parallax measurements through image simulations as noted above.

Go to: • [the start of this section](#) • [the start of the chapter](#) • [the table of contents](#)

4.10 Milky Way Metrics: future work

Analysis of precursor data using the LSST stack is expected on a relatively short timescale (perhaps during 2016-2017)? The catalogs thus produced, and their source images, will provide the opportunity for very fine-grained information to be folded in to metrics that relate to crowded regions.

Go to: • [the start of this section](#) • [the start of the chapter](#) • [the table of contents](#)

5 Mapping Our Galaxy: Positions, Proper Motions and Parallax

Dave Monet, Dana Casetti, John Gizis, Michael Liu

While astrometry is not a science case, high astrometric accuracy enables a large number of science cases. Hence, the LSST Observing Strategy needs to be examined for systematic trends that might mitigate or even preclude precise measures of stellar positions, proper motions, parallaxes, and perturbations that arise from unseen companions. To highlight the various astrometric impacts of the strategy, three science cases have been chosen for particular attention:

- The tie between the Radio and Optical realizations of the International Celestial Reference System.
- Identification of Streams in the Galactic Halo using proper motions.
- The specific and ensemble agreement between LSST and Gaia parallaxes.

Each of these cases stresses different aspects of the LSST hardware, software, and observing strategies.

The measurement of stellar parallax puts the most constraints on the observing cadence. There are two major issues:

- Sampling over a wide range of parallax factor.
- Breaking the correlation between Differential Color Refraction and parallax factor.

The parallax factors characterize the ellipse of the star's apparent motion as seen during the year. The shape of the ellipse is given by the Earth's orbit and is not a free parameter in the astrometric solution. The amplitude of the RA parallax factor is close to unity while the amplitude of the Dec parallax factor is dominated by the sine of ecliptic latitude. The RA parallax factor has maximum amplitude when the star is approximately six hours from the Sun, so the optimum time for parallax observing is when the star is on the meridian near evening or morning twilight. Atmospheric refraction displaces the star's apparent position in the direction of the zenith by an amount characterized by both the wavelength of the light and the distance to the zenith. Whereas the measured position of star is a function of the total refraction, the measurement of parallax and proper motion depends on the differences in the refraction as a function of the color of each star and the circumstances of the observations. This dependence is called Differential Color Refraction (DCR). The combination of parallax factor and DCR leads to the these two rules well known to those who make astrometric observations.

1 Observations need to cover the widest possible range in parallax factor.

- 2 The correlation between parallax factor and hour angle in the observations needs to be minimized.

The search for faint proper motion stars has two key components. The first is the need to identify stars that move from the ensemble of other image features that can cause confusion. For example, a compact group of stars that contains one or more stars of variable brightness can confuse the catalog correlation algorithm. The other is the need to establish the zero point. For the case of relative astrometry, meaning the measurement of relative positions in an image, the question remains on how to remove the mean motion of the reference frame. For example, astrometry on certain classes of galaxies might produce a zero point of sufficient accuracy. This leads to a third constraint on the observing cadence.

- 3) Observations must cover a sufficient range of epochs so that stars with linear or periodic motions can be identified at a high level of confidence.

The tie between the radio and optical reference frames relies on measuring accurate positions for objects visible in both wavelength regimes. Whereas there are optical variable stars with radio emission, most have associated optical nebulosity that degrades the accuracy of the optical positions. The typical radio+optical object is a QSO. Unfortunately, many QSOs have detectable optical or radio structures that degrade the positions or suggests a displacement between the location of the sources of the radio and optical radiation. The major contribution from LSST will be the identification of a large number of QSOs based on their colors that have minimal (if any) spatially extended structure. The impact of this search has no obvious impact on the cadence other than temporal coverage to identify variability.

In summary, there are three metrics for the observing strategy that have direct relevance on the quality of LSST astrometric measurements. These were identified years ago and are already in the suite of MAF utilities, but they should be reviewed prior to making final decisions.

- A) For each LSST field, the parallax factors at each epoch of observation need to be computed. The ensemble of these must be checked for sufficient coverage of the parallactic ellipse. In particular, the number of measures with RA parallax factor less than -0.5 and greater than +0.5 needs to be tallied because these carry the most weight in the solution for the amplitude (parallax).
- B) For each LSST field, the hour angle of the observation needs to be computed, and the correlation between hour angle and parallax factor needs to be examined for significance. The observing strategy must minimize the number of fields with this correlation.
- C) The epochs of observation for each field must be checked for a reasonable coverage over the duration of the survey and to avoid collections of too many visits during a few short intervals.

Finally, it must be noted that these MAF metrics are only part of the study of LSST's predicted astrometric performance. Detailed simulations and studies need to be done in many other areas as part of the prediction and verification of LSST's astrometric performance. Among the most important are the following.

- Can we use galaxies as reference objects, and if so are certain shapes or colors better than others?

-
- Can we identify QSOs and sense optical structure that might mitigate using certain ones in the Radio-Optical reference frame link?
 - Given the LSST exposure time, site, and physical characteristics, how can we mitigate the limitations on astrometric accuracy imposed by the seeing and local atmospheric turbulence?
 - At what star densities does the measurement of a centroid become difficult or impossible, and does difference imaging allow us to work in these crowded areas?
 - What tools do we need to compare the general and specific agreement between the *Gaia* results and the LSST results?
 - Does the “brighter-wider” effect in the deep depletion CCDs introduce a magnitude term into the centroid positions?

Go to: • [the start of this section](#) • [the start of the chapter](#) • [the table of contents](#)

6 Variable and Transient Sources in the Galaxy and Beyond

Mike Lund, Ashish Mahabal, Stephen Ridgway, Lucianne Walkowicz, Rahul Biswas, Michelle Lochner, Jeonghee Rho...

Confirmed leads for Stellar variability and Fast Stellar Transients: Mike Lund, Ashish Mahabal, Stephen Ridgway, Lucianne Walkowicz

Confirmed leads for cosmological SNe: Rahul Biswas, Michelle Lochner, Jeonghee Rho

Confirmed leads for extragalactic transients: Ashish Mahabal

Confirmed leads on rolling cadence: Stephen Ridgway

6.1 Introduction

The observation of variable targets investigates the time domain, and thus realizes the essence of a synoptic survey. Variable and transient studies are all about sampling, and different types and time scales of phenomena benefit from different sampling strategies - sometimes significantly different. Competing objectives described in this chapter are at the heart of LSST observing strategy and cadence design.

Target types are here grouped in subsections by variability characteristics, but as will be seen, this does not mean that all targets in a group require a common cadence, since the times scales may vary dramatically. Acquiring suitable data for a wide range of time scales presents a fundamental problem for LSST, since the available 800 visits to a field over the survey cannot be deployed so as to usefully sample all time scales at all times. This fact leads to the concept of a non-uniform survey, in which parts of the sky are visited more frequently part of the time. The merits of such options must be traded against the benefits of a more uniform survey strategy.

When evaluating a particular observation or series of observations in light of how they perform for a specific science case, it may be helpful to think of metrics as lying along a continuum between discovery and characterization. Discovery requires a minimum amount of information to recognize an event or object as a candidate of interest, which necessarily involves some level of bare-bones characterization (upon which said recognition is based); rich characterization, on the other hand, implies that an event may not only be recognized as a candidate of interest, but basic properties of the event or object may be determined from the observation (e.g. including but not limited to classification of the event). The interpretation of a given metric along this continuum has implications for the subsequent action and analysis required, particularly as regards possible follow-up observations with other facilities.

6.2 Metrics for Transients and Variables

As the science cases outlined below are grouped by temporal behavior (rather than underlying physical causes), the metrics developed to evaluate them may be generic and applicable to seemingly disparate science cases. Here, we describe metrics that are either already coded into the sims_maf_contrib repo or proposed. Individual subsections below should refer back to these metric descriptions.

6.2.1 Existing Metrics

Lund et al. (2015; <http://arxiv.org/pdf/1508.03175.pdf>) discuss three metrics that have been incorporated into the MAF. Two of these metrics deal explicitly with time variable behavior: a) observational triplets, and b) detection of periodic variability.

Observational triplets (`TripletMetric`)

This metric provides a means of evaluating whether a transient event on some timescale of interest has been detected, by testing for a sequence of three observations. The object must be detected in quiescence, followed by two subsequent detections above some threshold; this sequence of observations allows the magnitude of the change to be measured, as well as its timescale.

This metric may be used for a variety of astrophysical phenomena, in particular transient events on variable objects (e.g. novae, stellar flares), in that it is general with respect to the amplitude of the brightness variation as well as the timescale of said change. The requirement of a detection prior to outburst does constrain it to objects that have already been detected in quiescence (in other words, not necessarily “true” transients), although there may be some cases where this is not the case (e.g. a supernova occurring on a previously detected galaxy). In practice, the time lapse between the first and second and second and third observations must be comparable (between 10^2 and 10^5 seconds) for discovery. This metric may be calculated for a given OpSim run and then further reduced to a histogram in logarithmic time bins; the minimum number of bins to construct an interesting sample of objects is source-dependent.

Periodogram purity function (`PeriodicMetric`)

This metric calculates the Fourier power spectral window function of each field (Roberts et al. 1987) as a means of quantifying the completeness of phase coverage for a given periodic variable. The periodogram purity is defined as 1 minus the Fourier power spectral window function; in the perfect case, all power is concentrated in a delta function at the correct frequency, and is zero elsewhere. As power “leaks” away from the correct frequency as a consequence of discrete, non-ideal data sampling, the periodogram becomes more structured. For the purposes of MAF metrics, which are designed to quantify performance as a single number, the periodogram purity is quantified as the minimum value away from the correct frequency.

Phase Gap Metric (PhaseGapMetric)

Histogram of the median and maximum phase gaps achieved in all fields

Period Deviation Metric (PeriodDeviationMetric)

This metric computes the percent deviation of recovered periods from pure sine variability.

Transient Metric (transientAsciiMetric)

Calculate what fraction of transients would be detected using an ascii input file for the lightcurve.

6.2.2 Proposed Metrics

The following is a raw list of metric ideas; these need specificity and further description.

The triplet metric may also be altered to include filter constraints, such that the triplets are drawn from a single filter or subset of filters.

Color evolution constraint: triplets of observations in a specific color (really requirement of two triplets in multiple filters)

2D Histogram of delta t's between observations constituting a triplet

FWHM of the window function (to quantify sampling)

Maximum hour angle difference

Fraction of discoveries vs fractional duration of eclipse

Fraction of targets vs survey duration, for which the period can be determined to 5-sigma confidence

Fraction of targets vs survey duration, for which a period change of 1% can be determined with 5-sigma confidence

Histogram of median visit series length vs maximum visit spacing within the series

Number of events adequately sampled

6.3 Periodic Variable Stars

Author Name(s)

Some stars may be strictly periodic, or sufficiently so to be treated as such for some purposes, in which case data from different cycles can be combined according to phase to provide a more fully sampled light curve. It is unreasonable to suppose that LSST visits will be synchronized with variable stars, and visits will occur effectively at random phases. In a 10-year survey, most periodic stars of almost any period will benefit from excellent phase coverage in all filters. Only a very small period range close to the sidereal day will be poorly observed. There is no reason to believe that any likely LSST observing strategy could seriously disturb good sampling of periodic variables.

Eclipsing binaries are discussed here with variable stars, as detection of eclipses is dependent on adequate sampling of the phase curve. However, study of the features of an eclipse, particularly one of short duration in phase, may require sampling more appropriate to the discussion of transients.

6.3.1 Nearly Periodic Variables

Stars with a drifting period will be served well with sampling which constrains period variations frequently through the survey. For targets with a wide range of periods, this will be most effectively accomplished with sampling that is rather uniform through the survey. A considerable degree of uniformity is needed for many science objectives, and distribution of visits over the full survey is more important than the exact timing.

Some variable stars do not exhibit a strictly repeating light curve, and show variations in light curve structure from period to period. For observational purposes, these targets are better described as periodic transients, discussed in a later section.

6.3.2 Targets and Measurements

Periodic Variable Type	Examples of target science	Amplitude	Timescale
Periodic binaries	Eclipses, physical properties of stars, distances, ages, evolution, apsidal precession, mass transfer induced period changes, Applegate effect	small	hr-day
RR Lyrae	Galactic structure, distance ladder, RR Lyrae properties	large	day
Cepheids	Distance ladder, cepheid properties	large	day
Long Period Variables	Distance ladder, LPV properties	large	weeks
Short period pulsators	Instability strip, white dwarf interior properties, evolution	small	min
Rotational Modulation	Gyrochronology, stellar activity	small	days

These targets share the requirement for good sampling over the variation phase curve.

For each target, the coverage of the phase curve sampling will accumulate randomly, and particular measurements or discoveries will become possible at a rate that is somewhat linear with number of acquired visits (hence linearly with time in a uniform survey).

With millions of different periods, it is difficult to imagine designing the survey to optimize this sampling, but the sampling achieved can be predicted with appropriate metrics.

6.3.3 Metrics

Metric	Description
Eclipsing binary discovery	Fraction of discoveries vs fractional duration of eclipse
Transiting exoplanets (depth dependent)	Fraction of discoveries vs fractional duration of eclipse
Phase gap	Histogram vs period of the median and maximum phase gaps achieved in all fields
Period determination (period dependent)	Fraction of targets vs survey duration, for which the period can be determined to 5-sigma confidence
Period variability (period dependent)	Fraction of targets vs survey duration, for which a period change of 1% can be determined with 5-sigma confidence

The period metrics can be based on a standard variable curve (e.g.sinusoid) of fiducial amplitude and brightness, and/or a realistic model population of a particular variable type. These metrics can be informative for science programs. However, it is not clear that the survey strategy can or should attempt to control these metrics, as the requirements are specific to each target, and all targets benefit from a generally uniform distribution of visits.

6.3.4 OpSim Analysis

Current simulations show for the main survey a broad uniformity of visits, with thorough randomization of visit phase per period, giving very good phase coverage with minimum phase gaps.

6.3.5 Discussion

For periodic variable science, two cadence characteristics should be avoided:

- an exactly uniform spacing of visits (which is anyway virtually impossible);
- a very non-uniform distribution, such as most visits concentrated in a few survey years.

A metric for maximum phase gap will guard against the possibility that a very unusual cadence might compromise the random sampling of periodic variables.

In each case, it would help to jump-start science programs if some fraction of targets had more complete measurements early in the survey.

Go to: • [the start of this section](#) • [the start of the chapter](#) • [the table of contents](#)

6.4 Non-periodic Variables

Author Name(s)

Some variable star types are not strictly periodic. These include multi-period stars, for which Fourier analysis may be useful, but only if the underlying frequencies are at least critically sampled. Irregularly variable stars may have so little repeatable structure that neither phase stacking nor harmonic analysis is very useful, but patterns may become evident over observing intervals of years or decades.

Non-periodic variable stars may benefit from complete phase coverage over a single cycle, or other time interval of interest, repeated in consecutive intervals, or in intervals distributed over the survey. Variable stars for which thorough sampling of limited duration is required, including eruptive variables, are considered below with transients.

Active galactic nuclei are mentioned here as well, as they may show variable and/or transient activity, in most cases with no or only weak periodicity. Other non-stellar variable objects may be discussed here as well.

6.4.1 Targets and Measurements

The class of non-periodic variables includes a heterogeneous assortment of objects and phenomena.

Variable Type	Examples of target science	Amplitude	Timescale
Long Period Variables	Pulsation modes, internal structure, evolution	large	weeks
Multimode pulsation	Pulsation mechanisms, internal structure	small	weeks
Semi-regular variables	Pulsation mechanisms, convection	large	weeks
Pulsating irregular variables	Chaotic dynamics	small	days
Epsilon Aurigae systems	Circumstellar material, dark companions	large	months
FU Ori systems	Accretion events, jets	large	months
Young Stellar Objects	Accretion, jets, disks, binarity, flaring, rotation, spots, magnetic phenomena	small	days
Active galactic nuclei	Galaxy evolution, reverberation mapping, black hole physics	large	weeks

In each case, the observational challenge is to discover and then to characterize the targets, utilizing the power of the LSST survey to increase by orders of magnitude the number of well-studied targets known. Most of the targets in the table have variation time scales of $\simeq 1$ week or greater, and will receive sampling commensurate with the time scale of variation under a natural LSST cadence (~ 800 visits over 10 years). Where a higher sampling rate is needed, these will need customized attention to the time scale and the number and duration of sampled intervals.

6.4.2 Metrics

Metric	Description
Non-periodic variables	Histogram of median visit series length vs maximum visit spacing within the series

6.4.3 OpSim Analysis

Current simulations provide reasonable sampling (~ 2 samples per time constant) for variables that change brightness on a time scale of >1 week. For faster variations, an enhanced sampling rate should be studied.

6.4.4 Discussion

Special cadences offer the opportunity to extend LSST studies to non-periodic phenomena with time scales ≤ 1 week, rather than the >1 week that is naturally achieved with a uniform survey.

The need for contemporaneous color information has not been addressed, and needs consideration, as with novel targets and non-repeating signals, it may not be possible to infer color relations.

Go to: • [the start of this section](#) • [the start of the chapter](#) • [the table of contents](#)

6.5 Periodic Transient Events

Author Name(s)

This section is a place holder in case periodic transients deserve focus. However, they may fit into the previous sections.

6.5.1 Targets and Measurements

Describe the discoveries and measurements you want to make for a generic transient, with additional comment on specific variable types which have any special requirements.

Example events: eclipsing binary stars, exoplanet eclipses

Now, describe their response to the observing strategy. Qualitatively, how will the science project be affected by the observing schedule and conditions? In broad terms, how would we expect the observing strategy to be optimized for this science?

6.5.2 Metrics

Quantifying the response via MAF metrics: definition of the metrics, and any derived overall figure of merit.

6.5.3 OpSim Analysis

OpSim analysis: how good would the default observing strategy be, at the time of writing for this science project?

6.5.4 Discussion

Discussion: what risks have been identified? What suggestions could be made to improve this science project's figure of merit, and mitigate the identified risks?

Go to: • [the start of this section](#) • [the start of the chapter](#) • [the table of contents](#)

6.6 Transient Events

Stephen Ridgeway, Ashish Mahabal, Ohad Shemmer

Transient events may benefit from substantial temporal sampling (matched to the time constant of the event) with color information (perhaps contemporaneous) to support characterization and classification, obtained over the limited duration of interest. Transient events slower than \sim weeks may be adequately sampled by a uniform LSST cadence. Faster events may require special scheduling strategies. For some event types, LSST can only be expected to provide a discovery service, and followup will necessarily be performed elsewhere.

6.6.1 Targets and Measurements

The class of transients includes a heterogeneous assortment of objects and phenomena.

Transient Type	Examples of target science	Amplitude	Time Scale
Flare stars	Flare frequency, energy, stellar age	large	min
Cataclysmic variables	Interacting binaries, stellar evolution, compact objects, explosive events	small	min
Supernovae	SN physics, mass loss, distance scale, cosmology	large	days
Active galactic nuclei	Galaxy evolution, reverberation mapping, black hole physics	large	weeks
Stellar microlensing	Exoplanet statistics	large	hours
Gamma ray bursts	Optical discovery and characterization	large	min
LIGO detections	Source position and characterization	unknown	min
Serendipity	Discovery and characterization	unknown	unknown
Tidal Disruption Events	Discovery and characterization	large	days

Among the targets in this list, only AGN are likely to be sampled with sufficient resolution by a uniform LSST cadence - in fact for AGN, a challenge may be to spread visits sufficiently in time to avoid excessive seasonal gaps.

For very short lived phenomena (stellar flares, CV outbursts, GRBs, LIGO events) it appears that the function of LSST will be to provide discoveries and/or simple characterization. Followup to discovery/identification, if required, will surely take place elsewhere.

For events requiring intensive monitoring (stellar microlensing, exoplanet transits), the followup will certainly take place elsewhere.

Supernovae fall in an intermediate time range. LSST will provide multiple visits in multiple filters during the typical SN duration. This sampling may be insufficient for many (including key) science objectives. However, a moderate, and feasible, change to LSST observing strategy, may enhance the sampling for part of the sky part of the time, greatly enhancing the usefulness of SN observations.

For Tidal Disruption Events, where the fading time-scale is much more gradual (over weeks to months) than the rise time-scale it will be worth checking - through a metric - how many will be missed (as alerts). Ref. Science Book: 10.6.1. Also ref. recent papers.

Serendipitous discoveries are of course harder to plan for. An ideal transient discovery survey would include heavy coverage of all time scales. LSST will cover longer time periods well, but will have to make some choices of emphasis in coverage of shorter time-scales.

6.6.2 Metrics

Metric	Description
SNe	Number of events adequately sampled
Serendipity	Histogram of median visit series length vs maximum visit spacing within the series

The metrics for SNe will be highly specialized and based on the best available understanding of SN light curve analysis and the expected event population.

The suggested metric set for serendipity is based on the simple-minded idea that a novel transient will be characterized by a band-limited, finite waveform, and that a useful observation series will consist of a series of samples extending over the duration of the event, with at least critical sampling of the fastest variations. Since for some event durations the number of useful time series will be small, it may be useful to look not at the median length, but the median length of a subset size preselected as possibly useful (e.g. the 10^3 longest series).

6.6.3 OpSim Analysis

Analysis shows that current simulations provide poor coverage in any one filter for transient events longer than a deep drilling session (~ 30 minutes) and shorter than \sim weeks.

Simulated performance for SN observations must be analyzed for both main survey and mini-survey (deep drilling) productivity. It is considered that current simulated schedules give inadequate performance for SN science.

6.6.4 Discussion

Community studies are providing improving SNe metrics, and continuing communication between the SN and LSST communities is essential to tuning the observing strategy to deliver the SN time series that are needed and possible.

Improving LSST science return for SNe will also improve sampling of all transients with similar or somewhat shorter characteristic times. Non-uniform survey strategies (rolling cadence) can significantly improve the LSST performance for faster transients. Interpretation of multiple filters for novel events may be powerful, or problematic, since color may be uncertain.

Some insight into fast transients may be available from image pairs or triples (as opposed to more complete series). These include the pair of images in a visit - which could be useful in studying the rise time of an extremely fast event. This includes the characteristic grouping of visits (typically 0.5 to 1.0 hour separation) planned for purposes of identifying asteroids. It also includes fortuitous multiple sampling due to field overlap, providing additional sampling, which may be random or systematic, depending on the scheduling, on a time scale of minutes to hours. The sampling benefits of this fortuitous overlap have not yet been investigated.

Go to: • [the start of this section](#) • [the start of the chapter](#) • [the table of contents](#)

6.7 Rolling Cadence

Stephen Ridgway, ...

With a total of 800 visits spaced approximately uniformly over 10 years, and distributed among 6 filters, it is not clear that LSST can offer the sufficiently dense sampling in time for study of transients with typical durations less than or $\simeq 1\text{ week}$. This is particularly a concern for key science requiring well-sampled SNIa light curves. Rolling cadences stand out as a general solution that can potentially enhance sampling rates by $2\times$ or more, on some of the sky all of the time and all of the sky some of the time, while maintaining a sufficient uniformity for survey objectives that require it.

6.7.1 The Uniform Cadence

Current schedule simulations allocate visits as pairs separated by 30-60 minutes, for the purposes of identifying asteroids. For most science purposes, the 30-60 minute spacing is too small to reveal temporal information, and a pair will constitute effectively a single epoch of measurement. If the expected 824 (design value) LSST visits are realized as 412 pairs, and distributed uniformly over 10 observing seasons of 6 months each, the typical separation between epochs will be 4 days. The most numerous visits will be in the r and i filters, and the repeat visit rate in either of these will be $\simeq 20$ days.

The possibility is still open that, for asteroid identification, visits might be required as triples or quadrupoles, in which case the universal temporal sampling will be further slowed by 1.5 or $2\times$.

Under a strict universal cadence it is not possible to satisfy a need for more frequent sample epochs. This leads the simulations group to investigate the options opened up by reinterpreting the concept of a universal cadence. Instead of aiming for a strategy which attempts to observe all fields “equally” all the time, it would allow significant deviations from equal coverage during the survey, returning to balance at the end of the survey.

Stronger divergence from a universal cadence, allowing significant inhomogeneities to remain at the end of the survey, is of course possible, but is not under investigation or discussed here.

There is currently considerable interest in the community in strategies that provide enhanced sampling over a selected area of the sky, and rotating the selected area in order to exercise enhanced sampling over all of the survey area part of the time. The class of cadences that provides such intervals of enhanced visits, with the focus region shifting from time to time, is termed here a rolling cadence. As a point of terminology, observing a single sky area with enhanced cadence for a period of time will be described as a “roll”.

6.7.2 Rolling Cadence Basics

Assume a fixed number of observing epochs for each point on the sky, nominally distributed uniformly over the survey duration. A subset of these can be reallocated to provide improved sampling of a sky region. This will have the inevitable effects of: (1) reducing the number of

epochs available for that sky region during the rest of the survey, and (2) displace observations of other sky regions during the time of the improved temporal sampling. In short, the cadence outside the enhanced interval will be degraded.

The essential parameters of rolling cadence are: (1) the number of samples taken from the uniform cadence, and (2) the enhancement factor for the observing rate. The LSST document 16370, “A Rolling Cadence Strategy for the Operations Simulator”, by K. Cook and S. Ridgway, contains more detailed discussion and analysis.

6.7.3 Supernovae and Rolling Cadence

Author Name(s)

Supernovae as a science topic are addressed elsewhere. In this section, the demands of SN are used to directly constrain or orient the rolling cadence development.

Pending more quantitative guidance, the SN objective for rolling cadence is to obtain multicolor time series significantly longer than the typical SN duration, with a cadence significantly faster than uniform. As an example we discuss the option of a rolling cadence with the regular distribution of filters.

As a simple example, consider improving the cadence by a factor of 2 or 3. If we accept that some regions of the sky will be enhanced every year, and that uniform sky coverage will only arrive at the end of 10 years, then we could use, e.g., 10% of the total epochs in a single roll. If the enhancement is $2\times$, each roll would last for $\simeq 6$ months, with high efficiency for capture of complete SN events. If the enhancement is $4\times$, each roll would last for 2 months, with lower efficiency.

If it is important to achieve survey uniformity after 3 years, the available visits for each roll would be reduced also. With a $2\times$ enhancement of epoch frequency, a roll would last 2 months.

Some leverage would be gained by using more than 10% of the available visits for a single roll. However, this begins to impact the sampling of slow variables reduce schedule flexibility and robustness, and should be approached with caution.

From these examples, it appears that a $2\times$ enhancement with uniformity closure after 10 years is relatively feasible and promising. Much higher gains, or more rapid closure, require additional compromises.

6.7.4 Fast Transients and Rolling Cadence

Author Name(s)

Fast transients as a science topic are addressed elsewhere. In this section, the demands of fast transients are used to directly constrain or orient the rolling cadence development.

By “fast transients”, we are referring to events that are sufficiently fast that they are not addressed by the rolling cadence designed for SN observations, and slow enough that they are not covered in “deep drilling” type mini-surveys. For higher tempo rolls, it is quite difficult to obtain full color data, because of the constraints on filter selection. For this example, we will examine a

rolling cadence utilizing only the r and i filters, as they are used for most visits. They are close in wavelength, and we assume that sufficient color information will be obtained by the “background” uniform survey that continues during a roll.

Again using 10% of the available visits from the full 10 year survey for a single roll, we find that there would be enough epochs for each roll to acquire 1 visit per day for 21 consecutive days, giving an enhancement of 10 \times .

Alternatively, the same epochs could be used to observe a target every 20 minutes for 12 hours during a single night (here it is assumed that visit pairs are not required, doubling the available epochs) for an enhancement of 300 \times .

Several different possible redeployments of portions of a uniform survey have been described, each using 10% of available time. Of course it is possible in principle to implement multiple options, sequentially or maybe in parallel in some cases. This may pose considerable challenges to the scheduling strategy design by introducing incompatible boundary conditions.

While rolling cadences are powerful, they have limitations. For example, sampling events that last longer than \simeq 1 day and less than \simeq 1 week have the obvious problem of diurnal availability. In this example, intermediate cadences could be implemented in the circumpolar region, where diurnal access is much extended. This is an example of a case in which a mini-survey of a limited number of regions could be considered as an alternative to a rolling cadence applied to the entire main survey.

6.7.5 Constraints, Trades and Compromises for Rolling Cadences

While rolling cadences offer some attractive benefits, it is important to realize that rolling cadences are very highly constrained, and that they do bring disadvantages and compromises.

There are strong arguments against beginning a rolling cadence in the first, or even the second year of the survey. Early in the survey, it is important to obtain for each field/filter combination, an adequate number of good quality photometric images, and at least one image in excellent seeing, to support closure of photometry reductions and to support generation of template images.

Since major science goals require a significant degree of survey homogeneity, it may be advisable to implement a strategy that brings the survey to nominal uniform depth at several times, e.g. after 3 or 5 years. This would strongly constrain rolling cadences.

Some science objectives favor certain distributions of visits. For astrometry, visits early and late in the survey and at large parallax factors, are beneficial. Slow variables may benefit from uniform spacing. Rolling cadences might impact these constraints either favorably or unfavorably.

Many objectives are served by randomization of observing conditions for each field. Some rolling cadences could tend to reduce this randomization, for example by acquiring a large number of observations during a meteorologically favorable or unfavorable season, or during a period of instrument performance variance.

Dithering does not work gracefully with a rolling cadence, reducing temporal coverage at the boundaries of the selected sky region. This is negligible for small dithers, but important for large dithers, which are under consideration.

These cautions illustrate that evaluation of rolling cadences must be based on the full range of schedule performance metrics, and not just those targeted by rolling cadence development.

Go to: • [the start of this section](#) • [the start of the chapter](#) • [the table of contents](#)

7 Keeping It Even: Accurate Cosmological Measurements on the Largest Scales

Eric Gawiser , Peter Kurczynski, Phil Marshall , Ohad Shemmer , Timo Anguita and others to follow

7.1 Introduction

Cosmology is one of the key science themes for which LSST was designed. Our goal is to measure cosmological parameters, such as the equation of state of dark energy, or departures from General Relativity, with sufficient accuracy to distinguish one model from another, and hence drive our theoretical understanding of how the universe works, as a whole. To do this will necessarily involve a variety of different measurements, that can act as cross-checks of each other, and break parameter degeneracies in any single one.

The Dark Energy Science Collaboration (DESC) has identified five different cosmological probes enabled by the LSST: weak lensing (WL), large scale structure (LSS), type Ia supernovae (SN), strong lensing (SL), and clusters of galaxies (CL). In all cases, the primary concern is residual systematic error: the shapes and photometric redshifts of galaxies, and the properties of supernova and lensed quasar light curves, will all need to be measured with extraordinary accuracy in order for LSST’s high statistical power to be properly harnessed. This accuracy will come from the abundance and heterogeneity of the individual measurements made, and the degree to which they can be modeled and understood. This latter point implies a need for uniformity in the survey, which enables powerful simplifying assumptions to be made when calibrating on the largest, cosmologically most important scales. The need for heterogeneity also implies uniformity, in the sense that the nuisance parameters that describe the systematic effects need to be sampled over as wide a range as possible (examples include the need to sample a wide range of roll angles to minimize shape error, and observing conditions to understand photometric errors due to the changing atmosphere).

In this chapter we look at some of the key measurements planned by the Dark Energy Science Collaboration, and how they depend on the Observing Strategy.

7.2 Large Scale Structure: Testing Dithering Patterns and Timescales to Improve Survey Uniformity

Humna Awan, Eric Gawiser, Peter Kurczynski, Lynne Jones

Three of the key cosmology probes available with LSST represent “static science” insensitive to time-domain concerns. These are Weak Lensing, Large-Scale Structure, and Galaxy Clusters. Nonetheless, due to the need to track and correct for the survey “window function” in all of these probes, cosmology with LSST will benefit greatly from achieving survey depth as uniform as possible over the WFD area. OpSim tiles the sky in hexagons inscribed within the nearly-circular LSST field-of-view. It has been shown in [Carroll et al. \(2014\)](#) that the default LSST survey strategy implemented in OpSim runs leads to a strongly non-uniform “honeycomb” pattern due to overlapping regions on the edges of these hexagons receiving double the observing time. A pattern of large dithers proves sufficient to greatly reduce these overlaps, leading to an increase in median survey depth in each filter of 0.08 magnitudes.

In this section, we report results from an investigation by Awan et al. (in preparation) of several geometrical patterns for dithers performed on timescales varying from once per observing season to once per night to every visit.

EG: Flesh out WL, LSS, and Clusters dependence on survey uniformity to make this section more clearly science-driven.

7.2.1 Dithering Patterns and Timescales

7.2.2 Metrics

Our primary metric is total uncertainty in the derived window function over relevant angular scales, modeled via variations in the angular power spectrum of fake galaxy fluctuations between *gri* bands. Intermediate metrics include the number of galaxies in each pixel, fluctuations in this number, total power in the angular power spectrum of a skymap of those fluctuations, and residual power that angular power spectrum after subtracting a smooth fit to it.

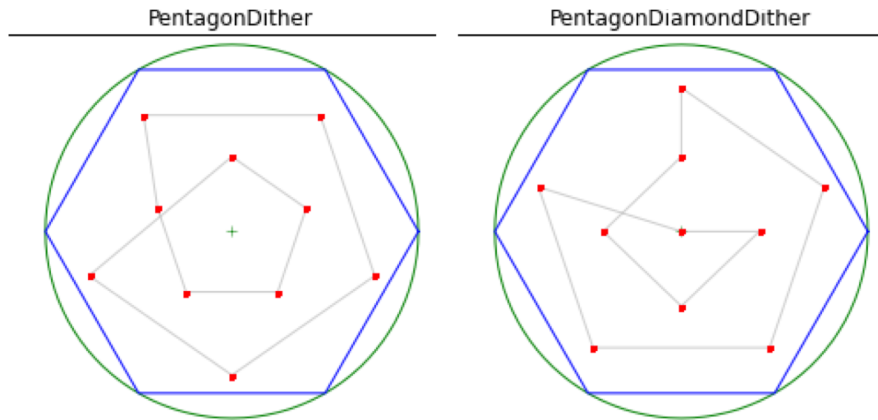
7.2.3 OpSim Analysis

In this section we present our ongoing OPSIM/ MAF analysis, as we try to answer the question “what dithering strategies produce acceptable variations in survey uniformity, and which appears optimal?”

7.2.4 Results

EG: Improve figures to originals rather than screen-captures.

EG: Input fuller results and text from Awan et al. draft.



: Fig. 1.— Geometries for by season dithering strategies.

Figure 7.1:

7.2.5 Discussion

Go to: • [the start of this section](#) • [the start of the chapter](#) • [the table of contents](#)

7.3 Suppressing systematic effects

Stephen Ridgway, Josh Myers, ...

Much of cosmology science may be limited by systematic errors rather than photon signal-to-noise.

7.3.1 Target Measurements

It is expected that even after maximal optimization of camera optics and electronics, that systematic image shape errors will be associated with the orientation of the camera focal plane. These can be partially reduced by randomization of the orientation of the camera with respect to the sky. This is represented by the parameter RotSkyPos.

Similarly, the telescope optics may harbor systematic aberrations, and these also could be mitigated by recording images with varying parallactic angle. Another relevant parameter, RotTelPos, is indicative of the projected angle of the telescope optics on the sky.

Uniformity of depth is essential - metrics and requirements will be added.

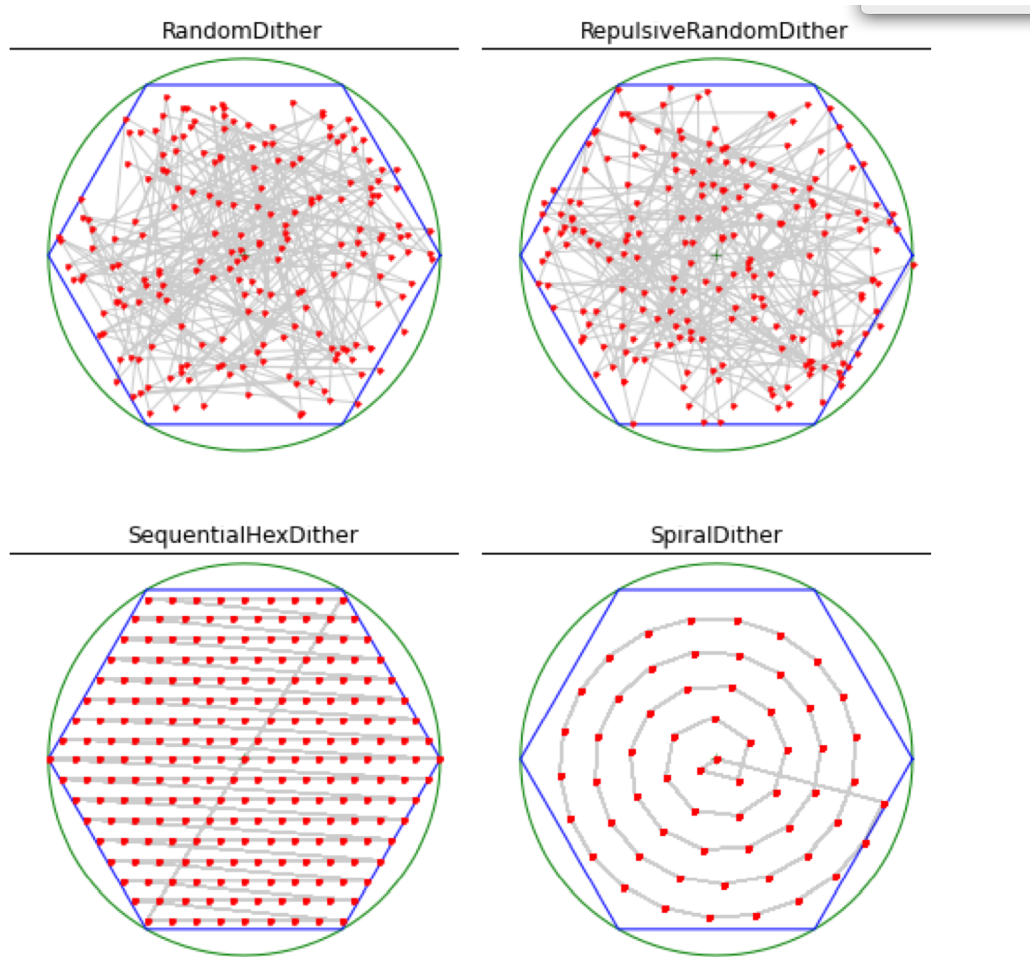


Fig. 2.— Geometries for by visit and by night dithering strategies.

Figure 7.2:

7.3.2 Metrics

A metric is available for RotSkyPos. The metric computes, for any selected filter and simulation, a histogram of the distribution of rms values of RotSkyPos computed per field. It also computes basic statistics of these distributions.

7.3.3 OpSim Analysis

The distribution of rms values by filter is shown in Figure 7.6 for the current candidate baseline simulation, enigma_1189. As shown, the rms values cluster around the value 1 radian, with typical values 1 ± 0.3 radian. This compares to a completely uniform distribution over the half circle with an rms of 1.14.

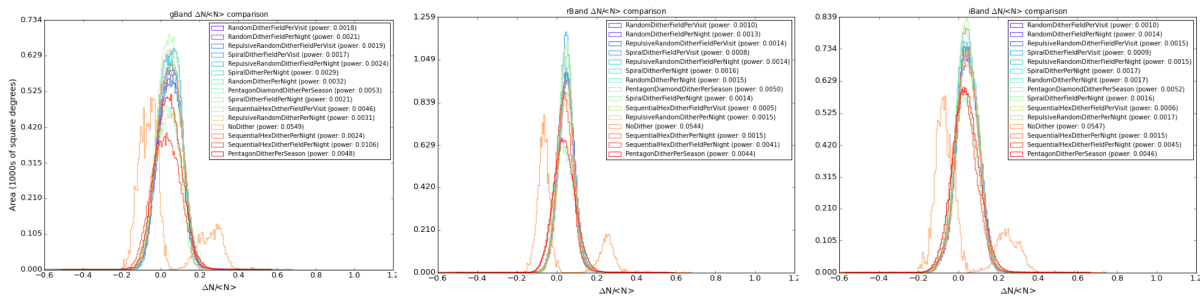


Fig. 4.— Histograms for artificial fluctuations in galaxy counts in gri bands for various

dithering strategies.

Figure 7.3:

7.3.4 Discussion

The RotSkyPos metric analysis shows that the majority of fields have a good randomization of detector angles projected on the sky.

There are several limitations to this observation.

First, we do not have at present a quantitative requirement for randomization of this parameter. In future development of weak lensing analysis, a criterion should be developed.

Second, a significant fraction of fields have median values that are lower or higher than expected for a random distribution, with some far from uniformly distributed. Regardless of the *perfield* criterion, it is desirable to avoid the incidence of individual discrepant fields.

The recommended criterion for randomization of RotSkyPos is not the behavior of the majority of the fields, but of the minority with the least random behavior. The number of non-random fields should be minimized. A recommended metric is the count of fields with median RMS less than 0.8 or greater than 1.5 radians (these values to be reviewed again as additional experience is gained with additional OpSim schedule simulations and weak lensing analysis.)

It is certain that actively controlling the statistics of RotSkyPos will require additional slewing of the camera rotator. At present, the operations plan is to only slew when necessary to prepare for a filter change - that could be estimated at the equivalent of $\simeq 3$ complete rotations per day. Figure 7.6 shows that to render the distribution completely uniform would require moving all observing angles an average of $\simeq 30$ degrees, or 300 complete rotations per night. The timing of this has not been considered. Whether or not this uniformity could be achieved with less slew time if implemented in scheduling remains to be demonstrated.

A similar metric for RotTelPos should be developed.

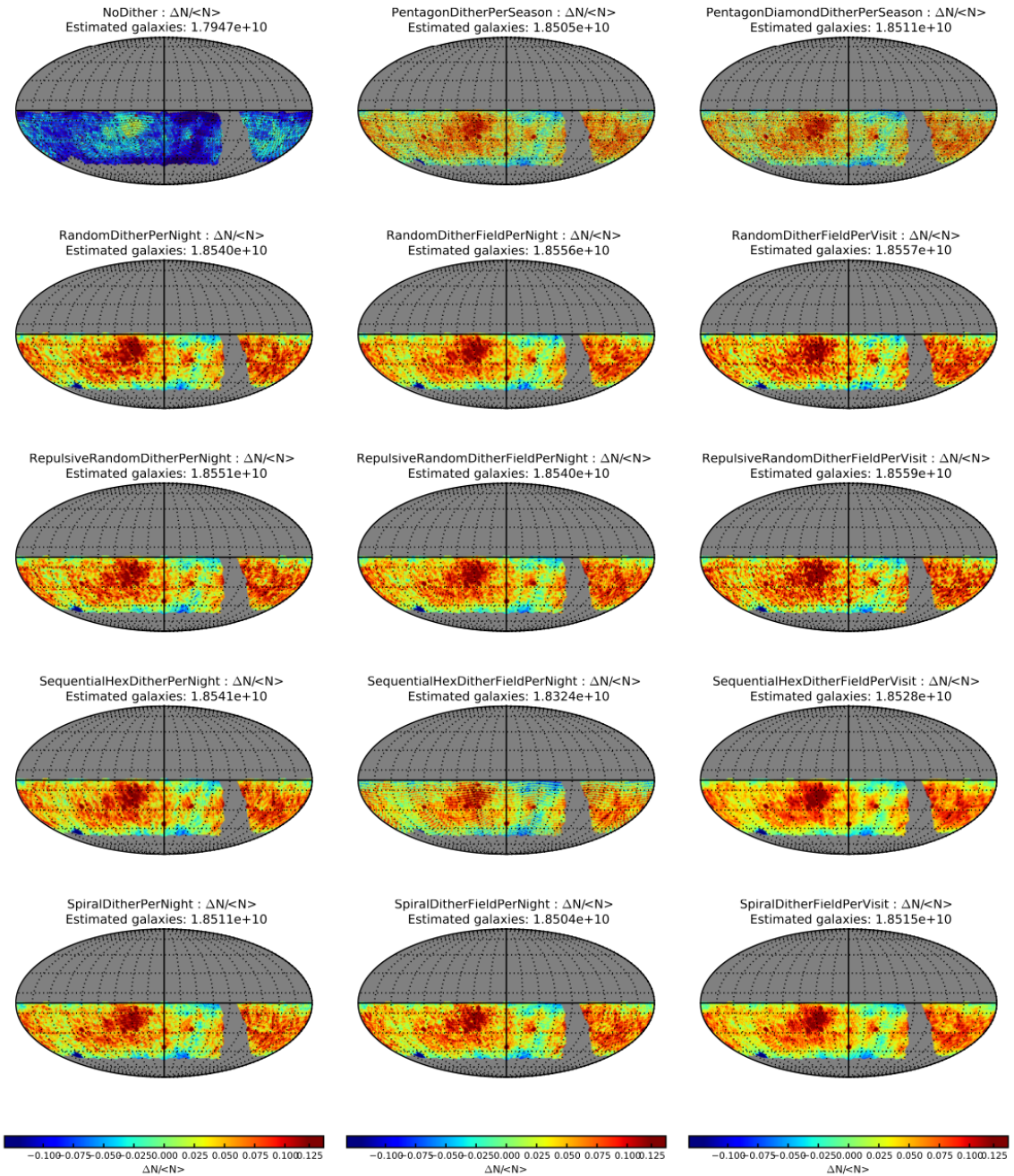


Fig. 5.— Skymaps for r-band differential galaxy counts from various dithering strategies.

Figure 7.4:

7.4 Supernova Cosmology and Physics

Jeonghee Rho, Michelle Lochner, Rahul Biswas, Seth Digel

This section is concerned with the detection and characterization of supernovae (SNe) over time with LSST and their various scientific applications. The most important application is the use of supernovae type Ia (SNIa) and potentially some core-collapse SN (like type IIP) to trace the recent expansion history of the universe, and confront models of the physics driving the late time accelerated expansion of the universe.

This objective of SN cosmology follows (at least for SNIa) results from several highly successful surveys; improvement in knowledge of cosmology could come from substantially larger numbers of well-characterized SNe. This goal is not directly tied to the unprecedentedly large survey area of LSST. However, we shall argue that in practice, even this goal would benefit from the spatial scale offered by the WFD component of the LSST survey.

On the other hand, the WFD aspect will make the LSST survey potentially the first to scan the very large area of the entire Southern sky for SNe. SNe that are detected and well characterized by LSST will probe the isotropy of the universe. Peculiar velocities of SNe will probe the growth of structure. In addition, this large sample will enable further sharpening of our understanding of the properties of the SN population of different types. This last point is extremely important for SN cosmology goals: The success of SNIa cosmology has always been based on the empirical model that intrinsic peak brightnesses are related to the certain observable characteristics of SNe. The WFD SNIa sample will dramatically increase the size of the sample available to train such an empirical model, as well understand the probability of deviations and scatter from this model. Aside from issues like calibration which need to be addressed differently, a larger sample of such well measured SNe is probably the only way to address ‘systematics’ due to deviations from the empirical model. The anticipated sample can be thought of as consisting of two components: the low-redshift sample which is more likely to be complete, and the higher-redshift sample that will be able to constrain evolution.

7.4.1 Target measurements and discoveries

SNe of different types are visible over time scales of about a few weeks (e.g., type Ia) to nearly a year (type IIP). During the full ten-year survey, LSST will scan the entire southern sky repeatedly with a WFD cadence, and certain specific locations of the sky called the Deep Drilling Fields (DDF) with special enhanced cadence.

This spatio-temporal window should contain millions **RB: remember to check** of SNe, that will have apparent magnitudes brighter than the single exposure limiting magnitude of LSST. However, the actual sequence of observations by LSST, defined by the series of field pointings as a function of time in filter bands (along with weather conditions), will determine the extent to which each SN can be detected and characterized well. Characterization of the SNe is at the core of a number of science programs that use them as bright, abundant objects with empirically determined intrinsic brightnesses. For LSST, this goal entails (a) detection of SNe, (b) photometric typing of SNe, (c) estimating photometric redshifts of SNe (or identifying host galaxies and obtaining their redshifts from photometry or follow-up spectroscopy), (d) estimation of intrinsic brightnesses of the SNe, and finally (e) use of these data in addressing our science goals of cosmological inference, etc. The efficacy of photometric typing, redshifts and estimation of intrinsic brightnesses are all dependent on the amount of information available in the observed light curves of SNe. While these steps

are not necessarily independent, it is useful to think of the requirements on some of these steps separately; it is not unlikely that combinations of some of the steps would still be affected by similar requirements.

Our first objective is to detect such SNe, by which we mean selecting SNe from among the transient sources detected by LSST. In brief, this process consists of defining a set of image subtractions between a high-resolution ‘template’ image of a sky section, and a set of single exposures at different times (usually of lower resolution) of the same region, after accounting for the different resolutions of images, and alignments. These sets of image subtractions associated with a single object will be used to detect the object as a transient and then classify the transient as an SN. Clearly, detecting an SN depends on the number of such images recorded per object, the different filters used for those images, and the signal-to-noise ratios of the images. The efficiency of this step may be summarized as a threshold on the joint properties of an astrophysical candidate (apparent brightness, light curve characteristics, background) as well as observing conditions (astronomical seeing, etc.).

Our second objective is to photometrically classify different kinds of SNe. Previously, only spectroscopically typed SNe have been used for cosmology. Photometric typing from light curves alone has only been used to select candidates for spectroscopic follow-up (see, e.g., [Sako et al. \(2008\)](#)). However, LSST will simply find far too many candidates for even a significant fraction of them to be followed up spectroscopically. In order to avoid discarding the majority of the SN dataset, we need to use techniques capable of determining cosmological parameters from a potentially contaminated photometric SN dataset.

Several techniques have been proposed recently to solve this problem. One approach involves applying stringent cuts to the photometric dataset to obtain a nearly pure sample of SNIa ([Bernstein et al. 2012](#); [Campbell et al. 2013](#)) and running the standard SNIa cosmology analysis with this sample. Another approach, BEAMS ([Kunz et al. 2007](#); [Newling et al. 2011](#); [Hlozek et al. 2012](#); [Knights et al. 2013](#)), makes use of an entire dataset, coping with contamination by using a mixture model for the likelihood, thus allowing for multiple populations. Whatever the technique ultimately used for cosmological analysis, it will rely on accurate initial classifications of SN type and unbiased estimates for the probability of each type.

Current state-of-the-art photometric classification techniques rely on fitting empirically determined templates of SNe to light curves ([Jha et al. 2007](#); [Guy et al. 2007](#); [Sako et al. 2011](#)). However in recent years, new approaches have been developed in response to the 2010 ‘Supernova Photometric Classification Challenge’ ([Kessler et al. 2010b](#)). Many of these use novel light curve parameterization and employ machine learning algorithms to perform the classification (see [Kessler et al. \(2010a\)](#) and references therein).

While many of these methods have been tested on standard sets of simulated data and (in some cases) on SDSS data, which technique (if any) is superior in all situations is unclear. For example, some techniques are dependent on the availability of reliable redshift information. Some techniques may be more robust to non-representative datasets [Not sure what this means] than others, and how the techniques will respond to changes in cadence, filter sets, signal-to-noise, etc., is unclear.

With this in mind, we propose the use of a multifaceted classification system which employs several different methods for extracting features from the light curves (e.g., fitting parametric functions or templates) and several different classification algorithms. This system is highly modular, allowing new approaches for direct comparison with existing techniques to be added easily. This also allows

direct analysis of different observing strategies, without requiring an initial choice of classification technique.

Our third objective is to characterize SNe in terms of empirical light curve models.

The ultimate goal of using SNe (type SNIa or SNIIP) for cosmology requires estimating the intrinsic brightnesses of the SN. The first (and sometimes only, depending on the light curve model) step is fitting the calibrated fluxes to a light curve model with a set of parameters. According to the ansatz used in SN cosmology, the intrinsic brightness of SNe is largely determined by the parameters of the light curve model; hence the uncertainties on the inferred parameters largely determine the uncertainties on the inferred peak intrinsic brightness or distance moduli of the SNe.

7.4.2 Metrics

Quantifying the response via MAF metrics: definition of the metrics, and any derived overall figure of merit.

To be added: discussion of the ROC curve as a useful metric for photometric supernova classification

7.4.3 OpsSim Analysis

OpSim analysis: how good would the default observing strategy be, at the time of writing for this science project?

As noted above the scientific goal of characterizing SNe is to a large extent dependent on how well the light curves of individual SNe are sampled in time and filters. To study this, we re-index the OpsSim output on spatial locations rather than use the temporal index. There are different methods (which will be merged), and here we will first illustrate this in terms the cadence in an example LSST field.

7.4.4 Discussion

Discussion: what risks have been identified? What suggestions could be made to improve this science project's figure of merit, and mitigate the identified risks?

- Intrinsic Dispersion, environmental effects, newer analysis methods
- Follow-up procedures: What is feasible? Where will our training samples for classification and light curve models come from (other experiments, our own sub-samples with spectroscopic follow-up?), spectroscopic follow-up of host galaxies. Can hosts be identified?
- ‘Systematics’: In what ways will the real data not match the assumptions made in analysis. Having a large sample of SN, to understand the astrophysics would be useful for this.

Go to: • [the start of this section](#) • [the start of the chapter](#) • [the table of contents](#)

- 12 -

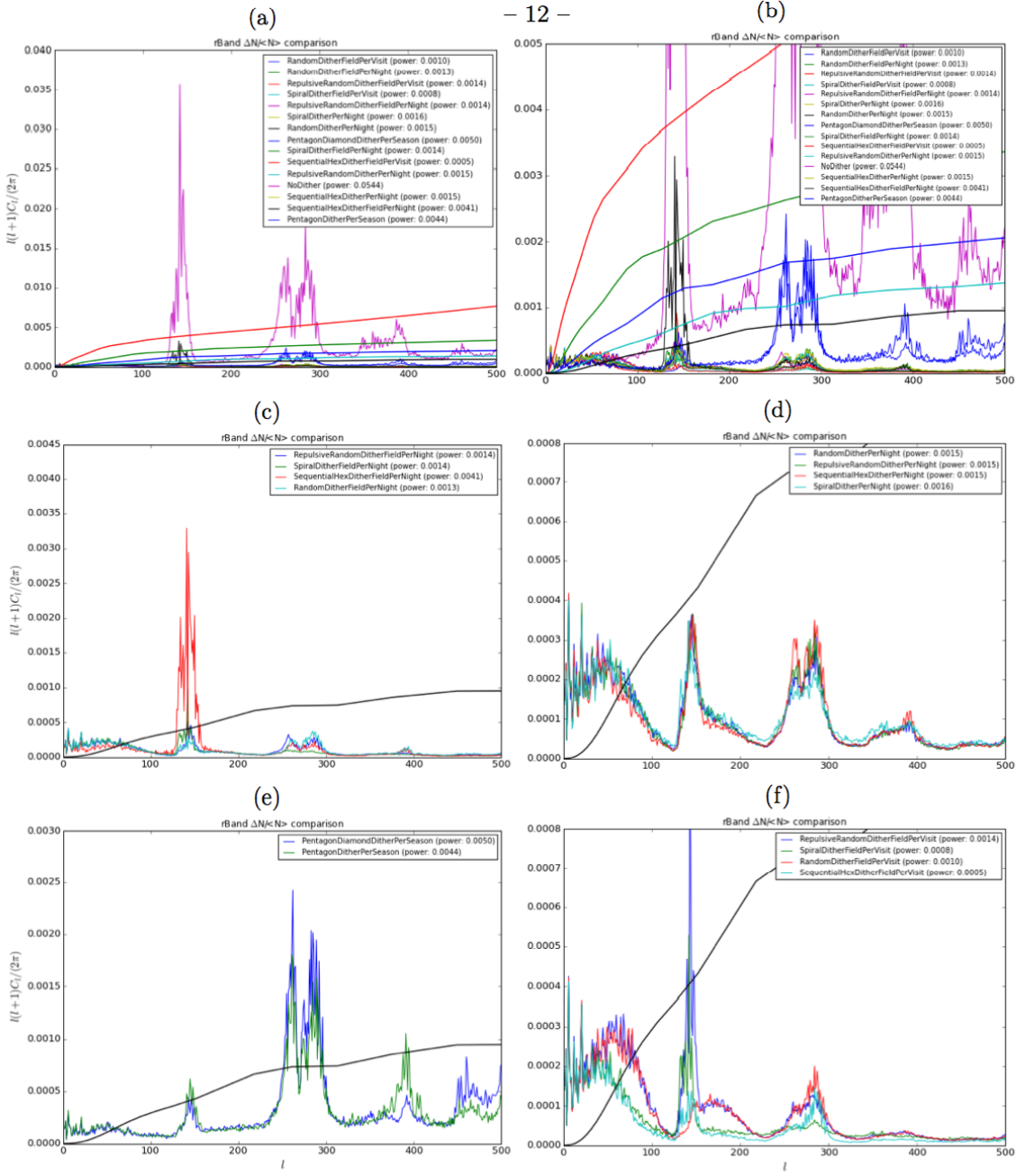


Fig. 6.— Angular power spectra for artificial fluctuations in r-band galaxy counts from various strategies. Panel (a) includes the spectra for all strategies, with its zoomed version shown in Panel (b). Panel (c) includes those for FieldPerNight strategies, Panel (d) for PerNight, Panel (e) for PerSeason, and Panel (f) for FieldPerVisit strategies. Thick curves are an example BAO signals, where the red one is for $0.15 < z < 0.37$, green for $0.37 < z < 0.66$, blue for $0.66 < z < 1$, cyan for $1 < z < 1.5$, and black for $1.5 < z < 2$.

Figure 7.5:

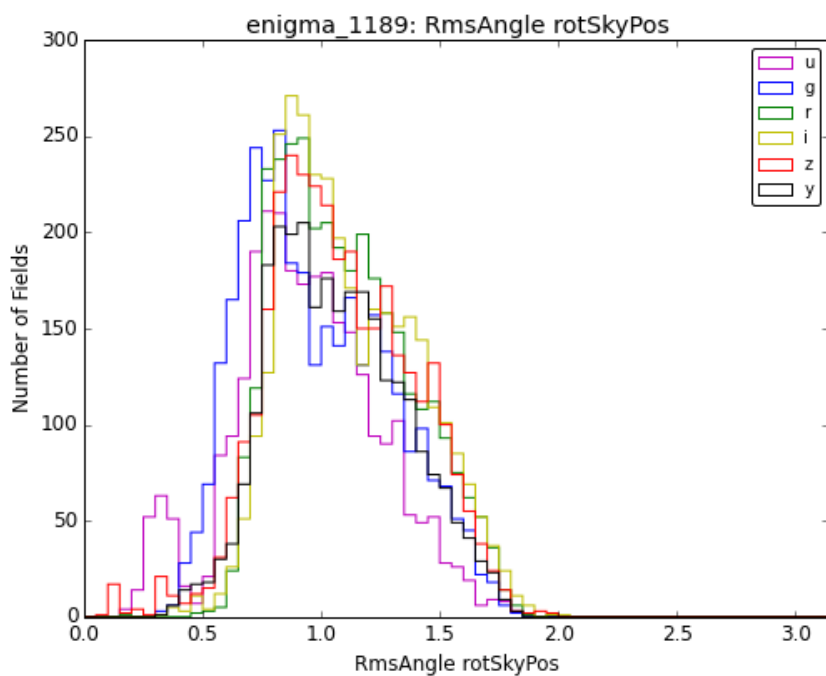


Figure 7.6: The relative angle of the detector plane with respect to the sky, RotSkyPos, as a histogram showing the number of fields vs. rms of the parameter.

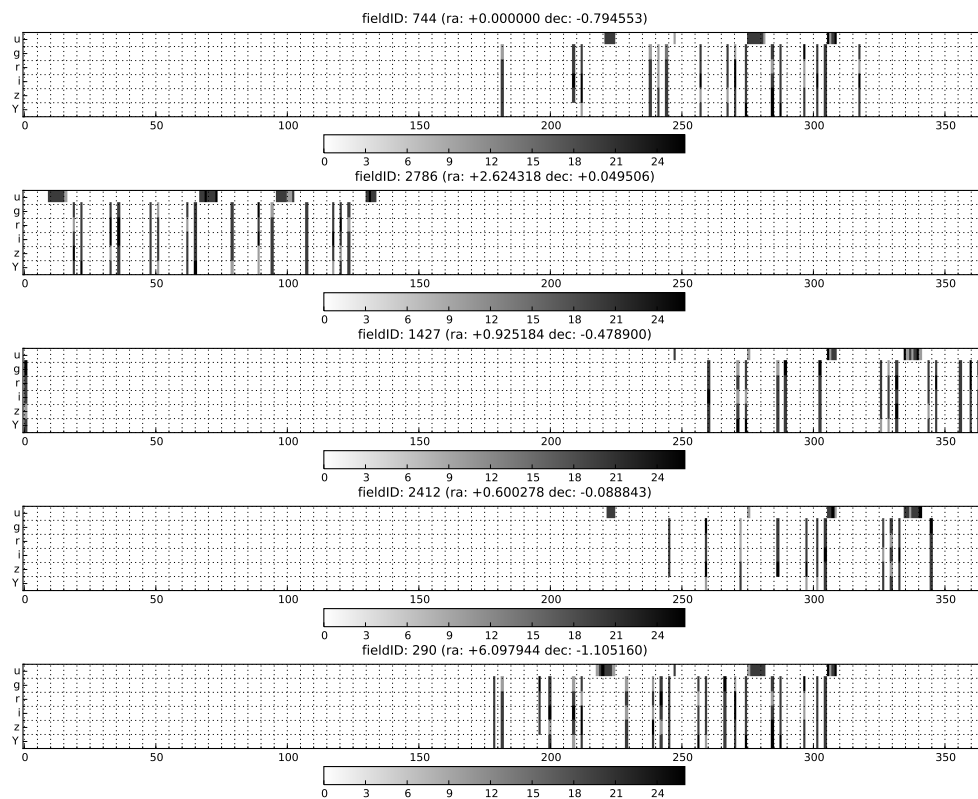


Figure 7.7: Cadence in different filters for a few LSST DDFs in the the ouptut of OpSim version Enigma 1189. This ignores issues of chip gaps and overlaps between LSST pointings. These issues have been addressed in (Carroll et al. 2014) and Awan et.al. (2015, in prep.). We will add these to this analysis.

7.5 Strong Gravitational Lens Time Delays

Phil Marshall , Lynne Jones

The multiple images of strongly lensed quasars and supernovae have delayed arrival times: variability in the first image will be observed in the second image some time later, as the photons take different paths around the deflector galaxy, and through different depths of gravitational potential. If the lens mass distribution can be modeled independently, using a combination of high resolution imaging of the distorted quasar/SN host galaxy and stellar dynamics in the lens galaxy, the measured time delays can be used to infer the “time delay distance” in the system. This distance enables a direct measurement of the Hubble constant, independent of the distance ladder.

7.5.1 Target measurements and discoveries

For this cosmological probe to be competitive with LSST’s others, the time delays of several hundred systems (which will be distributed uniformly over the extragalactic sky) will need to be measured with bias below the sub-percent level, while the precision required is a few percent per lens. In galaxy-scale lenses, the kind that are most accurately modeled, these time delays are typically between several days and several weeks long, and so are measurable in monitoring campaigns having night-to-night cadence of between one and a few days, and seasons lasting several months or more.

To obtain accurate as well as precise lensed quasar time delays, several monitoring seasons are required. Lensed supernova time delays have not yet been measured, but their transient nature means that their time delay measurements may be more sensitive to cadence than season or campaign length.

7.5.2 Metrics

Anticipating that the time delay accuracy would depend on night-to-night cadence, season length, and campaign length, we carried out a large scale simulation and measurement program that coarsely sampled these schedule properties. In [Liao et al. \(2015\)](#), we simulated 5 different light curve datasets, each containing 1000 lenses, and presented them to the strong lensing community in a “Time Delay Challenge.” These 5 challenge “rungs” differed by their schedule properties, in the ways shown in [Table 7.1](#). Focusing on the best challenge submissions made by the community, we derived a simple power law model for the variation of each of the time delay accuracy, time delay precision, and useable sample fraction, with the schedule properties cadence, season length and campaign length. These models are shown in [Figure 7.8](#), reproduced from [Liao et al. \(2015\)](#),

Rung	Mean Cadence (days)	Cadence Dispersion (days)	Season (months)	Campaign (years)	Length (epochs)
0	3.0	1.0	8.0	5	400
1	3.0	1.0	4.0	10	400
2	3.0	0.0	4.0	5	200
3	3.0	1.0	4.0	5	200
4	6.0	1.0	4.0	10	200

Table 7.1: The observing parameters for the five rungs of the Time Delay Challenge. Reproduced from [Liao et al. \(2015\)](#).

and are given by the following equations:

$$|A|_{\text{model}} \approx 0.06\% \left(\frac{\text{cad}}{3\text{days}} \right)^{0.0} \left(\frac{\text{sea}}{4\text{months}} \right)^{-1.0} \left(\frac{\text{camp}}{5\text{years}} \right)^{-1.1}$$

$$P_{\text{model}} \approx 4.0\% \left(\frac{\text{cad}}{3\text{days}} \right)^{0.7} \left(\frac{\text{sea}}{4\text{months}} \right)^{-0.3} \left(\frac{\text{camp}}{5\text{years}} \right)^{-0.6}$$

$$f_{\text{model}} \approx 30\% \left(\frac{\text{cad}}{3\text{days}} \right)^{-0.4} \left(\frac{\text{sea}}{4\text{months}} \right)^{0.8} \left(\frac{\text{camp}}{5\text{years}} \right)^{-0.2}$$

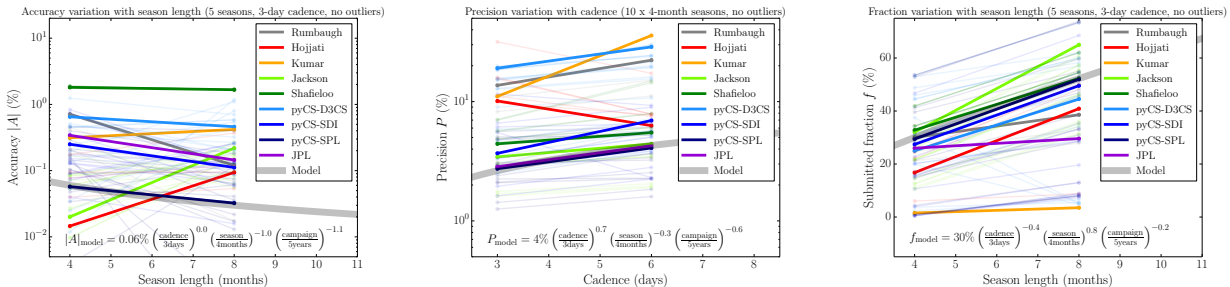


Figure 7.8: Examples of changes in accuracy A (left), precision P (center) and success fraction f (right) with schedule properties, as seen in the different TDC submissions. The gray approximate power law model was derived by visual inspection of the pyCS-SPL results; the signs of the indices were pre-determined according to our expectations. Reproduced from [Liao et al. \(2015\)](#).

All three of these metrics would, in an ideal world, be optimized: this could be achieved by decreasing the night-to-night cadence (to better sample the light curves), extending the observing season length (to maximize the chances of capturing a strong variation and its echo), and extending the campaign length (to increase the number of effective time delay measurements). A combined figure of merit should therefore be readily available. The quantity of greatest scientific interest is the *accuracy in cosmological parameters*: efforts to derive such a figure of merit in terms of the Hubble constant are underway.

Table 7.2: Lens Time Delay Metric Analysis Results.

OPSIM run	Filters	cadence	season	campaign	Accuracy	Precision	Fraction	timedelayFoM
enigma_1189	<i>ri</i>	XXX	XXX	XXX	XXX	XXX	XXX	???
enigma_1189	<i>ugrizy</i>	XXX	XXX	XXX	XXX	XXX	XXX	???
ops2_1075	<i>ri</i>	XXX	XXX	XXX	XXX	XXX	XXX	???
ops2_1075	<i>ugrizy</i>	XXX	XXX	XXX	XXX	XXX	XXX	???

Notes: see the text for the definitions of each metric, and sky maps and histogram plots of them. The Figure of Merit is still under development.

7.5.3 OpSim Analysis

In this section we present the results of our ongoing OPSIM/ MAF analysis, as we try to answer the question “how good would the proposed observing strategies be, for time delay lens cosmography?”

We used the `SeasonStacker` to work with seasons.

We used `ops2_1075` for most of our tests, but we need to now re-run on `enigma_1189`, and others from ??.

PJM: Correct the above paragraphs and add more links to MAF code.

Figure 7.9 shows the results of our MAF analysis of one OPSIM database, `ops2_1075`, where we have assumed that all filters were able to be used in the light curve analysis (as was implicitly assumed when applying the results of Liao et al.). These sky maps show that, over the main (WDF) survey area, the time delay accuracy, time delay precision and time delay lens success fraction are consistently maintained, indicating that the global average values of these metrics could conceivably used as higher level metrics or even figure of merit.

Table 7.2 shows the global (i.e. al-sky) average values of our metrics, for two different OPSIM databases and two different filter set assumptions.

PJM: Compute global average lens time delay metrics and discuss.

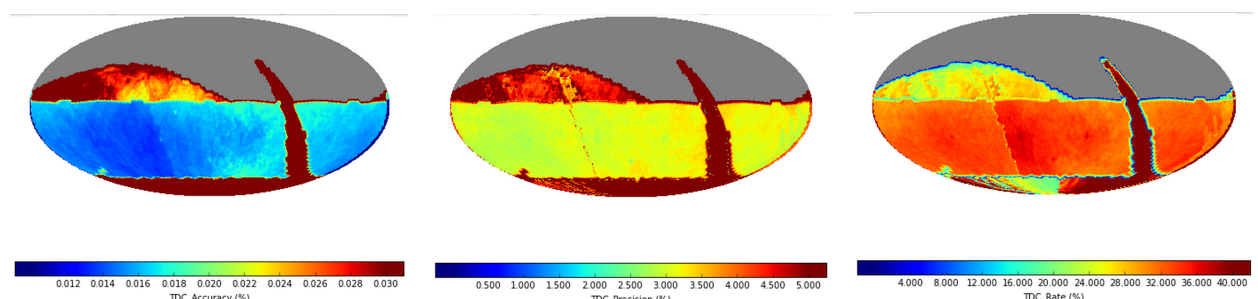


Figure 7.9: Sky maps of the accuracy A (left), precision P (center) and success fraction f (right) metrics, for the `ops2_1075` OPSIM database and assuming all filters (*ugrizy*) are used in the analysis according to the assumptions described in the text.

7.5.4 Discussion

Discussion: what risks have been identified? What suggestions could be made to improve this science project's figure of merit, and mitigate the identified risks?

PJM: Write lens time delays discussion section.

Go to: • [*the start of this section*](#) • [*the start of the chapter*](#) • [*the table of contents*](#)

7.6 AGN Science

Ohad Shemmer Timo Anguita ?? ?? ??

7.6.1 AGN Selection and Census

About 10^7 – 10^8 AGNs will be selected in the main LSST survey using a combination of criteria, split broadly into four categories: colors, astrometry, variability, and multiwavelength matching with other surveys. The LSST observing strategy will affect mostly the first three of these categories.

Colors: The LSST observing strategy will determine the depth in each band, as a function of position on the sky, and will thus affect the color selection of AGNs. This will eventually determine the AGN $L - z$ distribution and, in particular, may affect the identification of quasars at $z \gtrsim 6$ if, for example, Y -band exposures will not be sufficiently deep.

Variability: AGNs can be effectively distinguished from (variable) stars, and from quiescent galaxies, by exhibiting certain characteristic variability patterns (e.g., [Butler & Bloom \(2011\)](#)). Non-uniform sampling may “contaminate” the variability signal of AGN candidates.

Astrometry: AGNs will be selected among sources having zero proper motion, within the uncertainties. The LSST cadence may affect the level of this uncertainty in each band, and may therefore affect the ability to identify (mostly fainter) AGN. Differential chromatic refraction (DCR), making use of the astrometric offset a source with emission lines has with respect to a source with a featureless power-law spectrum, can help in the selection of AGNs and in confirming their photometric redshifts ([Kaczmarek et al. 2009](#)). The DCR effect is more pronounced at higher airmasses. Therefore, it’d be advantageous to have at least one visit, per source, at airmass greater than about 1.4. AGN selection and photometric redshift confirmation may be affected since the LSST cadence will affect the airmass distribution, in each band, for each AGN candidate.

7.6.2 AGN Clustering

Measurements of the spatial clustering of AGNs with respect to those of quiescent galaxies can provide clues as to how galaxies form inside their dark-matter halos and what causes the growth of their supermassive black holes (SMBHs). The impressive inventory of LSST AGNs will enable the clustering, and thus the host galaxy halo mass, to be determined over the widest range ranges of cosmic epoch and accretion power. The LSST cadence will not only affect the overall AGN census and its $L - z$ distribution, but also the depth in each band as a function of sky position that can directly affect the clustering signal.

7.6.3 AGNs and the Time Domain

AGN Variability: A variety of AGN variability studies will be enabled by LSST. These are intended to probe the physical properties of the unresolved inner regions of the central engine. Relations will be sought between variability amplitude and timescale vs. L , z , λ_{eff} , color, multi-wavelength and spectroscopic properties, if available. The LSST sampling is expected to provide

high-quality power spectral density (PSD) functions for a large number of AGNs; these can be used to constrain the SMBH mass and accretion rate/mode. Furthermore, LSST AGNs exhibiting excess variability over that expected from their luminosities will be further scrutinized as candidates for lensed systems having unresolved images with the excess (extrinsic) variability being attributed mainly to microlensing.

Photometric reverberation mapping (PRM), measuring the time-delayed response of either the flux of the broad emission line region (BELR) lines to the flux of the AGN continuum or between the continuum flux in one (longer wavelength) band to the continuum flux in another (band with shorter wavelength), will be one of the cornerstones of AGN research in the LSST era (e.g., [Chelouche \(2013\)](#); [Chelouche & Zucker \(2013\)](#); [Chelouche et al. \(2014\)](#); [?](#); [?](#)). For example, LSST is expected to deliver BELR line-continuum time delays in $\sim 10^5 - 10^6$ sources, which is unprecedented when compared to $\sim 50 - 100$ such measurements conducted via the traditional, yet much more expensive (per source) spectroscopic method. Sources in the deep-drilling fields (DDFs) will benefit from the highest quality PRM time-delay measurements given the factor of ~ 10 denser sampling. The PRM measurements will probe the size and structure of the accretion disk and BELR, in a statistical sense, and may provide improved SMBH mass estimates for sources that have at least single-epoch spectra.

The PRM method is very sensitive to the sampling in each band, therefore the ability to derive reliable time delays can be affected significantly by the LSST cadence. The best results will be obtained by having the most uniform sampling equally for each band. Additionally, there is a trade-off between the number of DDFs and the number of time delays that PRM can obtain ([Chelouche et al. 2014](#)). For example, an increase in the number of DDFs, with similarly dense sampling in each field, can yield a proportionately larger number of high-quality time delays, down to lower luminosities, but at the expense of far fewer time delays (for relatively high luminosity sources) in the main survey.

Potentially periodic AGN variability, leading to tentative discoveries of binary SMBHs (e.g., [?](#)) may also benefit from uniform sampling. Over the ten-year survey, LSST will be sensitive to periods of a few days up to ~ 3 yr.

Time Delays in Gravitationally Lensed Quasars: This aspect is discussed in detail in the lens time delays section ([Section 7.5](#)).

AGN Size and Structure with Microlensing: Microlensing due to stars projected on top of individual lensed quasar images produce additional magnification. Using the fact that the Einstein radii of stars in lensing galaxies closely match the scales of different emission regions in high-redshift AGNs (micro-arcseconds), analyzing microlensing induced flux variations statistically on individual systems allows us to measure “sizes” of AGN regions. Assuming a thermal profile for accretion disks, sizes in different emission wavelengths will be probed and as such, constraints on the slope of this thermal profile will be placed. Given the sheer number of lensed systems that LSST is expected to discover (~ 8000), this will allow us to stack systems for better constraints and hopefully determine the evolution of the size and profile. Due to the typical relative velocities of lenses, microlenses, observers (Earth) and source AGN, the microlensing variation timescales are between months to a few decades.

The quasar microlensing optical depth is ~ 1 , so every lensed quasar should be affected by microlensing at any given point in time. However, measurable variability can occur on longer

timescales. [Mosquera & Kochanek \(2011\)](#) studied all known lensed quasars. They found the median timescale between high magnification events (Einstein crossing time scales) in the observed *I*-band is of the order of ~ 20 yr (with a distribution between 10 and 40 yr). However, the source crossing time (duration of a high magnification event) is ~ 7.3 months (with a distribution tail up to 3 yr). This basically means that out of all the lensed quasar *images* (microlensing between images is completely uncorrelated) about half of them will be quiescent during the 10 yr baseline of LSST. However, since the typical number of lensed images is either two or four, it means that, statistically, in every system, one (for doubles) or two (for quads) high magnification events should be observed in 10 yr of LSST monitoring.

Note that, the important cadence parameter is the source crossing time, as it is the length of the event to be as uniformly sampled as possible. The 7.3 months crossing time is the median for the observed *i*-band, but this time would be significantly shorter for bluer bands: for a thermal profile with slope α : $R_\lambda \propto \lambda^\alpha$ implies source crossing time $t_s \propto \lambda^{1/\alpha} \rightarrow t_u = t_i \times (\lambda_u/\lambda_i)^{1/\alpha}$. For a Shakura-Sunyaev slope of $\alpha = 0.75$ this would correspond to $7.3 \times (3600/8140)^{4/3}$ months which is ≈ 2.5 months in the *u*-band.

In terms of the cadence, at least three evenly sampled data points per band within two to three months would be preferred to be able to map the constraining high magnification event(?). Hopefully uniformly spaced. Very tight cadence (e.g., DDFs) would increase the constraints significantly. However, since lensed quasars are not that common, this smaller area would mean only a few (~ 80 ?) suitable systems monitored in the DDFs. Regarding the season length, the “months” timescale of high magnification events very likely means that we can/will miss high magnification events in the season gaps, at least in the bluer bands. Killer: observations spread on timescales larger than 3 months(?). This would likely miss the high magnification events. In those cases we could perhaps consider close consecutive photometric bands as equivalent accretion disk regions, however this would mean weaker constraints on the thermal profile. Important Note: all this science needs to be done on lensed quasars with measured or very short time delays to remove the intrinsic variability signal, which might significantly reduce the sample.

Microlensing Aided Reverberation Mapping: Given that microlensing mostly affects continuum emission rather than BELR line emission, microlensing may enable disentangling the BELR line plus the continuum emission in single photometric bands, allowing the use of single broad band PRM measurements ([Sluse & Tewes 2014](#)). As with the two-band PRM method discussed above, the denser (and the longer) the sampling, the more accurate are the constraints that can be obtained for the time delays.

Transient AGN and TDEs: This aspect is discussed in detail in the non-periodic variables section ([Section 6.4](#)).

7.6.4 Metrics

AGN Selection: Need to compute the mean *Y* band magnitude across the sky for the nominal OpSim. Compare this magnitude to the one required for identifying ≥ 1000 quasars at $z \geq 6$. Currently, for enigma.1189, the single-epoch 5-sigma depth in *Y* is 22.36 mag, and for the final co-added 5-sigma depth is *Y* = 24.4. These limits are deeper than the original predictions.

PRM: Need to compute the average and the dispersion in the number of visits, per band, across the sky for the nominal OpSim (during the entire survey). Since PRM works best for uniform sampling, need to compare the distributions of the number of visits in each band, averaged across the sky, and identify ways to minimize any potential differences between these distributions. By running PRM simulations, identify the 1) minimum number of visits (in any band) that can yield any meaningful BELR-continuum lag estimates, and 2) the largest difference in the number of visits between two different bands that can yield any meaningful BELR-continuum lag estimates. Repeat these simulations by doubling the nominal number of DDFs. Assess the number of meaningful BELR-continuum time delays that can be obtained with the nominal OpSim, and point out potential perturbations in the cadence to improve the number and quality of such time delays.

Microlensing: Need to compute the dispersion in the time gap between visits in the same band, across the sky, in order to assess the fraction of microlensing events that might be missed (on top of seasonal gaps).

7.6.5 Discussion

Some additional considerations/thoughts that came up during the workshop:

1) Assuming we will have 10 DDFs, perhaps one of those fields could be sampled more heavily than the others and would be visited nightly (or even more frequently, e.g., from ~ 1 to ~ 1000 min) per band. This can be justified by the fact that a) very few AGNs have been monitored at these frequencies on such a long baseline, leaving room for discovery, and b) this may probe intermediate-mass black holes ($\sim 10^4 - 10^5 M_\odot$) via PRM or PSDs. Good candidate fields are the CDF-S and the MCs. Need to suggest a strategy for an OpSim (or commissioning).

2) Need to assess the effects of the LSST cadence on the ability to detect periodic AGNs and quasi-periodic oscillations (QPOs) in AGNs.

3) Needs from OpSim: in order to have informative metrics, we need to have accurate model light curves that can reproduce how the fiducial light curves appear in different bands, at different inherent luminosities, and at different redshifts.

: Compare the current science content with the AGN chapter in the Science Book as well as with the Ivezić et al. overview paper (<http://arxiv.org/pdf/0805.2366v4.pdf>).

: Compare the Y-band (and other bands) depths, single epoch and final co-added, from enigma_1189 with other OpSims.

: Assess the effect of non-simultaneous colors on AGN selection.

: Based on the current OpSim, need to specify the magnitude limits at the highest airmass and assess the limitations of the DCR method in the $L-z$ plane. Should check this with MAF and if indeed AM := 1.4, need to add a request in: <https://github.com/LSSTScienceCollaborations/OpSim>

: Assess whether, e.g., a pair of ~ 2.5 min exposures (i.e., ~ 10 times longer than the standard exposures) at airmass ~ 2 would get deep enough for useful DCR constraints for a large fraction of the AGNs. This may be a non-negligible perturbation of the

expected 56-184 visits per band, and may even be impossible given current upper limits on exposure times, but this would help improve photo-z's for galaxies and SNe too.

- : For PRM and microlensing: obtain distributions (mean and dispersion) of the number of visits, per band, across the sky for the nominal OpSim (during the entire survey).
- : Add a discussion about blazars and LSST cadence (e.g., Isler+15?). Would blazar science benefit from a specific cadence requirement?
- : Check the Astrometry chapter and assess the astrometric precision for AGN selection. For example, we may require very good depth at least in the 1st and 10th year of the survey.
- : Indicate the properties (frequency range and sampling) for obtaining optimal PSDs required for QPO detection (given MBH, spin, and L/LEdd). Based on current OpSim, assess the potential of discovering QPOs in the main survey and in the DDFs.

Go to: • [the start of this section](#) • [the start of the chapter](#) • [the table of contents](#)

8 Drilling Deep: Options for a Small Number of Enhanced Observation Fields

Niel Brandt, Lynn Jones

8.1 Introduction

9 Special Surveys

Knut Olsen, David Nidever, more to come

9.1 Introduction

The four main LSST science themes, as defined by the Science Book, drive the design of LSST’s main Wide-Fast-Deep survey. However, it has always been recognized that many important scientific projects, including some that are highly relevant to LSST’s main science themes, are not well served by the areal coverage and/or cadence constraints placed on the WFD survey. The LSST Project thus set aside a nominal 10% of the observing time to serve what are collectively called “special surveys”. In addition, the LSST commissioning period may be available for use by special programs. Projects that will certainly make use of this 10% time not dedicated to the WFD survey include the Deep Drilling fields and Galactic Plane surveys described separately in this paper, as well as any survey wishing to observe at declinations below -60° , such as the Magellanic Clouds. These special programs heavily oversubscribe the nominal 10% of time assigned to them. It is of thus critical importance for these programs to define compelling science cases, clearly justify their observing requirements, and derive metrics to quantify the performance of a given schedule for the program. An extra degree of freedom that these special surveys

As mentioned previously, the Deep Drilling and Milky Way plane surveys are described separately in this paper. In this section, we describe the goals of two special surveys designed to serve scientific goals related to the Magellanic Clouds. Descriptions of other special surveys, including candidate commissioning programs, are welcome here.

9.2 The Magellanic Clouds

David L. Nidever, Knut Olsen

The Magellanic Clouds have always had outsized importance for astrophysics. They are critical steps in the cosmological distance ladder, they are a binary galaxy system with a unique interaction history, and they are laboratories for studying all manner of astrophysical phenomena. They are often used as jumping-off points for investigations of much larger scope and scale; examples are the searches for extragalactic supernova prompted by the explosion of SN1987A and the dark matter searches through the technique of gravitational microlensing. More than 17,000 papers in the NASA ADS include the words “Magellanic Clouds” in their abstracts or as part of their keywords, highlighting their importance for a wide variety of astronomical studies.

An LSST survey that did not include coverage of the Magellanic Clouds and their periphery would be tragically incomplete. LSST has a unique role to play in surveys of the Clouds. First, its large $A\Omega$ will allow us to probe the thousands of square degrees that comprise the extended periphery of the Magellanic Clouds with unprecedented completeness and depth, allowing us to detect and map their extended disks, stellar halos, and debris from interactions that we already have strong evidence must exist (REFS). Second, the ability of LSST to map the entire main bodies in only a few pointings will allow us to identify and classify their extensive variable source populations with unprecedented time and areal coverage, discovering, for example, extragalactic planets, rare variables and transients, and light echoes from explosive events that occurred thousands of years ago (REFS). Finally, the large number of observing opportunities that the LSST 10-year survey will provide will enable us to produce a static imaging mosaic of the main bodies of the Clouds with extraordinary image quality, an invaluable legacy product of LSST.

We propose two distinct mini-surveys to meet the goals of LSST Magellanic Clouds science:

- A mini-survey covering the 2700deg^2 with $\delta < -60$ to the standard LSST single-exposure depth and to stacked depths of XXX, with cadence sufficient to detect and measure light curves of RR Lyrae stars
- A mini-survey covering $\sim 250\text{deg}^2$ of the main bodies of the Clouds with cadence sufficient to detect exoplanet transits and other variable objects; a subset of these images should be taken with seeing of $0.5''$, with stacked depth reaching the confusion limits in the Clouds

Figure X shows a rough map of the proposed mini-surveys. These surveys will support several important scientific goals:

1. What are the stellar and dark matter mass profiles of the Magellanic Clouds? Map extended disk, halo, debris, and streams. Use streams as probes of total mass profile. RR Lyrae give potential for three-dimensional stellar profile.
2. What is the satellite population of the Magellanic Clouds? Discovery of dwarfs by DES and other surveys illuminating for understanding distribution of dark matter subhalos and how galaxies form in them (REFS)
3. What are the internal dynamics of the Magellanic Clouds? Proper motions from HST and from the ground (REFS) have measured the bulk motions of the Clouds and have, in combination with spectroscopy, begun to unravel the three dimensional internal dynamics of the Clouds...
4. How do exoplanet statistics in the Magellanic Clouds compare to those in the Milky Way? Lund calculation shows can measure transits of Jupiter-like planets, Clouds are lower metallicity environment
5. Identify and characterize the variable star and transient population of the Clouds. Population studies, linking to star formation and chemical enrichment histories, etc, from Szkody et al. DD white paper.
6. Light echoes from supernovae and explosive events. Echoes can give view of such events unavailable by any other means, ref. papers by Rest et al.

Two main overarching science themes:

1. **Galaxy formation evolution:** The study of the formation and evolution of the Large and Small Magellanic Clouds (LMC and SMC, respectively), especially their interaction with each other and the Milky Way. The Magellanic Clouds (MCs) are a unique local laboratory for studying the formation and evolution of dwarf galaxies in exquisite detail. LSST's large FOV will be able to map out the three-dimensional structure, metallicity and kinematics in great detail.
2. **Stellar astrophysics & Exoplanets:** The MCs have been used for decades to study stellar astrophysics, microlensing and other processes. The fact that the objects are effectively all at a single known distance makes it much easier to study them than in, for example, the Milky Way. LSST will extend these studies to fainter magnitudes, higher cadence, and larger area.

Many different types of objects and measurements with their own cadence “requirements” will fall into these two broad categories (with some overlap). These will be outlined in the next section.

A very important aspect of the “galaxy evolution” science theme is not just the cadence but also the sky coverage of the Magellanic Clouds “mini-survey”. A common misunderstanding is that the MCs only cover a few degrees on the sky. That is, however, just the central regions of the MCs akin to the thinking of the Milky Way as the just the bulge. The full galaxies are actually much larger with LMC stars detected at $\sim 21^\circ$ (~ 18 kpc) and SMC stars at $\sim 10^\circ$ (~ 11 kpc) from their respective centers. The extended stellar debris from their interaction likely extends to even larger distances. Therefore, to get a complete picture of the complex strucure of the MCs will require a mini-survey that covers ~ 2000 deg 2 . At this point, it not entirely clear how to include this into the metrics. Note, that for the second science case this is not as much of an issue since the large majority of the relevant objects will be located in the high-density, central regions of the MCs.

9.2.1 Target measurements and discoveries

1. Deep Color Magnitude Diagrams
2. Proper Motions
3. Variable stars
4. Transients
5. Transiting Exoplanets
6. Astrometric binaries
7. Gyrochronology
8. Astroseismology

9.2.2 Metrics

Quantifying the response via MAF metrics: definition of the metrics, and any derived overall figure of merit.

9.2.3 OpSim Analysis

OpSim analysis: how good would the default observing strategy be, at the time of writing for this science project?

9.2.4 Discussion

Discussion: what risks have been identified? What suggestions could be made to improve this science project's figure of merit, and mitigate the identified risks?

Go to: • [the start of this section](#) • [the start of the chapter](#) • [the table of contents](#)

9.3 Short Exposure Survey- Introduction

The current LSST requirements stipulate a minimum exposure time of 5 seconds, with an expected default exposure time of 15 seconds. This document advocates for decreasing the minimum exposure time requirement from 5 to 0.1 seconds. This would increase the dynamic range for bright sources (compared to the default 15 sec time) by about 5 magnitudes, to a total of 13 astronomical magnitudes (where dynamic range is the difference between the brightest unsaturated source and the faintest point source detectable at 5 sigma). This is a large factor, and would enable a wide range of science goals, outlined below. One interesting aspect of this is that it would allow us to operate the LSST system during twilight times that would otherwise saturate the array due to background sky brightness. This would allow a number of the goals described below to be carried out without impacting the primary survey by conducting observations during twilight sky conditions that would saturate the array at longer exposure times.

Since the twilight sky brightness is an important factor discussed below, we provide here a very brief outline of the temporal evolution of the background sky brightness.

Tyson and Gal (1993) provide a simple framework that serves our purposes well. They provide observational data as well as a simple model for the evolution of twilight sky brightness. Figure 1 from that paper is included below. They show that a good model for the sky brightness evolution is given by an exponential with $\log_{10}(S) = (k/\tau)t + C$, where S is the sky brightness in electrons per pixel per second, C is the dark sky background, $k = (10.6 \text{ minutes})^{-1}$ is a universal (band-independent) timescale during which the sky's surface brightness changes by a factor of ten (at latitude -30 degrees), and τ is a season-dependent factor that ranges from 1.0 at the equinox to 1.07 in austral winter and 1.20 in austral summer. So the rule of thumb is that we should expect it to take 4.25 minutes for the sky background to change by one magnitude per square arc sec. (In what follows we'll ignore the increased twilight time in summer and winter.)

For current generation typical astronomical camera systems that take over a minute to read out, this 4.2 minute time scale means that only a handful of images can be obtained during twilight time. But for the LSST camera with a 2 second readout time, we can obtain hundreds of short exposures during twilight. Even if we are limited to a 15 second cadence due to thermal stability or data transfer limitations there is a large amount of time opened up that we can use.

What do we stand to gain in operational time with shorter exposures? If the standard survey terminates taking 15 second exposures due to some sky brightness criterion, by shifting to 0.1 sec images at that point we will have changed the sky flux per pixel by $2.5 \log_{10}(150) = 5.4$ magnitudes. This brings us back into a high dynamic range regime, as described below.

Figure 2 illustrates the principles that underpin this proposal. LSST is a unique combination of hardware and software, that will deliver reliable catalogs of both the static and the dynamic sky. By pushing towards shorter integration times we can greatly expand the scientific reach of the system.

The dynamic range in magnitudes that we can achieve for a given integration time depends on the sky background, the read noise, and the full well depth per pixel. We will adopt a typical value of 100Ke for the full well depth, but the arguments presented below are essentially independent of this value. The dynamic range in magnitudes is limited on the bright end by the point source whose PSF peak exceeds full well, and on the faint end by the 5σ point source sensitivity, which depends on sky brightness per pixel. So we are squeezed between the two parameters of full well depth and sky background.

The 5 sigma limiting flux scales as the square root of the sky brightness, while the saturation flux decreases linearly as sky brightness increases. So the two curves in Figure 2 have slopes that differ by a factor of two. Operating during bright-sky time with short exposures adds about 20 minutes of observing per twilight, or 40 minutes per night. This is a non-trivial resource!

Figure 2 shows one reason why it is not advantageous to go below 0.1 second exposures- we would lose the overlap between a twilight survey and the standard LSST object catalog.

Having set the stage for the opportunity to operate at shorter exposure times either during dark sky time, or during twilight, or both, we now describe some of the scientific motivations for doing so.

9.3.1 Science Drivers for Shorter Exposures

Discovery space at short time scales.

LSST is a time domain discovery machine. It is hard to anticipate the importance of being able to detect astronomical variability on short time scales. By extending the time domain sensitivity to phenomena with a characteristic time of less than 5 seconds, we will have added 1.5 orders of magnitude in time domain sensitivity.

Taking short exposures does not necessarily imply a requirement on fast image cadence. Periodic variability can be readily detected and characterized with a succession of short images that do not satisfy the Nyquist criterion, as long as we know the time associated with each data point to adequate accuracy. But it does seem appropriate to investigate the maximum possible rapid-fire imaging rate for LSST, presumably limited by either data transfer bottlenecks or by thermal issues within the camera.

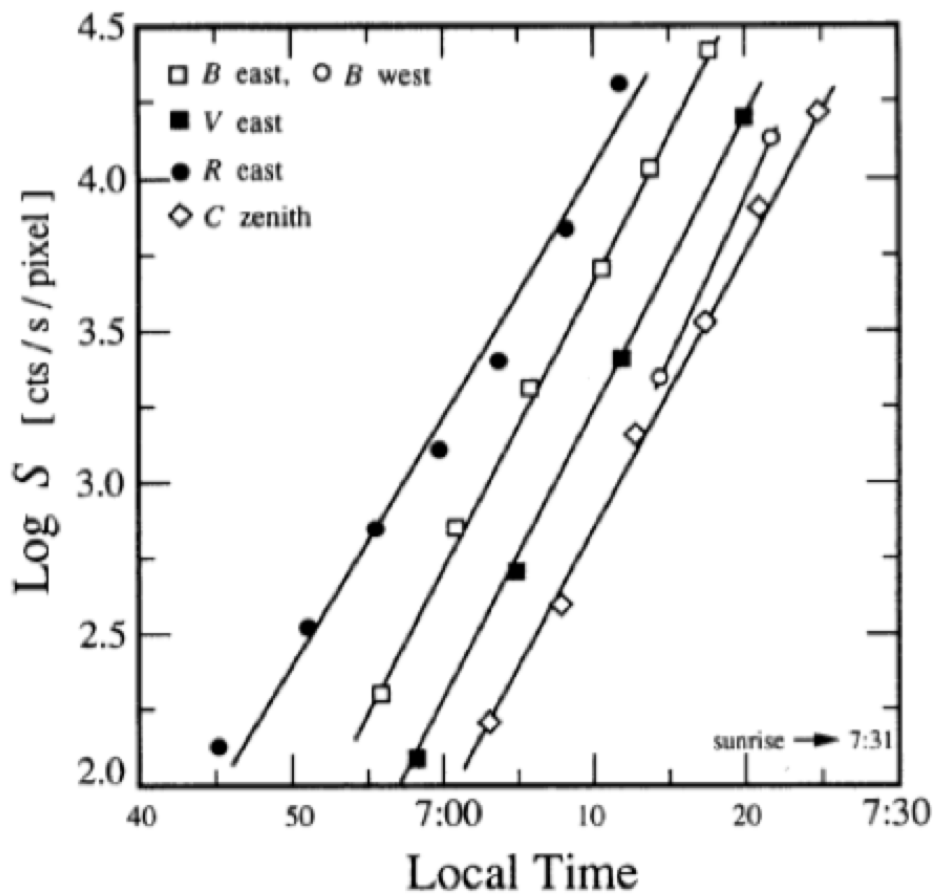


FIG. 1. Log of the twilight sky surface brightness vs local time for four broadband filters: Washington C ($\lambda_{\text{eff}} = 3900 \text{ \AA}$), and Harris B , V , R . All filters display a similar rate of change of surface brightness. This effect appears to be independent of direction (within 2 airmasses of the zenith) as evidenced by the similarity of slopes for data obtained while pointing east, west, and toward the zenith before sunrise.

Figure 9.1: (reproduced from Tyson et al, 1993). This plot shows that the sky brightness changes by one magnitude in a 4.2 minute interval, essentially independent of passband.

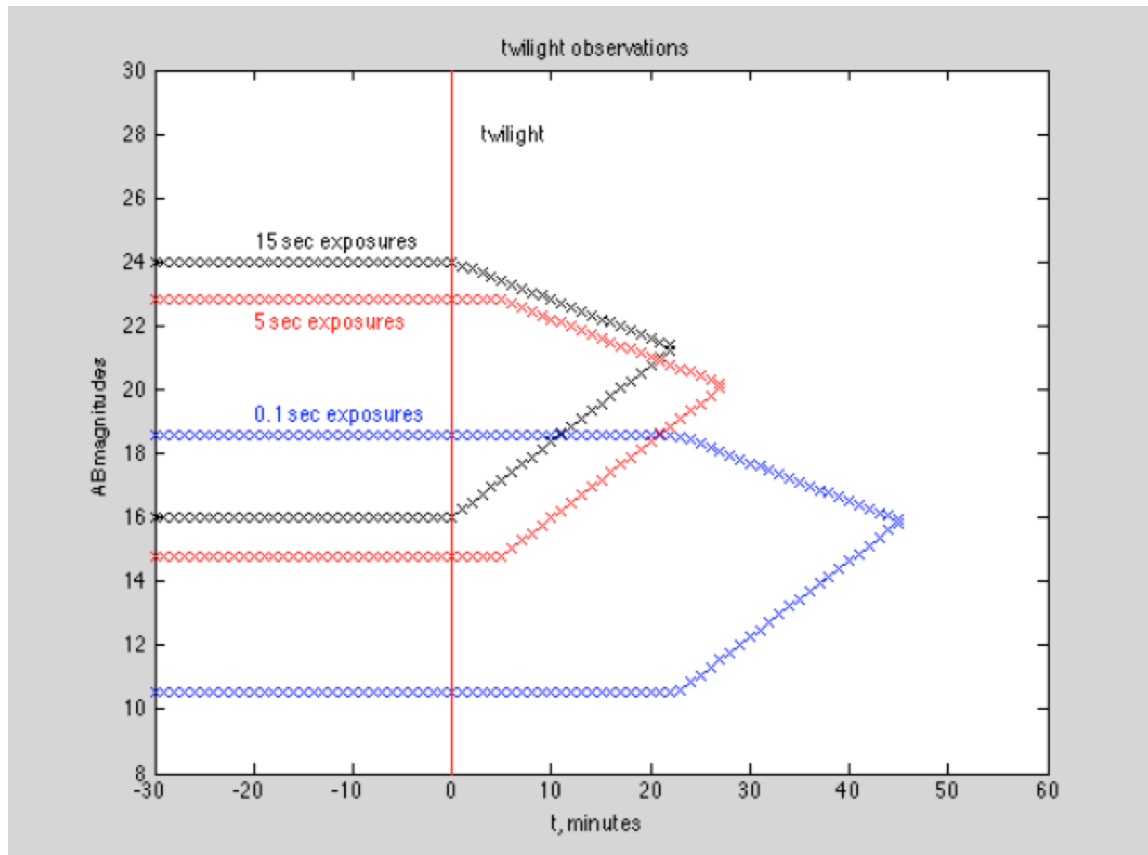


Figure 9.2: Twilight dynamic range. As we enter morning twilight time, the increasing sky brightness requires brighter sources for 5 sigma detection, and also limits unsaturated objects to increasingly fainter sources. Eventually the gap between these goes to zero. But operating at shorter exposure times allows us to push useful survey operations into brighter twilight time, and also to increase the dynamic range of the LSST survey products. The black lines correspond to 15 second integrations (nominally in the r band), the red lines to 5 second exposures, and the blue curves to 0.1 second exposures. The upper lines in each case represent the 5 sigma point source detection threshold while the lower line corresponds to the source brightness that produces saturation in the peak pixel of the PSF. Adding shorter exposure times increases our dynamic range in flux, and adds valuable observing time.

Distances to Nearby SN Ia- an essential ingredient in using supernovae to probe dark energy.

The determination of the equation of state parameter of the Dark Energy using type Ia supernovae entails measuring the redshift dependence of the luminosity distances to objects over a range of redshifts. The low end of this redshift range is limited by peculiar velocities to considering supernovae at redshifts $z > 0.01$. At this distance (distance modulus of $\mu = 33$) the peak brightness of a type Ia supernova is $r=15$ and exceeds the expected LSST point source saturation limit.

Moreover, the rate on the sky of these bright nearby supernovae is so low that in the standard cadence we don't expect to obtain well-sampled multiband light curves for them. But we will discover many of them on the rise. Using twilight time with short exposures to obtain appropriate temporal and passband coverage will allow us to extend the LSST SN Hubble diagram across the entire redshift range of 0.01 to 1.

It is vitally important that we obtain these nearby-SN light curves on the same photometric system, reduced with the same data reduction pipeline, as the distant sample. This means we really must use the LSST instrument and software in order to avoid systematic errors arising from differences in photometric systems or algorithmic issues.

We stress that this twilight SN followup campaign can be accomplished without impacting the main survey, during the roughly 20 minutes per night of twilight that would otherwise unusable at the default exposure time. We would use the brighter twilight time to obtain pointed observations on nearby supernovae, motivated by the importance of photometric uniformity described above.

A Bright Star Survey for Galactic Science.

We could also use the added twilight time to conduct a bright star survey, and the precise astrometry and photometry from LSST can then be used in conjunction with archived data ranging from 11th to 27th AB magnitudes. This short-exposure domain would extend the LSST dynamic range in fluxes by two orders of magnitude, towards the bright end. Moreover, obtaining precise positions, fluxes and variability at these brighter magnitudes would greatly increase the overlap with the historical archive of astronomical information, including from digitized plate data. We would be able to obtain astrometric and color information to high precision, as well time series for variability studies.

An example of an application to Milky Way structure studies comes from RR Lyrae variable stars. With a saturation magnitude of around 16th in the standard LSST survey, RR Lyrae closer than 20 kpc will be saturated in the standard LSST images. So we will lose nearly all Galactic RR Lyrae. Extending the surveys bright limit to 11th magnitude will allow us to collect light curves for RR Lyrae beyond ~ 100 parsecs, collecting essentially all Southern hemisphere Galactic RR Lyrae.

Another application for stellar population studies is measuring the fraction of binary stars as a function of stellar type, metallicity, age and environment. By conducting a variability survey in the 11-18 magnitude range we can capitalize on temperature and metallicity data already in hand for many of these objects.

Another application of a bright star survey would be to search for planetary transits in the magnitude range appropriate for radial velocity followup observations using 30 meter class telescopes. For high dispersion spectrographs at the 4m aperture class, most targets are currently around 8th magnitude, so we should expect 30m telescopes to attain similar radial velocity precisions for sources of magnitude $8 + 5\log(30/4) = 12$. By going to shorter exposures we obtain almost an hours additional observing time per night when these sources dont saturate, whereas they are far beyond saturation in the default 15 second LSST survey images.

A typical ($r-K$) color between SDSS and 2MASS is $r-K=3$. The 2MASS catalog is complete down to $K \sim 14$ which corresponds to $r \sim 17$. So most 2MASS stars will be saturated in the standard LSST 15 second observations. A bright star survey will allow a multiband match to the 2MASS data, as well as an astrometric comparison between the two catalogs.

Finally, the apparent magnitude of solar system objects depends on their distance from us and from the sun, as well as illumination and observation geometry. Extending the bright limit will allow us to track asteroid positions as they approach opposition.

9.3.2 Counterarguments

What About Scintillation Effects?

Short exposure times suffer from scintillation effects. An estimate for uncertainty due to scintillation is provided by <http://astro.corlan.net/gcx/scint.txt>. For a 0.1 second integration we expect a fractional flux uncertainty of 0.15 at 2 airmasses and 0.043 at 1 airmass, for a 10 cm aperture. Scaling this up to the 8.5m aperture of LSST by a factor $D^{2/3}$ predicts fractional flux variations of below one percent, even at two airmasses, for a 0.1 second exposure. So scintillation should not impact our ability to make precision measurements of flux and position.

What about just doing this with smaller telescopes?

A possible counter-argument to the proposal of allowing for shorter exposure times is that much of this can be done with smaller telescopes. But its important to bear in mind that LSST is a system, and the data reduction and dissemination tools are as important as the hardware. We intend to deliver accessible, high-quality, well-calibrated photometry on a common photometric system and correspondingly good positions. If we do so from a co-added point source depth of 27th to the short-exposure bright limit of 11th magnitude we will span over six decades in flux on a well-calibrated flux scale. We would also have the ability to study astrophysical variability on time scales from 0.1 second to 10 years, which is nine decades in the time domain. This combination of temporal and flux dynamic range would be a truly remarkable achievement, and would yield science benefits far beyond the illustrative examples provided above. Much of this discovery space is enabled by going to shorter exposures.

9.3.3 Proposed Implementation and Impacts

The implementation of this would simply entail taking short-exposure images during twilight time that would otherwise go unused. The data rate would go up, and the number of shutter cycles per night would also increase.

Go to: • [the start of this section](#) • [the start of the chapter](#) • [the table of contents](#)

10 Tensions and Trade-offs

...

Discussion and conclusions chapter, at the end, highlighting the issues that we will need to figure out. Possible topics include the cost/benefit tradeoffs between competing objectives.

References

- Bernstein, J. P., Kessler, R., Kuhlmann, S., Biswas, R., Kovacs, E., Aldering, G., Crane, I., D'Andrea, C. B., Finley, D. A., Frieman, J. A., Hufford, T., Jarvis, M. J., Kim, A. G., Marriner, J., Mukherjee, P., Nichol, R. C., Nugent, P., Parkinson, D., Reis, R. R. R., Sako, M., Spinka, H., & Sullivan, M. 2012, *ApJ*, 753, 152
- Butler, N. R. & Bloom, J. S. 2011, *AJ*, 141, 93
- Campbell, H., D'Andrea, C. B., Nichol, R. C., Sako, M., Smith, M., Lampeitl, H., Olmstead, M. D., Bassett, B., Biswas, R., Brown, P., Cinabro, D., Dawson, K. S., Dilday, B., Foley, R. J., Frieman, J. A., Garnavich, P., Hlozek, R., Jha, S. W., Kuhlmann, S., Kunz, M., Marriner, J., Miquel, R., Richmond, M., Riess, A., Schneider, D. P., Sollerman, J., Taylor, M., & Zhao, G.-B. 2013, *ApJ*, 763, 88
- Carroll, C. M., Gawiser, E., Kurczynski, P. L., Bailey, R. A., Biswas, R., Cinabro, D., Jha, S. W., Jones, R. L., Krughoff, K. S., Sonawalla, A., & Wood-Vasey, W. M. 2014, in Society of Photo-Optical Instrumentation Engineers (SPIE) Conference Series, Vol. 9149, Society of Photo-Optical Instrumentation Engineers (SPIE) Conference Series, 0
- Chelouche, D. 2013, *ApJ*, 772, 9
- Chelouche, D., Shemmer, O., Cotlier, G. I., Barth, A. J., & Rafter, S. E. 2014, *ApJ*, 785, 140
- Chelouche, D. & Zucker, S. 2013, *ApJ*, 769, 124
- Guy, J., Astier, P., Baumont, S., Hardin, D., Pain, R., Regnault, N., Basa, S., Carlberg, R. G., Conley, A., Fabbro, S., Fouchez, D., Hook, I. M., Howell, D. A., Perrett, K., Pritchett, C. J., Rich, J., Sullivan, M., Antilogus, P., Aubourg, E., Bazin, G., Brionner, J., Filhol, M., Palanque-Delabrouille, N., Ripoche, P., & Ruhlmann-Kleider, V. 2007, *A&A*, 466, 11
- Hlozek, R., Kunz, M., Bassett, B., Smith, M., Newling, J., Varughese, M., Kessler, R., Bernstein, J. P., Campbell, H., Dilday, B., Falck, B., Frieman, J., Kuhlmann, S., Lampeitl, H., Marriner, J., Nichol, R. C., Riess, A. G., Sako, M., & Schneider, D. P. 2012, *ApJ*, 752, 79
- Ivezic, Z., Tyson, J. A., Allsman, R., Andrew, J., Angel, R., & for the LSST Collaboration. 2008, ArXiv e-prints
- Jha, S., Riess, A. G., & Kirshner, R. P. 2007, *ApJ*, 659, 122
- Kaczmarszak, M. C., Richards, G. T., Mehta, S. S., & Schlegel, D. J. 2009, *AJ*, 138, 19
- Kessler, R., Bassett, B., Belov, P., Bhatnagar, V., Campbell, H., Conley, A., Frieman, J. A., Glazov, A., González-Gaitán, S., Hlozek, R., Jha, S., Kuhlmann, S., Kunz, M., Lampeitl, H., Mahabal, A., Newling, J., Nichol, R. C., Parkinson, D., Philip, N. S., Poznanski, D., Richards, J. W., Rodney, S. A., Sako, M., Schneider, D. P., Smith, M., Stritzinger, M., & Varughese, M. 2010a, *PASP*, 122, 1415
- Kessler, R., Conley, A., Jha, S., & Kuhlmann, S. 2010b, ArXiv e-prints
- Knights, M., Bassett, B. A., Varughese, M., Hlozek, R., Kunz, M., Smith, M., & Newling, J. 2013, *JCAP*, 1, 39
- Kunz, M., Bassett, B. A., & Hlozek, R. A. 2007, *Phys. Rev. D*, 75, 103508
- Liao, K., Treu, T., Marshall, P., Fassnacht, C. D., Rumbaugh, N., Dobler, G., Aghamousa, A., Bonvin, V., Courbin, F., Hojjati, A., Jackson, N., Kashyap, V., Rathna Kumar, S., Linder, E., Mandel, K., Meng, X.-L., Meylan, G., Moustakas, L. A., Prabhu, T. P., Romero-Wolf, A., Shafieloo, A., Siemiginowska, A., Stalin, C. S., Tak, H., Tewes, M., & van Dyk, D. 2015, *ApJ*, 800, 11
- Mosquera, A. M. & Kochanek, C. S. 2011, *ApJ*, 738, 96
- Newling, J., Bassett, B. A., Hlozek, R., Kunz, M., Smith, M., & Varughese, M. 2011, ArXiv e-prints
- Sako, M., Bassett, B., Becker, A., Cinabro, D., DeJongh, F., Depoy, D. L., Dilday, B., Doi, M., Frieman, J. A., Garnavich, P. M., Hogan, C. J., Holtzman, J., Jha, S., Kessler, R., Konishi, K., Lampeitl, H., Marriner, J., Miknaitis, G., Nichol, R. C., Prieto, J. L., Riess, A. G., Richmond, M. W., Romani, R., Schneider, D. P., Smith, M., SubbaRao, M., Takanashi, N., Tokita, K., van der Heyden, K., Yasuda, N., Zheng, C., Barentine, J., Brewington, H., Choi, C., Dembicky, J., Harnavek, M., Ihara, Y., Im, M., Ketzeback, W., Kleinman, S. J., Krzesiński, J., Long, D. C., Malanushenko, E., Malanushenko, V., McMillan, R. J., Morokuma, T., Nitta, A., Pan, K., Saurage, G., & Snedden, S. A. 2008, *AJ*, 135, 348
- Sako, M., Bassett, B., Connolly, B., Dilday, B., Cambell, H., Frieman, J. A., Gladney, L., Kessler, R., Lampeitl, H., Marriner, J., Miquel, R., Nichol, R. C., Schneider, D. P., Smith, M., & Sollerman, J. 2011, *ApJ*, 738, 162

Chapter 10: References

Sluse, D. & Tewes, M. 2014, *A&A*, 571, A60